"Global Change Research Related to the Earth's Energy and Hydrologic Cycle"

Final and Third Year Report

For The Period

September 30, 1997 – September 29, 2000

Under
Cooperative Agreement: NCC8-141

Submitted to:

The George C. Marshall Space Flight Center
Marshall Space Flight Center
Huntsville, Alabama 35812

Prepared By

Linda R. Berry, Coordinator
Earth System Science Center
The University Of Alabama In Huntsville
Huntsville, AL 35899

Submitted by:

John Christy
Principal Investigator
Earth System Science Center
The University Of Alabama In Huntsville
Huntsville, AL 35899

For the past seven years the University of Alabama in Huntsville (UAH), Universities Space Research Association (USRA), and the National Aeronautics and Space Administration (NASA) Marshall Space Flight Center (MSFC) Global Hydrology Research Office (HR) have worked together to create an environment where collaborative research and education centered on the role of water in the energetics and dynamics of the Earth's atmosphere and physical climate system can grow and prosper through two different cooperative agreements NCC8-22 and NCC8-141. This report is the final report for NCC8-141. This collaboration has evolved into the creation of the Global Hydrology and Climate Center (GHCC). The mission of the "Global Change Research Related to the Earth's Energy and Hydrologic Cycle" is to enhance the scientific knowledge and educational benefits obtained from NASA's Earth Science Enterprise and the U.S. Global Change Research Program, University of Alabama in Huntsville (UAH) scientists have cooperated with Marshall Space Flight Center scientists to :

- Facilitate research with and access to Earth Observing System and other Earth data sets, and to assist scientists with the utilization and application of these data to global change research. Specifically, proposed global change research programs include:
  - Using surface- and space-based observations to determine fluxes of water and energy to analyze components of the hydrologic cycle.
  - Employing conceptual, diagnostic, and numerical models to integrate and interpret the observations and analyses of the hydrologic cycle.
  - Contributing to the prediction of global change by increasing understanding of hydrologic processes affecting global change.
  - Developing specifications and requirements for development of future observing systems.

- Participate in data management activities that aid scientific research. Specifically, proposed data management activities include:
  - Participating in field studies and the processing, quality control, and archival of large data sets.
  - Developing specifications and requirements for development of data management systems and analysis tools.

Research results have been presented at various conferences and meetings and have been published in reports and refereed journals (See Appendix A: Staff Travel Activities and Appendix B: Publications and Presentations).

- Integrate research and educational programs to help universities prepare future global change scientists and to aid university and secondary teachers to communicate the importance and challenges of global change science. Specifically, proposed educational initiatives include:
  - Developing visiting graduate student programs to promote student and faculty interest in global change research.
  - Establishing both university-based and pre-college education programs to encourage development of Earth system science curricula.

See Appendix C: Education Activities and Appendix D: Students.

- Stimulate involvement of university, private-sector and government agency scientists who seek to develop long-term collaborative research in global change science. Specifically, proposed scientific outreach functions include:
  - Sponsoring, organizing and coordinating scientific seminars, meetings, workshops, and colloquia related to global change research, as well as encouraging and supporting visits by scientists from universities and other organizations.

See Appendix E: Seminars.

Additional projects were added to the Cooperative Agreement during the three years. An update on these projects can be found in Appendix F

Appendix A:

Staff Travel Activities
Years 1 through 3

*Please note that this is a representative list of travel activities that occurred during Years One through Three and may not include all travel that occurred during Years One through Three of NCC8-141.

YEAR 1 – STAFF TRAVEL ACTIVITIES

NAME	DATES	LOCATION	REASON
Beaumont, B.	2/10-13/98	Greenbelt, MD	To attend/participate in the Earth On-Line Workshop.
Blair, A.	8/10-22/98	Orlando, FL	To attend field experiment of Camex3 Project
Botts, M.	5/4-7/98	Washington, D.C.	To participate in NASA EOS ESIP Federation Meeting (1st)
Bowdle, D.	12/16-19/97	Boulder, CO	Participate in Turbulence Working Group Meeting
Bowdle, D.	FL1/20-22/98	Key West, FL	To present a paper at the NOAA Working Group Meeting on Space-Based Lidar Winds
Bowdle, D.	3/22-4/9/98	Boulder, CO	To participate in flight tests of NASA DFRC Airborne Coherent LIDAR for Advanced In-flight Measurements (ACLAIM)
Buechler, D.	8/18-19/98	Greenbelt, MD	Collaborative research with Goddard Space Flight Center
Chambers, D.	8/19-21/98	Livermore, CA	Visit Lawrence Livermore National Laboratory to view facilities and discuss collaboration
Chang, F.	10/26-11/1/97	Silver Spring, MD	To participate in the First International Conference on Reanalysis and present a paper.
Chang, F.	5/22-30/98	Paris, France	To participate, present paper at the 9th conference on Satellite Meteorology & Oceanography
Christopher, S.	4/19-22/98	Baltimore, MD	To attend TOMS Science Team Meeting
Conover, H.	2/10-13/98	Greenbelt, MD	To attend/participate in the Earth On-Line Workshop.
Conover, H.	6/9-11/98	Greenbelt, MD	To attend/participate in the EOSDIS Technology Transfer Workshop.
Conover, H.	8/18-20/98	Greenbelt, MD	Meeting with Israeli delegation to discuss data center development and data system inter-operability .
Conover, H.	8/18-20/98	Greenbelt, MD	Meeting with Israeli delegation to discuss data center development and data system inter-operability .
Conway, D.	10/14-17/97	Pasadena, CA	AMSR Data Format Meeting
Conway, D.	3/30-4/2/98	Washington, D.C.	To attend AMSR Meeting
Conway, D.	7/6-8/98	Seattle, WA	To attend AMSR Meeting
Conway, P.	4/15-16/98	Greenbelt, MD	To participate in the Virtual Digital Earth Workshop at NASA GSFC, MD (PM ESSIP)
Cox, G.	2/3-5/98	LRC, VA	To attend a NASA Office of Earth Science Outreach Working Group meeting.
Cruise, J.	2/25-28/98	SSFC, MS & Baton Rouge, LA	Attend Gulf Coast Regional Workshop
Cutten, D.	7/27-8/8/98:.	DFRC - Edwards, CA	To participate in CAMEX-3 checkout DC-8 flights at DFRC
Cutten, D.	8/31/98-9/9/98	Patrick AFB, FL	To participate in NASA CAMEX-3 Expt. (MACAWS
Driscoll, K.	11/12-15/97	College Park, MD	To attend a Workshop on "Observing the Highest Energy Particles from Space"
Amzajerdian , F.	7/7-9/98	Annapolis, MD	Attend and present a paper at the International Laser Radar Conference (ILRC'98)
Graves, S.	10/7-9/97	Washington, D.C.	To attend EOSDIS Review Group.
Graves, S.	2/3-5/98	Washington, D.C.	To attend/participate in the EOSDIS External Review Group.

NAME	DATES	LOCATION	REASON
Graves, S.	6/9-11/98	Greenbelt, MD	To attend/participate in the EOSDIS Technology Transfer Workshop.
Hardin, D.	7/25-30/98	Greenbelt, MD	To participate in the DAAC Manager's Meeting
Hardin, D.	10/27-30/97	Greenbelt, MD	To participate in the CAMEX3 Meeting at GSFC, MD.
Harrison, S.	11/17-20/97	Pasadena, CA	To attend NASA User Services Working Group Meeting.
Larsen, S.	1/10-15/98	Phoenix, AZ	To attend AMS Annual Meeting
Larsen, S.	8/4-5/98	Tifton, GA	To support NASA research
Lerner, J.	1/10-16/98	Phoenix, AZ	Attend Annual AMS Conference
Lerner, J.	5/22-30/98	Paris, France	To attend the 9th Conference on Satellite Meteorology & Oceanography
Lobl, E.	10/14-17/97	Los Angeles, CA	To attend AMSR Data Format Meeting with NASDA
Lobl, E.	10/24-11/1/97	Tokyo, Japan	To attend ADEOS II 2nd Workshop, Joint AMSR Science Team Meeting
Lobl, E.	3/30/98-4/2/98	GSFC, MD	To attend AMSR-E Science Team Meeting PM-1 Validation Workshop.
Lobl, E.	7/3/98-7/8/98	Seattle, WA	To attend US AMSR Science Team Meeting
Mach, D.	8/23-9/16/98	KSC, FL	To participate in field program
McNider, R.T.	5/12-13/98	Washington, D.C.	To meet with U.S. Global Change Managers regarding Southeast Regional Assessment.
McNider, R.T.	5/26-28/98	Morgantown, WV	Attend Appalachian Regional Assessment Workshop
Podgorny, S.	7/27-8/5/98	Edwards AFB, CA	To attend ER-2 Aircraft Integration
Podgorny, S.	8/10-22/98	Orlando, FL	To attend Field Experiment for CAMEX3 Project
Ritschard, R.	10/24/98	Washington, D.C.	To present draft proposal on Southeast Regional Assessment toNASA HQ and other federal agencies.
Ritschard, R.	11/11-14/97	Washington, D.C.	To attend the National Forum on impacts on Climate Variability And Change
Ritschard, R.	11/4/97	Atlanta, GA	Attend EOS to make a presentation at the SE Regional Assess. Workshop.
Ritschard, R.	11/21/97	Washington, D.C.	To meet w/Alex Tuychov (NASA HQ) and discuss two proposals: SE Regional Assessment and an unsolicited proposal on agricultural crop assessments.
Ritschard, R.	12/1-2/97	Beltsville, MD	To attend NASA/USDA Working Session of USDA on Agriculture and Remote Sensing.
Ritschard, R.	12/8-9/97	Baton Rouge, LA	To attend NASA/USDA Working Session of USDA on Agriculture and Remote Sensing.
Ritschard, R.	6/25-26/98	Washington, D.C.	To meet with NASA program managers (Maynard) and with USGCRP/NACO (Mike McCracken & Paul Dressler)
Ritschard, R.	7/21-23/98	Miami, FL	To attend USGCRP Workshop on Climate Change and Extreme Events
Ritschard, R.	7/26-8/3/98	Monterey, CA	To attend Summer Workshop - U.S. National Assessment.
Smith, M.	2/10-13/98	Greenbelt, MD	To attend/participate in the Earth On-Line Workshop.
Stewart, M.	7/27-31/98	Edwards AFB, CA	To attend ER-2 Aircraft Integration
Wohlman, R.	8/11-29/98	Cape Canaveral, FL	Support work on CAMEX-3

YEAR 2 – STAFF TRAVEL ACTIVITIES

NAME	DATES	LOCATION	REASON
Bowdle, D.	11/16-20/98	New York, NY	To attend first meeting of the NASA Science Team on Aerosol Radiative Forcing and present a paper.
Bowdle, D.	1/18-22/99	Key West, FL	To present a paper at the NOAA Working Group Meeting on Space-Based Lidar Winds
Bowdle, D.	6/27/99-7/9/99	Timberline, OR	Present papers at the Coherent Laser Radar Conference (6/28-7/2/99) and the NOAA/NASA Working Group on Satellite Doppler Winds (7/6-9/99).
Buechler, D.	6/6-11/99	Guntersville, AL	To attend ICAE99 Conference.
Chambers, D.	10/5-9/99	Baltimore, MD	To attend and present at the Optical Society of America's Annual Meeting.
Chambers, D.	1/26-28/99	Greenbelt, MD	To present a paper to the Earth Science and Technology Strategy Team.
Chambers, D.	6/26-7/3/99	Mt. Hood, OR	Present a paper to the Tenth Biennial Coherent Laser Radar Technology and Applications Conference.
Chambers, D.	August 1999	Jena, Germany	To attend and present a paper at the European Optical Society's Topical Meeting on Diffractive Optics.
Chambers, D.	September '99	Santa Clara, CA	To attend a present at the Optical Society of America's Annual Meeting.
Chang, F.	1/9-15/99	Dallas, TX	To participate in the 79th AMS Annual Meeting; to present a paper at the 14th conference on Hydrology and to present a paper at the 23rd Conference on Hurricane and Tropical Meteorology.
Christopher, S.	11/17-20/98	New York, NY	To attend First Aerosal Science Team Meeting.
Christy, J.	10/12-14/98	Washington, D.C.	To present a paper at the A&WMA Meeting.
Christy, J.	10/20-22/98	University of Maryland	To participate in GOSSP Committee Meeting.
Christy, J.	11/3-5/99	Irvine, CA	To participate in NRC/NAS Committee on Earth Studies Meeting.
Christy, J.	11/28-12/3/99	Paris, France	To attend lead author meeting of IPCC.
Christy, J.	1/10-16/99	College Station, TX	To present a paper at the annual meeting of AMS and participate as a contributor in IPCC meeting in College Station, TX.
Christy, J.	3/7-10/99	Ashville, NC	To attend NCDC Satellite Comparison Review.
Christy, J.	4/20-22/99	Washington, D.C.	To attend WMO Meeting on Upper Air Temperatures from Satellites.
Christy, J.	6/7-9/99	Washington, D.C.	To attend NRC Committee on Earth Studies Meeting.
Conway, D.	11/6-13/98	Tokyo, Japan	To attend ADEOS II Workshop and Joint AMSR Science Team Meeting.
Conway, D.	2/21-28/99	Honolulu, HI	To attend Joint Japanese/AMSR MOM and Data Format Meetings
Conway, D.	9/13-17/99	Washington D.C.	To attend HDF-EOS Workshop.

NAME	DATES	LOCATION	REASON
Conway, R.	7/11-21/99	Lancaster, CA	To attend AMPR Flight Test prior to travel to Kwajalein Marshall Island
Conway, R.	8/8/99-9/4/99	Kwajalein Marshall Island	To attend Kwajex Experiment.
Driscoll, K.	12/2-10/98	San Francisco, CA	To attend AGU Workshop and Conference.
Driscoll, K.	6/5-11/99	Guntersville, AL	To attend ICAE99 Conference.
Driscoll, K.	8/15-23/99	Rio De Janerio, Brazil	To attend and present paper at the Sixth International Conference of Brazilian Geophysical Society.
Iwai, Hisaki	1/9-15/99	Dallas, TX	To attend the AMS Conference and present a paper he and Gary Jedlovec have co-authored which covers a portion of his research.
Kerr, K.	12/2-7/98	San Francisco, CA	To attend ICAE Organization Meeting.
Kerr, K.	6/5-11/99	Guntersville, AL	To attend ICAE99 Conference.
Li, Ye	February 1999	Tucson, AZ	To attend training on the Advanced Systems Analysis Program.
Lobl, E.	11/6-13/98	Tokyo, Japan	To attend ADEOS II Workshop and Joint AMSR Science Team Meeting.
Lobl, E.	10/17-21/98	Durham, NH	To attend EOS IWG Meeting.
Lobl, E.	3/14-4/5/99	Florence, Italy	To attend AMSR Validation Meeting and attend the MICRORAD'99 Conference.
Lobl, E.	7/6-8/99	Oklahoma City, OK	To attend joint AMSR Science Team Meeting and Validation.
Lobl, E.	9/6-8/99	Greenbelt, MD	To attend AMSR-E Round System Interface Meeting
Lobl, E.	9/22-27/99	Los Angeles, CA	To attend CEOS Working Group on Calibration and Validation Microwave Sub-Group Meeting
Mach, D.	1/24-2/9/99	Brazilia, Brazil	To participate in the Tropical Rainfall Measuring Mission of the Large Scale Biosphere Atmosphere Experiment in the Amazon.
Mach, D.	6/6-11/99	Guntersville, AL	To attend ICAE99 Conference.
McNider, R.	3/29-31/99	Boulder, CO	To attend U.S. Weather Research Program Meeting and meet with EPA.
Perkey, D.	10/31-11/8/98	Albuquerque, NM	To attend and present paper at the AMS 23rd Conference on Agricultural and Forest Meteorology.
Podgorny, S.	8/26/99-9/18/99	Kwajalein Island	To participate in NASA Kwajaex Campaign Support.
Ritschard, R.	2/17-18/99	Washington, D.C.	To attend Program Meeting with N. Maynard & L. Whittsett (NASA/ESE) Proposal Meeting with R. Pulwark (NOAA/OSP).
Ritschard, R.	2/28-3/4/99	Baltimore, MD	Member of NASA Proposal Review Committee; Reviewing Proposals for NRA-98-OES-09 (Agriculture and Remote Sensing).
Ritschard, R.	3/15-16/99	Tuscaloosa, AL	To attend annual NIGEC Conference. Member of NIGEC Advisory Board.
Ritschard, R.	3/16-17/99	Atlanta, GA	To attend a one-day meeting of the SE Regional Assessment Team.

NAME	DATES	LOCATION	REASON
Ritschard, R.	4/11-14/99	Atlanta, GA	To attend National Assessment 1999 Workshop.
Ritschard, R.	5/10-12/99	Atlanta, GA	To attend AWRA Special Session on Co. of Climate Change in Water Resources.
Ritschard, R.	8/14-22/99	Sacramento, CA	To attend International Ecosystem Health Congress Conference on Managing Ecosystem Health and presenting a paper.
Stewart, M.	3/25-26/99	Grand Forks, ND	To inspect North Dakota School of Mines Citation Aircraft for installation of electric field mills.
Stewart, M.	6/5-11/99	Guntersville, AL	To attend ICAE99 Conference.
Stewart, M.	6/21-24/99	Grand Forks, ND	To assist in the installation of electric field mills at the North Dakota School of Mines Citation Aircraft.

YEAR 3 - STAFF TRAVEL ACTIVITIES

NAME	DATES	LOCATION	REASON
Lobl, E.	9/6-8/99	Greenbelt, MD	To attend 8th AMSR-E Ground System/PM-1 Interface Meeting
Lobl, E.	9/22-27/99	Los Angeles, CA	To attend CEOS Working Group on Calib. & Validation Microwave Subgroup Meeting
Conway, P.	10/12-14/99	Dryden, CA	To attend UAV Demonstration.
Lobl, E.	10/14-17/99	Greenbelt, MD	To attend AQUA Working Group Meeting; Presented Status of AMSR-E.
Buechler, D.	12/1-3/99	Asheville, NC	Attend NEXRAD Workshop at the National Climatic Data center
Lobl, E.	12/3-11/99	Kyoto, Japan	Attend ADEOS II Workshop; Lead Joint AMSR Science Team Validation Meeting.
Fong Chiau Chang	1/8-14/00	Long Beach, CA	Attend AMS Conference in Long Beach, CA
Stewart, M.	1/24-27/00	KSFC, FL	To attend AFFM/LLD Meeting at Kennedy Space Flight Center.
Ritschard, R.	2/24-25/00	Baton Rouge, LA	To attend a meeting of the Southern Gulf National Disaster Virtual Consortium at LSU
Lobl, E.	3/13-14/00	GSFC, MD	To attend ATBD Review and Science Team Meeting
Conway, D.	3/13-14/00	Washington, D.C.	To attend AMSR Meeting
Ritschard, R.	3/15/00	Washington, D.C.	To attend a meeting of the Committee on Global Environmental Data (CGED) and make a presentation on the NECIS Case
Ritschard, R.	3/16-17/00	LaFayette, LA	To attend a meeting at the University of Louisiana of the authors preparing report on ecological impacts on climate change on Gulf Coast sponsored by the Ecological Society of America & Union of Concerned Scientists
Chang, F.	5/13-18/00	Victoria, BC	To attend the Boreas Final Fling
Stewart, M.	5/24/00-6/19/00	Orlando/Coco Beach, FL	Participate in Field Mill Integration for ABFM-2000 and ABFM Field Program
Mach, D.	6/11/00-7/1/00	KSFC, FL	To participate in the NASA ABFM Program.
Podgorny, S.	6/13-30/00	Patrick AFB, FL	Engineering support for KSC ABFM Field Program
Lobl, E.	7/25/00-7/30/00	Honolulu, HI & Los Angeles, CA	To Attend Joint (US/Japan) AMSR Science Team Meeting; Joint Validation Planning in Los Angeles to visit TRW to see the integrated instrument.

*Please note that this is a representative list of travel activities that occurred during Year 3 and may not include all travel that occurred during Year 3 of NCC8-141.

Appendix B:

Publications and Presentations
Years One through Three

Year 1 Communications

Refereed Publications – Year 1

Submitted

Han, Q.Y., W.B. Rossow, J. Chou and R.M. Welch, 1998: On definition of cloud particle size used in satellite retrieval. Submitted, *J. Atmos. Sci.*

Newchurch, M.J., E.S. Yang, J. Staehelin and A.K. Weiss, 1998: A multivariate autoregressive combined harmonics approach to time series date: Analysis of dobson Umkehr and total ozone trends at Arosa 1979-1996. Submitted, *J. Geophys. Res.*

Norris, W. B., S.F. Mueller and J.E. Langstaff, 1998: Estimates of sulfate deposition in the eastern United States: 1975, 1990, and 2010. Submitted, *J. Air and Waste Mgmt. Assoc.*

Accepted – Year 1

Berendes, T.A., K.S. Kuo, R.M. Welch, B.A. Baum, A. Pretre, A.M. Logar, E. M. Corwin, and R.C. Weger, 1998: A comparison of paired-histogram, maximum likelihood and neural network approaches for daylight global cloud classification using AVHRR imagery. Accepted, *J. Geophys. Res.-Atmos.*

Christy, J. R., R. W. Spencer, and E. Lobl, 1998: Analysis of the merging procedure for the MSU daily temperature time series. Accepted, *J. Climate, 11.*

Christy, J. R., R. W. Spencer, and E. Lobl, 1997: Assessment of the merging procedure for the MSU daily temperature time series. Accepted, *J. Climate.*

Cutten, D.R., J.D. Spinhirne, R.T. Menzies, D.A. Bowdle, V. Srvastava, R.F. Pueschel, A.D. Clarke, and J. Rothermel, 1998: Intercomparison of pulsed lidar data with flight level CW lidar data and modeled backscatter from measured aerosol microphysics near Japan and Hawaii. Accepted, *J. Geophys. Res.-Atmos.*

Gillani, N.V., M. Luria, J.F. Meagher, R. Valente, R.E.Imhof, R.L. Tanner, 1998: Relative production of ozone and nitrates in urban and rural power plant plumes: I. Composite results based on data from ten measurement days. Accepted, *J. Geophys. Res.*

Gillani, N.V., M. Luria, J.F. Meagher, R. Valente, R.E.Imhof, R.L. Tanner, 1998: The loss rate of Noy from a power plant plume based on aircraft measurements. Accepted, *J. Geophys. Res.*

Han, Q.Y., W.B. Rossow, J. Chou and R.M. Welch, 1998: Global variation of droplet column concentration of low-level clouds. Accepted, *J. Geophys. Letts.*

Han, Q.Y., W.B. Rossow, J. Chou and R.M. Welch, 1998: Global survey of the relationship of cloud albedo and liquid water path with droplet size using ISCCP. Accepted, *J. Climate.*

Hubler, G., R. Alvarez, P. Daum, R. Dennis, N.V. Gillani, L. Kleinman, W. Luke, J. Meagher, D. Rider, M. Trainer, and R. Valente, 1998: An overview of the airborne activities during the SOS 1995 Nashville/Middle Tennessee ozone study. Accepted, *J. Geophys. Res.*

Knupp, K., J. Stalker, and E. W. McCaul, Jr., 1997: An observational and numerical study of a mini-supercell storm. Accepted, *Atmos. Res.*, **34**.

Rinsland, C.P., M.R. Gunson, P. Wang, R.F. Arduini, B.A. Baum, P. Minnis, A. Goldman, M.C. Abrams, R. Zander, E. Mahiew, R. J. Salawitch, H.A. Michelsen, F.W. Irion , and M.J. Newchurch, 1998: ATMOS/ATLAS 3 infrared profile measurements of clouds in the tropical and subtropical upper troposphere. Accepted, *J. Quant. Spec. Rad. Trans.*

Rinsland, C.P., M.R. Gunson, P. Wang, R.F. Arduini, B.A. Baum, P. Minnis, A. Goldman, M.C. Abrams, R. Zander, E. Mahiew, R. J. Salawitch, H.A. Michelsen, F.W. Irion , and M.J. Newchurch, 1998: ATMOS/ATLAS 3 infrared profile measurements of trace gases in the November 1994 tropical and subtropical upper troposphere. Accepted, *J. Quant. Spec. Rad. Trans.*

Rothermel, J., D. R. Cutten, R. M. Hardesty, R. T. Menzies, J. N. Howell, S. C. Johnson, D. M. Tratt, L. D. Olivier, and R. M. Banta, 1997: The Multi-center Airborne Coherent Atmospheric Wind Sensor, MACAWS. Accepted, *Bull. Amer. Meteor. Soc.*

Rothermel, J., L. D. Olivier, R. M. Banta, R. M. Hardesty, J. N. Howell, D. R. Cutten, S. C. Johnson, R. T. Menzies, and D M. Tratt, 1997. Accepted, *Optics Express.*

Valente, R.J., R.E. Imhoff, R.L. Tanner, J.F. Meagher, P.H. Daum, R.M. Hardesty, R. McNider, N.V. Gillani, 1998: Ozone production during an air stagnation episode over Nashville, TN. Accepted, *J. Geophys. Res.*

Published – Year 1

Han, Q.Y., W.B. Rossow, J. Chou, and R.M. Welch, 1998: Global variation of droplet column concentration of low-level clouds. Published, *J. Geophys. Letts.* **25**, 1419-1422.

Han, Q.Y., W.B. Rossow, J. Chou, and R.M. Welch, 1998: Global survey of the relationship of cloud albedo and liquid water path with droplet size using ISCCP.. Published, *J. Climate,* **11**, 1516-1528.

Kim, J.H., and M. Newchurch, 1998: Biomass-burning influence on troposheric ozone over New Guinea and South America. Published, *J. Geophys. Res.,* **103,** 1455-1461.

Mishchenko, M. I., L. D. Travis, W. B. Rossow, B. Cairns, B. E. Carlson, and Q. Han, 1997: Retrieving CCN column density from single-channel measurements of reflected sunlight over the ocean: A sensitivity study. Published, *Geophys.Res. Letts.,* **24**: 2655-2658.

Ritchie, A.A., Jr., M.R. Smith, H.M. Goodman, R.L. Schudalla, D.F. Conway, F.J. LaFontaine, D. Moss, and B. Motta, 1998: Critical analyses of data differences between FNMOC and AFGWC spawned SSM/I datasets. Published, *J. Atmos. Sci.,* **55:**9, 1601-1612.

Rothermel, J., D.R. Cutten, R.M. Hardesty, R.T. Menzies, J.N. Howell, S.C. Johnson, D.M. Tratt, L.D. Oliver, and R.M. Banta, 1998: The multi-center airborne coherent atmospheric wind sensor, MACAWS. Published, *Bull. Amer. Meteor. Soc.,* **79**, 581-599.

Conference Presentations and Publications – Year 1

Amzajerdian, F. G.D. Spiers, B.R. Peters, Y. Li, T.S.. Blackwell, J.M. Geary, 1998: "Design and Operational Characteristics of the Shuttle Coherent Wind Lidar". Presentation, *International Laser Radar Conference,* Baltimore, MD 7-9 July.

Chang, F.-C., G. J. Jedlovec, R.J. Suggs, and A.R. Guillory, 1998: Intercomparisons of total precipitable water from satellite and other long-term data sets. Presentation, *9th Conf. On Satellite Meteor. and Oceanogr.* (AMS), Paris, 25-29 May.

Chang, F.-C., 1997: Drought episodes and teleconnections in the geopotential height field during the Northern Hemisphere summer. Presentation, *First Internatl. Conf. on Reanalysis*, Silver Spring, MD, 27-31 Oct.

Christy, J. R., 1997: Upper-air temperature variations: Are we warming or cooling? Invited presentation, *EOS Transactions* (AGU Fall Mtg.), San Francisco, 7-11 Dec., F137.

Cruise, J., T. Boyington, A. Limay, Y. Kim, D. Perkey, and R. McNider, 1998: Macroscale hydrologic modeling of the southern Ohio River basin. Presentation, *GCIP Mississippi River Climate Conf.*, St. Louis, MO, 6-12 June.

Jedlovec, G.J., F.-C. Chang, R. J. Suggs, A.R. Guillory, 1998: Variations in atmospheric water vapor as seen in satellite data and model reanalysis fields. Proceedings, *9th Symp. On Global Change Studies and Namias Symp.. on the Status and Prospects for Climate Prediction*, Jan., 31-35.

Lerner, J.A., G.J. Jedlovec, and R.J. Atkinson, 1998: The use of a satellite climatological data set to infer large scale three-dimensional flow characteristics. Proceedings, *9th Conf. On Satellite Meteor. and Oceanogr.* (AMS), Paris, 25-29 May, 30-33.

McNider, R.T., W.B. Norris, A. Song, S.F. Mueller, and R. Bornstein, 1998: The role of convergence zones of producing extreme concentration events. Presentation, *10th Joint Conf. on the Applications of Air Pollution Meteor. with the Air and Waste Mgmt. Assoc.*, (AMS), Phoenix, AZ, 11-16 Jan.

Newchurch, M.J., et al., 1998: Trends in upper-stratospheric ozone. Invited presentation, *AGU Spring Mtg.*, Boston, 27 May.

Norris, W.B., S.F. Mueller, and J.E. Langstaff, 1998: Estimated changes in sulfur deposition in the mid-eastern United States resulting from compliance with Title IV of the 1990 clean Air Act. Presentation , *10th Joint Conf. on the Applications of Air Pollution Meteor. with the Air and Waste Mgmt. Assoc.*, (AMS), Phoenix, AZ, 11-16 Jan.

Workshops, Seminars and Other Communications – Year 1

Beaumont, B., M. Smith and G. Bacon, 1998: Earth On-Line Data Server Prototype, 20 Mar.

Beaumont, B., and M. Smith, 1998: Dataset Independent Subsetter for HDF-EOS Data, Rel. 1.1, 9 Feb.

Bowdle, D.A. and R.T. Menzies, 1998: Aerosol backscatter at 2um: Modeling and validation for SPARCLE and follow-on missions. Presentation, Space Readiness Coherent Lidar Experiment (SPARCLE) Session, *NOAA Working Group Mtg. On Space-Based Lidar Winds,* Key West, FL, 20-22 Jan.

Callen, M., 1998: Raw Metadata Ingest: LIS, OTD, RADRAIN, V. 1.0, 25 June.

Christy, J.R., 1998: Microwave Satellite Data. Faculty Lecture, UCAR/COMET, Boulder, CO, 4 June.

Christy, J.R., 1998: "Global Temperatures from Satellites and the Global Warming Issue." Presentation, Tennessee Valley Chapter, AMS, Huntsville, AL, 23 June.

Christy, J.R., 1998: "Global Temperatures from Satellites and the Global Warming Issue." Presentation, U.S. Congressional Staffers, Washington, D.C.. 19 June.

Christy, J.R., 1998: "Global Temperatures from Satellites and the Global Warming Issue." Presentation, Norwegian Academy of Science and Technology, Oslo, Norway, 11-12 June.

Christy, J.R., 1998: "Global Temperatures from Satellites and the Global Warming Issue." Presentation, North Alabama Science Center, Huntsville, AL, 8 May.

Christy, J.R., 1998: "Global Temperatures from Satellites and the Global Warming Issue." Presentation, University of Rochester, Rochester, NY, 15 Apr.

Christy, J.R., 1998: "Global Temperatures from Satellites and the Global Warming Issue." Presentation, Alabama State Science Fair Banquet, Huntsville, AL, 10 Apr.

Christy, J.R., 1998: "Global Temperatures from Satellites and the Global Warming Issue." Presentation, Max Planck Institute Fur Meteorologie, Hamburg, Germany, 1 Apr.

Christy, J. R., 1997: Briefing on global warming, Business Council of Alabama and Alabama's U. S. House of Representatives and U. S. Senate staff members, Montgomery, AL, 3 Dec.

Christy, J. R., 1997: Briefing on global warming to Kyoto-bound U. S. Senate and House of Representatives staff members, Washington, DC, 18 Nov.

Christy, J. R., 1997: Presentation on global warming to elected officials and interested citizens, Tucson, AZ, 11 Nov.

Christy, J. R., 1997: Presentation on global warming to Canadian industrial and political leaders, Fraser Institute, Vancouver, BC, 29 Oct.

Christy, J. R., 1997: Invited Member, Expert Panel for NIGEC to discuss Administration's live presentation on global warming, Tuscaloosa, AL, 6 Oct.

Conover, H., and S. Graves, 1998: Update on Date Storage Paradigms for Custom Order Processing, EOSDIS Technology Transfer Workshop, GSFC, Greenbelt, MD, 9-11 June.

Conover, H., B. Beaumont and M. Smith, 1998: Requirements Definition and Design Review. Earth On-line Workshop, GSFC, Greenbelt, MD, 10-13 Feb.

Conover, H., 1997: Overview of EOSDIS and the GHRC. *NASA Sci. and Tech. Adv. Council Symp, "A U. S.-Russia Space Science Interchange,"* Huntsville, AL, 10 Nov.

Criswell, E., 1998: GHRC Statistics Generation Software, V. 1, 20 Mar.

Criswell, E., and M. Smith, 1998: Web-based SSM/I Subset Software, v. 1, 23 Jan

Criswell, E., 1997: Digital Linear Tape Software, V. 1.0. Design and Implementation, 31 Oct.

Drewry, M., 1998: GDS Metadata Ingest, V.2.0, 28 May.

Drewry, M., 1998: GDS Metadata Ingest, V.2.0, 5 May.

Drewry, M., and M. Callen, 1998: LDAR Metadata Ingest, V. 1.0, 29 May.

Drewry, M., R. Newquist, and S. Redman, 1997: Lightning and Atmospheric Electricity Research at the GHCC Web Page. Design and implementation, Nov.

Graves, S., H. Conover, B. Beaumont, and M. Smith, 1998: Subsetting Splinter Mgt., EOSDIS Technology Transfer Workshop, GSFC, Greenbelt, MD, 10 June.

Graves, S., 1998: Chair, Earth Observing System Data and Information System (EOSDIS) External Review Group, Washington, D.C.., 3-5 Feb.

Graves, S., 1997: Chair, *NASA Headquarters EOSDIS Rev. Grp.*, Washington, 7-9 Oct.

Han, Q.Y., W.B. Rossow, J. Chou, and R.M. Welch, 1998: Two problems in satellite retrieval of ice particle sizes. Invited presentation, NASA/Goddard Institute for Space Studies Seminar, New York, 28 June.

Hardin, D., 1998: Web-based Dynamic Browse Calendar, V. 1.0, 14 Apr.

Harrison, S., S. Hardin, H. Conover, and S. Redman, 1997: Convection and Moisture Experiment (CAMEX) Web Page. Release, Dec.

Harrison, S., 1997: A dataset independent subsetting prototype. *NASA User Svcs. Wkg. Grp. Mtg.*, Pasadena, CA, 19 Nov.

Lobl, E., 1997: Statue of AMSR-E Science and Software. *NASDA 2nd AMSR Workshop*, Tokyo, 28-30 Oct.

Newchurch, M.J., et al., 1998: Stratospheric ozone trends: Summary of the IOC/SPARC ozone trends assessment. Invited presentation, NCAR, Boulder, CO, Apr.

Newchurch, M.J., 1998: The ozone deficit. Invited presentation, NCAR, Boulder, CO, Apr.

Newchurch, M.J., 1998: Report to the TOMS Science Team, GSFC, Greenbelt, MD, 20-22 April.

Newchurch, M. J. and E. S. Yang, 1997: Upper-stratospheric ozone trend. Presentation, SPARC/IOC Rev. Mtg. on Trends in the Vertical Distribution of Ozone, Cosener's House, Abingdon, UK, 14-16 Oct.

Newchurch, M. J. and E. S. Yang, 1997: Stratospheric ozone trends measured by Dobson/Umkehr, SAGE and SBUV. Presentation, POAM Science Team Mtg., Cool Font, WV, 8-10 Oct.

Regner, K., S. Harrison, and D. Hardin, 1998: Off-Site Contingency Tape Archive Implementation Plan and Procedures, V. 1.0, 22 May.

Smith, M., and E. Criswell, 1998: NLCN Browse Generation Software and Procedures, Rel. 1.0, 14 Apr.

Smith, M., and E. Criswell, 1998: LIS Browse Generation Software and Procedures, 9 June.

Smith, M., and E. Criswell, 1998: LIS WWW Calendar Page, V. 2.0, 9 June.

Smith, M., E. Criswell, and S. Jones, 1998: LDAR Browse Generation Software and Procedures, 27 Apr.

Smith, M., 1997: IDL Browse Product Generation Software for LIS, V. 1.0. Rev., 22 Dec.

Vaughan, W., 1997: NASA Technical Standards Awareness Initiative. Presentation, *NASA Engineering Standards Steering Committee Workshop*, NASA Langley Research Ctr., Langley, VA, 19-20 Nov.

Year 2 Communications

Refereed Publications – Year 2

Submitted – Year 2

Christopher, S. A., X. Li, R. M. Welch, P. V. Hobbs, J. S. Reid, T. F. Eck, and B. Holben, 1998: Estimation of downward shortwave irradiances in biomass burning regions during SCAR-B, submitted to JGR-Atmospheres

Goodman, S.J., D.E. Buechler, K. Knupp, K. Driscoll, and E.W. McCaul, Jr., 1999: The 1997-98 El Nino event and related wintertime lightning variations in the Southeastern United States. Submitted to *Geophys. Res. Lett.*

Han, Q. Y., W. B. Rossow, J. Chou, K. Kuo, and R. M. Welch, 1999e: Near-global survey of cloud susceptibilities using ISCCP data. [submitted to Geophys. Res. Letts.,]

Ritschard, R., J. Cruise, and U. Hatch 1999. Spatial and temporal analysis of agricultural water requirements in the Gulf Coast of the United States. Journal of American Water Resources Association (in review).

Accepted – Year 2

Boccippio, D.J., K. Driscoll, W. Koshak, R. Blakeslee, W. Boeck, D. Mach, D. Buechler, H.J. Christian, ans S.J. Goodman, 1999: The Optical Transient Detector (OTD): Instrument characteristics and cross-sensor validation. *J. Atmos. Oc. Tech* (In press).

Han, Q. Y., W. B. Rossow, J. Chou, K. Kuo, and R. M. Welch, 1999a: The Effects of aspect ratio and surface roughness on satellite retrievals of ice-cloud properties. *J. Quantitative Spectroscopy and Radiative Transfer* [in press]

Ritschard, R. Current. Environmental Biology (textbook being prepared for Pergamon Press).

Williams, E.R., B. Boldi, A. Matlin, M. Weber, S. Hodanish, D. Sharp, S. Goodman, R. Raghavan, and D. Buechler, 1999: The behavior of total lightning in severe Florida thunderstorms. *Atmos. Research* (In press)

Published – Year 2

Berendes, T. A., K.-S. Kuo, R. M. Welch, B. A. Baum, A. Pretre, A. M. Logar, E. D. Corwin, and R. C. Weger, 1998: A comparison of paired-histogram, maximum likelihood, and neural network approaches for daylight global cloud classification using AVHRR imagery. *J. Geophys. Res.*, 104(D6), 6199-.

Chambers, D. M., and G. P. Noordin, 1999: Stratified volume diffractive optical elements as high efficiency-gratings. *Journal of the Optical Society of America 116, 1184-1193.*

Christopher, S.A., J. Chou, R. M. Welch, D. V. Kliche and V. S. Connors, 1998: Satellite investigations of fire, smoke and carbon monoxide during April 1994 MAPS mission: Case studies over tropical Asia, *J. Geophys. Res 103*, 19327-19336.

Christopher, S. A., M. Wang, T. A. Berendes, R. M. Welch, and S.K. Yang, 1998: The 1985 Biomass Burning Season in South America: Satellite Remote Sensing of Fires, Smoke and Regional Radiative Energy Budgets. J. *Appl. Meteor.*, 37, 661-678.

Christopher, S.A., D. Kliche, V.S. Connors, and R.M. Welch, 1998: Satellite investigations of fires, smoke and Carbon Monoxide during the April 1994 MAPS missions, Part I : Case Studies, *J. Geophys. Res.*, 103, 19327-19336.

Christy, J.R., R.W. Spencer, and E. Lobl, 1998: Analysis of the merging procedure for the MSU daily temperature time series. *J. Climate*, 11, 2016-2041.

Christy, J.R., "Measuring Global Temperature", Do We Understand Global Climate Change?, Norwegian Academy of Technological Sciences, Trondheim June 1998. ISBN 82-7719-030-1, 201 pp.

Gill, Paul and William W. Vaughan: "The Changing Climate for Standards", *ASTM Standardization News*, May 1999

Han, Q., W. B. Rossow, J. Chou, and R. M. Welch, 1998: Global Survey of the Relationship between Cloud Droplet Size and Albedo using ISCCP *J.Climate, 11*, 1516-1528.

Greenwald, T. J., S.A., Christopher, J. Chou, and L. Liljegren, 1999: Intercomparison of Cloud Liquid Water Path Derived From the GOES-9 Imager and Ground Based Microwave Radiometers, *J. Geophys. Res.*, 104, 9251-9260

Greenwald, T. J., and S. A. Christopher, 1999: Daytime variation of Marine Stratocumulus Properties as observed from Geostationary Satellite, *Geophysical Research Lett.*, 26,1723-1726.

Kandel and the SCARAB science team : The SCARAB earth Radiation Budget Data Set, *Bull. Amer. Metorolo. Soc.*, 79, 765-783.

Kaufman, Y. J., P. V. Hobbs, V. W. J. H. Kirchoff, P. Artaxo, L. A. Remer, B. N. Holben, M. D. King, E. M. Prins, D. E. Ward, K. M. Longo, L. F. Mattos, C. A. Nobre, J. D. Spinhirne, Q. Ji, A. M. Thompson, J. F. Gleason, and S.A. Christopher, S.C. Tsay, 1998: Smoke, Clouds, and Radiation-Brazil (SCAR-B_ experiment. *J. Geophys. Res.*, 103, D24, 31783-31808.

Logar, A. M., D. E. Lloyd, E. M. Corwin, M. L. Penaloza, R. E. Feind, T. A. Berendes, K.-S. Kuo, and R. M. Welch, 1998: The ASTER polar cloud mask. *Trans. Geosci. Remote Sensing*, 36, 1302-1312.

Nair, U. S., R. C. Weger, K. S. Kuo and R. M. Welch, 1998: Clustering, randomness and regularity in cloud fields. 5: The nature of regular cumulus cloud fields. *J. Geophys. Res.*, 103, 11363-11380.

Newchurch, M. J., D. M. Cunnold, and J. Cao, Intercomparison of SAGE with Umkehr[64] and Umkehr[92] ozone profiles and time series: 1979-1991, *J. Geophys. Res.*, 103, 31,277-31,292, 1998.

Rinsland, C. P., R. J. Salawitch, M. R. Gunson, S. Solomon, R. Zander, E., Mahieu, A. Goldman, M. J. Newchurch, F. W. Irion, and A. Y. Chang, Polar stratospheric descent of NOy and CO and Arctic denitrification during winter 1992-93, *J. Geophys. Res.*, 104, 1847-1861, 1999.

Ritschard, R. 1999. Southeastern regional climate assessment: What did we learn about water? Proceedings of American Water Resources Association 337-340..

Thome, K., K. Arai, S. Hook, H. Kieffer, H. Lang, T. Matsunaga, A. Ono, F. Palluconi, H. Sakuma, P. Slater, T. Takashima, H. Tonooka, S. Tsuchida, R. M. Welch and E. Zalewski, 1998 ASTER preflight and inflight calibration and the validation of Level 2 products. *IEEE Trans Geoscience Remote Sensing 36*, 1161-1172.

Vaughan, W. W.: "The Start of the New Solar Cycle 23", *NASA Space Environment and Effects Bulletin*, NASA Marshall Space Flight Center, Huntsville, AL' Winter 1998 Issue.

Vaughan, W. W., S. D. Pearson, and J. Ehernberger: "Atmospheric Environment Annual Report of Significant Accomplishments", *Aerospace America*, December 1998

Weiss, J.M., S.A. Christopher, and R.M. Welch, 1998: Automatedcontrail detection and segmentation. *IEEE Transactions on Geoscience and Engineering.*, 36, 1609-1619.

Conference Presentations and Publications – Year 2

Blakeslee , R.J., K.T. Driscoll, D.E. Buechler, D.J. Boccippio, W.L. Boeck, H.J. Christian, S.J. Goodman, J.M. Hall, W.J. Koshak, D.M. Mach, M.F. Stewart, 1999: Diurnal Lightning Distribution As Observed By The Optical Transient Detector (OTD). Preprints, 11th International Conf. on Atmospheric Electricity. Guntersville, AL, June 7-11, 1999, 742-745.

Bowdle, D. A., Hannon, S.M., and R.K. Bogue, 1999: Comparison of predicted and measured 2 μm aerosol backscatter from the 1998 ACLAIM flight tests. Presented at Tenth Biennial Conference on Coherent Laser Radar Technology and Applications, Timberline Lodge, Mount Hood, Oregon, June 28-July 2, 1999. Optical Society of America., Washington, DC, p. 151.

Buechler, D.E., S.J. Goodman, K. Knupp, and E.W. McCaul, Jr., 1999: The 1997-98 El Nino event and related lightning variations in the Southeastern United States. Preprints, 11th International Conf. on Atmospheric Electricity. Guntersville, AL, June 7-11, 1999, 519-522.

Buechler, D.E., S.J. Goodman, H.J. Christian, K. and Driscoll, 1999: Optical Transient Detector (OTD) observations of a tornadic thunderstorm. Preprints, 11th International Conf. on Atmospheric Electricity. Guntersville, AL, June 7-11, 722-725.

Chambers, D. M., and G. P. Noordin, 1998: Design and Behavior of Stratified Diffractive Optic Gratings. Baltimore, MD, 5-9 October 1998.

Chambers, D. M., M. J. Kavaya, and G. P. Noordin, 1999: Stratified Volume Diffractive Optical Elements As Low-Mass Coherent Lidar Scanners. Mt. Hood, OR, 26 June – 3 July 1999.

Chambers, D. M. and G. P. Nordin, 1999: Fabrication of Stratified Volume Diffractive Optical Elements. European Optical Society Topical Meeting on Diffractive Optics, Jena, Germany, August 1999.

Chambers, D. M. and G. P. Nordin, 1999: Fabrication and Performance of Stratified Volume Diffractive Optical Elements, Optical Society of America's Annual Meeting, Santa Clara, CA, September 1999.

Chan, C. Y., L. Y. Chan, H. Y. Liu, Y. Qin, S. A. Christopher, 1999: Biomass Burning and Ozone Peak over the Lower Troposphere in Hong Kong. Sixth Scientific Conference of the International Global Atmospheric Chemistry Project (IGAC)", September 13-17, 1999, Bologna, Italy

Christian, H.J., R.J. Blakeslee, D.J. Boccippio, W.L. Boeck, D.E. Buechler, K.T. Driscoll, S.J. Goodman, J.M. Hall, W.J. Koshak, D.M. Mach, M.F. Stewart, 1999: Global Frequency And Distribution Of Lightning As Observed By The Optical Transient Detector (OTD). Preprints, 11th International Conf. on Atmospheric Electricity. Guntersville, AL, June 7-11, 1999, 726-729.

Christian, H.J., R.J. Blakeslee, S.J. Goodman, D.M. Mach, M.F. Stewart, , D.E. Buechler, W.J. Koshak, J.M. Hall, W.L. Boeck, K.T. Driscoll, and D.J. Boccippio, 1999: The Lightning Imaging Sensor. Preprints, 11th International Conf. on Atmospheric Electricity. Guntersville, AL, June 7-11, 1999, 746-749.

Christopher, S. A., J. Zhang, X. Li, J, Chou, 1999: Radiative Effects of Biomass Burning Aerosols, AMS Conference on Atmospheric Radiation, Wisconsin, Jun-July, 1999.

Christy, J.R., 1998: Global Atmospheric Variations Since 1979. Air and Waste Management Association & American Meteorological Society. 13-16 October, Crystal City, VA.

Christy, J.R., R. W. Spencer and W. D. Braswell, 1999: Orbital Decay And Drift Revisions For The MSU Tropospheric Temperature Datasets: Little Overall Change. America Meteorological Society, Dallas TX 12 January 1999.

Christy, J.R., 1999: Evidences (And Lack Thereof) For Climate Change. Formal Briefing to U.S. Congressman Peterson (PA). State College, PA, 22 Jan 1999.

Christy, J.R. 1999: MSU Temperature Products. National Research Council. Asheville NC, 8 March 1999

Conover, H. (UAH ITSC), J. Bedet, M. Nestler, and M. Solomon (Raytheon), 1998: "EOS Inventory Interoperability Experiments: Lessons Learned at IRE-RAS and Tel Aviv", Raytheon Science Data Center Symposium, Silver Spring, MD, 4 November.

Conover, H., S. Graves, C. Pearson, J. Rushing, and M. Smith (UAH ITSC), 1998: "Promoting Science Data through Innovative Information Systems", invited poster at American Geophysical Union meeting, San Francisco, CA, 7 December.

Goodman, S.J., D. Buechler, S. Hodanish, D. Sharp, E.R. Williams, B. Boldi, A. Matlin, and M. Weber, 1999: Total Lightning Activity Associated With Tornadic Storms. Preprints, 11th International Conf. on Atmospheric Electricity. Guntersville, AL, June 7-11, 1999, 515-518.

Greenwald, T. J., S. A. Christopher, 1999: Investigation Of Drizzling Marine Stratocumulus Using the GOES-9 Imager and C-Bad Radar, AMS Conference on Radiation, Wisconsin, June 1999

Han, Q., J. Chou, and R. M. Welch, 1999b, Uncertainties In Retrievals Of Cirrus Cloud Properties Using Satellite Data. Preprints, the 19th CERES Science Team Meeting, 26-28, Apr. 1999, Langley, VA.

Han, Q., W. B. Rossow, J. Chou, K-S Kuo, and R. M. Welch, 1999c: Calibration of Channel 3 of the AVHRR, Preprints, Infrared Spaceborne Remote Sensing VII, SPIE's International Symposium, 18-23 July 1999, Denver, CO.

Han, Q., W. B. Rossow, J. Chou, K-S Kuo, and R. M. Welch, 1999d: Observed Effects of Cloud Droplet Concentration on Albedo for Low-Level Clouds Using Satellite Data. Preprints, the 22nd General Assembly of the International Union of Geodesy and Geophysics, 18-30, July 1999, Birmingham, UK.

Han, Q., W. B. Rossow, J. Chou, K.-S. Kuo, and R. M. Welch, 1999: Calibration Of Channel 3 Of The AVHRR. Preprints, Infrared Spaceborne Remote Sensing VII, SPIE's International Symposium, Denver, CO, 18-23 July 1999.

Han, Q., W. B. Rossow, J. Chou and R. M. Welch, 1998: The Effect Of Nonspherical Shape On The Retrieval Of Ice Particle Sizes From Satellite Observations, Conference on Light Scattering by Nonspherical Particles: Theory, Measurements and Applications, NASA Goddard Inst. Space Studies, N.Y., 29 Sept - 1 Oct.

Hannon, S.M., H.R. Bagley, D.C. Soreide, D. A. Bowdle, R.K. Bogue, and L.J. Ehrenberger, 1999: Airborne turbulence detection and warning: ACLAIM flight test results. Invited paper, In Tenth Biennial Conference on Coherent Laser Radar Technology and Applications, Timberline Lodge, Mount Hood, Oregon, June 28-July 2, 1999. Optical Society of America., Washington, DC, pp 20-23.

Keiser, K., J. Rushing, H. Conover, S. Graves (UAH ITSC), 1999: "Data Mining Toolkit for Earth Science Data", Earth Observation (EO) & Geo-Spatial (GEO) Web and Internet Workshop '99, Silver Spring, MD, 9-11 February 1999.

Kuo, K.-S., and R. M. Welch, 1999: Retrievals Of Optical Thickness And Droplet Size In Broken Cloudiness: The Impact Upon Radiative Fluxes. Spring Meeting, American Geophysical Union, Boston, MA, 1-4 June 1999.

Li, X., S.A. Christopher, J. Zhang, J. Chou, and R. M. Welch, 1999: Aerosol Single Scattering Albedo Estimation from NOAA-14 Measurements: Case studies over Brazil, SPIE, Denver, July 1999

Li, X., S. A Christopher, J. Zhang, J. Chou, and R. M. Welch, 1999: Satellite Remote Sensing Of Fires, Smoke And Regional Radiative Energy Budgets, SPIE, Denver, July 1999

Li, Xiang, S. A. Christopher, J. Chou, and R. M. Welch, 1999: Impact Of Central America Fires On The Radiation Budget Over The ARM CART Site, SPIE conference, Denver, CO, 18-23 July 1999.

Li, X., S. A. Christopher, J. Chou, and R. M. Welch, 1999: Impact of Central American Fires on Radiation Budget over ARM CART Site, IAMAS Symposium/IUGG99, Birmingham, England, 18-30 July 1999.

Li, Xiang, J. Zhang, S. A. Christopher, J. Chou and R. M. Welch, 1999: Satellite Remote Sensing Of Fires, Smoke And Regional Radiative Energy Budgets Over South America and Africa, SPIE Conference, Denver, CO, 18-23 July 1999.

McCaul, E.W., Jr., Buechler, D.E., and S.J. Goodman, 1999: Cloud-to-Ground Lightning Characteristics Of A Major Tropical Cyclone Tornado Outbreak. Preprints, 11th International Conf. on Atmospheric Electricity. Guntersville, AL, June 7-11, 1999, 511-514.

Nair, U.S., R. A. Pielke, Jr., R. M. Welch, 1999: Influence Of Surface Characteristics On The Development Of Cumulus Cloud Fields Over Texas, SPIE Conference, Denver, CO, 18-23 July.

Nair, U.S., J.F. Rushing, R. P. Ramachandran, K.S. Kuo, R. M. Welch, S. J. Graves, 1999: Detection Of Cumulus Clouds In Satellite Imagery, SPIE Conference, Denver, CO, 18-23 July.

Nair, U.S. and R. M. Welch, 1999: Temporal Variability Of Cumulus Cloud Field Spatial Distributions Over Texas. IAMAS Symposium/IUGG99, Birmingham, England, 18-30 July.

Owens, J. K., K. O.Niehuss, and W. W. Vaughan: "Models for Future Estimation of Thermospheric Densities and Space Applications to Spacecraft Systems", AIAA Paper # 99-0632, 37th Aerospace Sciences Meeting, American Institute of Aeronautics and Astronautics, January 1999

Ritschard, R. 1999. Southeastern Regional Climate Assessment: What Did We Learn About Water? Specialty Conference on Potential Consequences of Climate Variability and Change to Water Resources of the United States, American Water Resources Association, Atlanta GA, May 10-12, 1999.

Ritschard, R. 1999. Application of Remote Sensing in Agriculture and Natural Resources. SRIEG-10 Conference, Huntsville, AL, May 20, 1999.

Ritschard, R. 1999. A Framework for Integrated Assessments of Climate Change: Southeastern United States. American Geophysical Union Spring Meeting, Boston, MA, May 31-June 4, 1999.

Ritschard, R. 1999. (*invited public lecture*) Integrated Assessments of Climate Variability and Change: A Southeastern U.S. Perspective. NASA/USRA Summer Lecture Series, Goddard Space Flight Center, Greenbelt, MD, June 9, 1999.

Srivastava, V., J. Rothermel, M.A. Jarzembski, A.D. Clarke, D.R. Cutten, D. A. Bowdle, J.D. Spinhirne, and R.T. Menzies, 1999: Backscatter modeling at 2.1 micron wavelength for space-based and airborne lidars using aerosol physico-chemical and lidar datasets. In Tenth Biennial Conference on Coherent Laser Radar Technology and Applications, Timberline Lodge, Mount Hood, Oregon, June 28-July 2, 1999. Optical Society of America., Washington, DC, pp 147-150.

Welch, R. M., R. O. Lawton and U. S. Nair, 1999: Land Use And Terrain Impacts On Cloud Field Development On The Caribbean Slope of Costa Rica and Nicaragua, IAMAS Symposium MI06 of IUGG99, Birmingham, England, 18-30 July.

Wielicki, B. A., B. R. Barkstrom, B. A. Baum, T. P. Charlock, R. N. Green, D. P. Kratz, R. B. Lee III, P. Minnis, G. L. Smith, T. Wong, D. F. Young, R. D. Cess, J. A. Coakley, Jr., D. A. H. Crommelynck, L. Donner, R. Kandel, M. D. King, A. J. Miller, V. Ramanathan, D. A. Randall, L.L. Stowe and R. M. Welch, 1998: Clouds and the Earth's Radiant Energy System (CERES): Algorithm Overview, IEEE

Vaughan, W. W., J. K. Owens, and K. O. Niehuss: "Sensitivity of Spacecraft Orbital Drag Predictions to Selection of Solar Activity Inputs", AIAA Paper #99-0633, 37th Aerospace Sciences Meeting, American Institute of Aeronautics and Astronautics, January 1999

Workshops, Seminars and Other Communications – Year 2

Bowdle, D. A., 1998: Characterization of elevated aerosol layers from MACAWS, ACLAIM, ATMOS, and SPARCLE. Presented at First Meeting of the Aerosol Radiative Forcing Science Team, Goddard Institute for Space Studies, New York, New York, November 18-20, 1998.

Bowdle, David A., 1999: SPARCLE SNR VALIDATION. Presented in the SPAce Readiness Coherent Lidar Experiment (SPARCLE) Session, Meeting of the NOAA Working Group on Space-Based Lidar Winds Key West, Florida, January 19-22, 1999.

Chambers, D. M., and G. P. Noordin, 1999: "Technology Studies To Enable Space Based Coherent Doppler Wind Lidar Missions Beyond SPARCLE" to Earth Science and Technology Strategy Team, Greenbelt, MD, January 26-28, 1999.

Conover, H. (UAH ITSC), 1999: CINTEX (Committee on Earth Observation Satellites (CEOS) Interoperability Extensions) Core Engineering Team Meeting, Greenbelt, MD, February 12-13.

Graves, S. and H. Conover (UAH ITSC), 1998: Federation Interoperability Group Workshop and ESIP WP-Federation Workshop, Santa Barbara, CA, 1-4 December.

Graves, Sara (UAH ITSC), 1999: New Data Information Systems and Services Meeting, Washington, DC, 19-22 January 1999.

Graves, Sara (UAH ITSC), 1999: New Data Information Systems and Services Meeting, Washington, DC, 22-24 February 1999.

Hardin, Danny (UAH ITSC), 1999: Quarterly DAAC Manager's Meeting, Greenbelt, MD, 18-20 February 1999.

Graves, Sara (UAH ITSC), 1999: Earth Systems Science Applications Advisory Committee Meeting, Washington, DC, 9-11 February 1999.

Software – Year 2

Beaumont, B. (UAH ITSC), 1998: Lightning Imaging Sensor Master Script - Monthly Processing, Part II, Version 1.0, 12 November.

Beaumont, B. and M. Smith (UAH ITSC), 1998: Hierarchical Data Format - Earth Observing System (HDF-EOS) Library Tools, Version 4.1, 30 November.

Criswell, E. and M. Smith (UAH ITSC), 1998: Web-based SSM/I Subsetter Software, Version 1.1, 15 November.

Smith, M., B. Beaumont, and Y. Jin (UAH ITSC), 1998: Overpass Time Analysis Software (for Optical Transient Detection Daily Browse), Version 1.1, 30 October.

Year 3 Communications

Refereed Publications – Year 3

Submitted – Year 3

Chang, F.C. and E.A. Smith, 2000: Hydrological and Dynamical Characteristics of Summertime Droughts Over U.S. Great Plains, *Journal of Climate.*

Han, Q., W.B. Rossow, J. Chou, and R.M. Welch, 1999: Near-global survey of column cloud susceptibility of water clouds using ISCCP data. Submitted, *Geophysic Research Letters.*

Han Q., W.B. Rossow, J. Chou, and R.M. Welch, 1999: The effects of size distribution on satellite retrievals of ice-cloud properties. Submitted, *Geophysic Research Letters.*

Johnson, D.L. and W.W. Vaughan, 1999: Lightning Strike Peak Current Probabilities As Related To Space Shuttle Operations. Submitted, *AIAA Journal of Spacecraft and Rockets.*

Knupp, K.R., J. Walters and E.W. McCaul, 1999: Doppler profiler observations of hurricane George during landfall. Submitted, *Geophysic Research Letters.*

Limaye A.S., J.F. Cruise, and M.T. Boyington, 1999: A macroscale modeling strategy for coupled hydrologic atmospheric models. Submitted, *ASCE Journal of Hydrologic Engineering.* Submitted a Revised Version following peer review.

Owens, J.K., W.W. Vaughan, K.O. Niehuss, and J. Minow, 1999: Space Weather, Earth's Neutral Upper Atmosphere (Thermosphere), and Spacecraft Orbital Lifetime/Dynamics. Submitted, *IEEE Transactions On Plasma Science.*

Srivastava, V., J. Rothermel, A. Clarke, J. Spinhirne, R. Menzies, D. Cutten, M. Jarzembski, D. Bowdle, and E. McCaul, Jr., 2000: Wavelength dependence of backscatter using aerosol microphysics and lidar datasets: Application to 2.1um wavelength for space-based and airborne lidars, *Applied Optics.*

Srivastava, V., J. Rothermel, A. Clarke, J. Spinhirne, R. Menzies, D. Cutten, M. Jarzembski, D. Bowdle, and E. McCaul, Jr., 2000: Wavelength dependence of backscatter using aerosol microphysics and lidar datasets: Application to 2 um wavelength for space-based and airborne lidars, *Applied Optics*

Wang, S., E. McCaul Jr., and K. Knupp, 2000: Large-eddy simulations of a strong wind shear-driven boundary layer, *American Meteorology Society*

Accepted – Year 3

Chang, F.C., and E.A. Smith, 1999: Hydrological and dynamical characteristics during droughts over U.S. Great Plains. Accepted, *Journal of the Atmospheric Sciences*, conditionally.

Goodman, S.J., D.E. Buechler, K. Knupp, K. Driscoll, and E.W. McCaul, Jr., 1999: The 1997-98 El Nino Event and Related Wintertime Lightning Variations in the Southeastern United States. Accepted, *Geophysical Research Letters.*

Goodman, S.J., D. Buechler, K. Driscoll, and K. Knupp, 1999: The 1997-98 El Nino event and related lightning variations in the Southeastern United States. Accepted, *Geophysical Research Letters.*

Han, Q. Y., W. B. Rossow, J. Chou, K. Kuo, and R. M. Welch, 2000: Near-global survey of cloud susceptibilities using ISCCP data. *Geophysical Research Letters*

Knupp, K., J. Walters, and E. McCaul, Jr., 2000: Profiler observations of hurricane George during landfall, *Geophysical Research Letters*

Published – Year 3

Boccippio, D.J., K. Driscoll, W.J. Koshak, R.J. Blakeslee, W. Boeck, D. Mach, D.E. Buechler, H.J. Christian, and S.J. Goodman, 2000: The Optical Transient Detector (OTD): Instrument Characteristics and Cross-Sensor Validation, *Journal Atmospherics Oceanic Technology*, 17, 441-458.

Buechler, D.E., K.T. Driscoll, S.J. Goodman, and H.J. Christian, 2000: Lightning Activity within a TornadicThunderstorm observed by the Optical Transient Detector (OTD), Geophysical Research Letters, 27, No. 15, 253-2256.

Christy, J.R., R.W. Spencer, and W.D. Braswell, 2000: MSU Tropospheric temperatures: Data set construction and radiosonde comparisons, *Journal of Atmospheric and Oceanic Technology*, 17, 1153-1170.

Cruise J.F., A.S. Limaye, and N. Al-Abed, 1999: Assessment of impacts of climate change on water quality in the southeastern United States. Published, *Journal of the American Water Resources Association,* vol. 35(6): 1539-1550.

Goodman, S.J., D.E. Buechler, K. Knupp, K. Driscoll and E.W. McCaul Jr., 2000: The 1997-98 El Nino event and related wintertime lightning variations in the Southeastern United States, *Geophysic Research Letters*, 27, 541-544

Han, Q., W.B. Rossow, J. Chou and R.M. Welch, 2000: ISCCP Data used to address a key IPCC climate issue: An approach for estimating the aerosol indirect effect globally, *GEWEX News*, Vol. 10, No. 1.

Koshak, W.J., M.F. Stewart, H.J. Christian, J.W. Bergstrom, J.M. Hall, and R.J. Solakiewicz, 2000: Laboratory Calibration of the Optical Transient Detector and the Lightning Imaging Sensor, *Journal Atmospheric Oceanic* Technology, 17, 905-915

Koshak, W.J., M.F. Stewart, H.J. Christian, J.W. Bergstrom, J.M. Hall, and R. J. Solakiewicz, 2000: Laboratory Calibration of the Optical Transient Detector and the Lightning Imaging Sensor, *Journal of Atmospheric Oceanic Technology* **17**, 905-915.

Mao, Q., S.F. Mueller and H-M. H. Juang, 2000: Quantitative precipitation forecasting for the Tennessee and Cumberland River Watersheds using NCEP regional spectral model, *Weather Forecasting*, 15, 29-45.

Vaughan, W.W., J.K. Owens, K.O. Niehuss, and M.A. Shea, 1999: The NASA Marshall Solar Activity Model For Use In Predicting Satellite Lifetime. Published, *Advances in Space Research*, vol. 23, No. 4, pp. 715-719.

Vaughan, W. W., S.T. Lai, T.P. Ratvasky, J. Roets, and H.L. Wesoky, 1999: Atmospheric Environment: 1999 Highlights. Published, *AIAA Aerospace America*, December issue.

Conference Publication and Presentations – Year 3

Chang, F-C., E.A. Smith, R.E. Hood, F.J. LaFontaine, J. Marengo, B.J. Sohn, S. Yang and S. Yuter, 2000: Direct Validation Analysis of TRMM Instantaneous Precipitation Retrievals. Presentation, *Annual Meeting of the AMS*, Long Beach, CA, January 9-14.

Goodman, S.J., D.E. Buechler, K. Driscoll, D.W. Burgess, and M.A. Magsig, 2000: Preprints, *20th Conference on Severe Local Storms*, "Tornadic Supercell on May 3, 1999 viewed from space during an overpass of the NASA TRMM observatory," Orlando, FL, September 11-15.

Graves, S., H. Conover, C. Pearson and R. Ramachandran, 2000: Migration of IMS Server to Java. Presentation, *Subsetting Technical Meeting*, Greenbelt, MD, February 3.

Han, Q., 2000: Presentation, *The NPOESS Meeting at NOAA GFDL*, "Monitoring Aerosol Indirect Effect from Space -- Satellite Observation Perspective," Princeton, NJ, September 13 –14.

Han, Q., J. Chou, and R. Welch, 2000: Presentation, *The 22nd CERES Science Meeting*, "Strategies of Monitoring Aerosol Indirect Effect from Space," Huntsville, AL, September 20-22.

Han, Q., W.B. Rossow, J. Chou and R.M. Welch, 2000: Retrieval of cloud column susceptibilities of water clouds using satellite data. Preprints, *10th Conference on Satellite Meteorology and Oceanography*, Long Beach, CA, January 9-13, 326-329.

Han, Q., J. Chou, and R.M. Welch, 1999: Effects of size distributions and effective variances on retrievals of ice crystal sizes. Preprints of the *Twentieth CERES Science meeting*, San Diego, CA, December 6-8.

Han, Q., J. Chou, and R.M. Welch, 1999: Column cloud susceptibility retrieved by ISCCP. *AGU Fall Meeting*, San Francisco, CA, December 13-17.

Kavaya, M. J. G.D. Spiers, and R.G. Frehlich, 2000: Preprint, *SPIE Second International Asia-Pacific Symposium on Remote Sensing of the Atmosphere, Environment, and Space;* "Potential Pitfalls related to space-based lidar remote sensing of the Earth with an emphasis on wind measurement," Conference 4153, Lidar Remote Sensing for Industry and Environment Monitoring, Sendai, Japan, October 9 –12.

Knupp, K.R., J. Walters, and E.W. McCaul Jr., 2000: Preprints, *24th Conference on Hurricanes and Tropical Meteorology*; Doppler profiler observations of the boundary layer within the eyewall of Hurricane George during landfall, Ft. Lauderdale, FL, May 29.

Knupp, K.R., J. Walters and E.W. McCaul, 2000: Presentation, 14th Symposium on boundary layer and turbulence; "Profiler observations of the boundary layer with hurricane George," Aspen, CO, August 7-11.

Knupp, K.R., J. Walters and E.W. McCaul Jr., 2000: Doppler profiler observations of the boundary layer within the eyewall of Hurricane George during landfall, the 24th Conference Hurricane Tropical Meteorology, *American Meteorology Society*, Ft. Lauderdale, FL.

McCaul, E., Jr., and D. Buechler, 2000: Preprints, *American Meteorology Society;* The Almena Kansas tornadic super-cell of June 3, 1999: A long-lived supercell with very little cloud-to-ground lightning, *Orlando, FL*

McCaul, E.W., Jr., and D.E. Buechler, 2000: Preprints, *20th Conference on Severe Local Storms*, "The Almena Kansas Tornadic Supercell of 3 June 1999: A long-lived supercell with very little cloud-to-ground lightning," Orlando, FL, September 11-15.

Mueller, S.F., and Q. Mao, 1999: Application of Markov Chain Model to Long-Range Temperature Prediction. Presentation submitted, *AMS 12th Conference on Applied Climatology*, Asheville, NC, May 8-11 2000.

Perkey, D.J., C.E. Hayes, and S.K. Bowen, 1999: Impact of Alabama precipitation variability on corn yields. Presented at the *American Water Resources Association 13th Annual Conference on Alabama Water Resources*, Gulf Shores, AL, September 8-10.

Perkey, D.J., 1999: Assessing the impact of the variability of precipitation on crop yields. Presentation, *G7 Global Climate Change Workshop*, Seoul, Korea, October 27.

Perkey, D.J., 1999: Hydrologic cycle research at the Global Hydrology and Climate Center. Invited paper presented at the *Fall Meeting of the Korean Meteorological Society*, Seoul, Korea, October 28-29.

Perkey, D.J., and P.J. Mulero, 2000: Presentation, *The 2000 Alabama Water Resources Conference*, "Impact of climate variability on Alabama county corn yields," Gulf Shores, AL, September 6-8.

Rothermel, J., D.R. Cutten, J.N. Howell, L.S. Darby, R.M. Hardesty, D.M. Tratt, and R.T. Menzies, 2000: Presentation, *24th Conference on Hurricanes and Tropical Meteorology;* Hurricane wind field measurements with scanning airborne Doppler lidar during CAMEX-3, Fort Lauderdale, FL, May 29 - June 2.

Walters, J., R. Decker, and K. Knupp, 2000: Presentation, 14th Symposium on boundary layer and turbulence; "Observations of stable nocturnal boundary layers over the hetereorgeneous surface of northern Alabama," Aspen, CO August 7-11.

Wang, S., E.W. McCaul Jr. and K.R. Knupp, 2000: Large-eddy simulations of the hurricane boundary layer, 24th Conference Hurricane Tropical Meteorology, *American Meteorology Society*, Ft. Lauderdale, FL.

Workshops, Seminars and Other Communications – Year 3

Conover, H., 1999: *NASA Data Mining Workshop*. Huntsville, AL, October 19-21.

Conover, H., 1999: *UAH Technologies for Digital Earth, 1st Digital Earth Prototype Group Workshop*. Goddard Space Flight Center, Greenbelt, MD, November 8.

Criswell, E., 1999: *National Lightning Detection Network (NLDN)/Brazil Lightning Detection Network (BLDN) Animator Software, Version 1.21*. October 20.

Criswell, E., 1999: *National Lightning Detection Network (NLDN)/Brazil Lightning Detection Network (BLDN) Animator Software, Version 1.22*. December 9.

Criswell, E., 1999: *NASA Data Mining Workshop*. Huntsville, AL, October 19-21.

Crosson, W., R. Inguva, C. Laymon, A. Limaye, and M. Schamschula, 1999: *Land Surface Hydrology Program Investigators Workshop*. Presented poster 'Assimilation of Remotely-Sensed Soil Moisture Estimates in a Distributed Surface Flux-Hydrology Model Using a Kalman Filter'. Columbia, MD, November 1-2.

Graves, S., 1999: *NASA Data Mining Workshop*. Huntsville, AL, October 19-21.

Graves, S., 1999: *Internet2 Members Meeting*. Seattle, WA, October 11-12.

Graves, S., 1999: *Applied Information System Review Panel*. Houston, TX, November 1-4.

Graves, S., 1999: *Terra/SAGEIII Science Operations Readiness Review (ORR)–Raytheon Systems Facility*. Washington, DC, November 8-10.

Graves, S., 1999: *NASA ESSAAC Meeting*. Washington, DC, November 17-19.

Graves, S., H. Conover, C. Pearson, M. Smith, and B. Beaumont, 1999: *GSFC ESDIS Site Visit at ITSC*. October 18.

Hanish, N., 1999: *NASA Data Mining Workshop*. Huntsville, AL, October 19-21.

Keiser, K., 1999: *NASA Data Mining Workshop*. Huntsville, AL, October 19-21.

Lobl E., 1999: *Validation presentation at the ADEOS II international workshop*. Kyoto, Japan, December 3-10.

Pearson, C., 1999: *NASA Data Mining Workshop*. Huntsville, AL, October 19-21.

Ramachandran, R., 1999: *NASA Data Mining Workshop*. Huntsville, AL, October 19-21.

Ramachandran, R., 1999: *NEXRAD Workshop*. Asheville, NC, December 2-3.

Smith, M., 1999: *NASA Data Mining Workshop*. Huntsville, AL, October 19-21.

Buechler D., 1999: *WSR-88D Workshop*. Asheville, NC, December 2-3.

Smith, M.R., 2000: *NASA EOSDIS Tools Training*, Greenbelt, MD, July 6-7.

Smith, M.R., 2000: *HDF-EOS Workshop IV*, Landover, MD, Sept. 19-21.

Conover, H., 2000: *ESTO/ESDIS Technology Transfer Workshop*; "Migration of IMS Server to Java", Greenbelt, MD, June 5-7.

Drewry, M., 2000: *EOS Data Gateway Development and Operations Meeting;* " Migration to the JAVA IMS Server," and "GHRC Data Center Status," Lanham, MD, June 21-23.

Graves, S., H. Conover, and R. Ramachandran, 2000: *ESIP II Technology Review*, Greenbelt, MD, June 8-9.

Harrison, S., 2000: *EOSDIS User Services Working Group (USWG) Meeting*, Fairbanks, Alaska, May 23-24.

Kavaya, M.J., F. Amzajerdian, G.D. Spiers, D.A. Bowdle, G.D. Emmitt, and T.L. Miller, 2000: *13th Meeting of the Working Group on Space-Based Lidar Winds* (was LAWS Science Team); "A Coherent Lidar Roadmap for Winds In The Long Run," Boulder, CO, June 21-23.

Ramachandran, R., 2000: *ESTO/ESDIS Technology Transfer Workshop*, "Earth Science Markup Language (ESML)", Greenbelt, MD. June 5-7.

Graves, S., D. Hardin and H. Conover, 2000: *The 4th Working Prototype Federation Meeting*, Houston, TX, January 19-21.

Graves, S., 2000: *NRC/CES Workshop on Climate Processing*, Washington, DC, February 6-8.

Hardin, D., 2000: *ESIP Evaluation Workshop*, Houston, TX, January 18.

Ramachandran, R., 2000: Passive Microwave - ESIP, Data for Science and Society, *The Second National Conference on Scientific and Technical Data*, Sponsored by the U.S. National Committee for CODATA, National Research Council, Washington, DC, March 13-14.

Ramachandran, R., 2000: Data Mining in Government, 2 Day Workshop *in Data Mining and Information Visualization, Alliance Center for Collaboration, Education, Science, and Software (ACCESS)*, Ballstone Metro Center Office Tower, Arlington, VA, March 14-15.

Conover, H., 2000: *ESTO/ESDIS Technology Transfer Workshop*; "Migration of IMS Server to Java", Greenbelt, MD, June 5-7.

Drewry, M., 2000: *EOS Data Gateway Development and Operations Meeting;* " Migration to the JAVA IMS Server," and "GHRC Data Center Status," Lanham, MD, June 21-23.

Graves, S., H. Conover, and R. Ramachandran, 2000: *ESIP II Technology Review*, Greenbelt, MD, June 8-9.

Harrison, S., 2000: *EOSDIS User Services Working Group (USWG) Meeting*, Fairbanks, Alaska, May 23-24.

Kavaya, M.J., F. Amzajerdian, G.D. Spiers, D.A. Bowdle, G.D. Emmitt, and T.L. Miller, 2000: *13th Meeting of the Working Group on Space-Based Lidar Winds* (was LAWS Science Team); "A Coherent Lidar Roadmap for Winds In The Long Run," Boulder, CO, June 21-23.

Ramachandran, R., 2000: *ESTO/ESDIS Technology Transfer Workshop*, "Earth Science Markup Language (ESML)", Greenbelt, MD, June 5-7.

Smith, M.R., 2000: *NASA EOSDIS Tools Training*, Greenbelt, MD, July 6-7.

Smith, M.R., 2000: *HDF-EOS Workshop IV*, Landover, MD, Sept. 19-21.

Software and Other Communications - Year 3

Callen, M., 2000: *Advanced Microwave Precipitation Radiometer(AMPR) Metadata Ingest Collection*, Version 1.1, March 21.

Callen, M., 2000: *Microwave Sounding Unit (MSU) Metadata Ingest Software*, Version 1.1, February 3.

Callen, M., 2000: *Convection and Moisture Experiment (CAMEX-3) Metadata Ingest Collection*, Version 1.1, April 5.

Callen, M., 2000: *IMS Guide Server Hyperlink Catalog*, Version 1.0, March 21.

Callen, M. and M. Drewry, 2000: *GHRC Statistics Report Collection*, Version 1.0, January 25.

Conover, H., M. Drewry and M. Callen, 2000: *GHRC IMS/EDG Server*, Version 7.0, March 10.

Conover, H. and M. Callen, 2000: *CINTEX IMS Server*, Version 6.1c, March 1.

Conover, H., M. Callen and M. Drewry, 2000: *SCRS Statistics Report Collection Version*, 1.0, February 21.

Drewry, M. and M. Callen, 2000: *LIS Statistics Report Collection Version*, 1.0, March 3.

Drewry, M. and M. Callen, 2000: *PM-ESIP Statistics Report Collection Version*, 1.0, March 28.

Drewry, M. and M. Callen 2000: *Lightning Imaging Sensor and Optical Transient Detector (LIS/OTD) Metadata Ingest Software* Version, 1.2, March 24.

Drewry, M. and M. Callen, 2000: *National Lightning and Detection Network Metadata Ingest Collection*, Version 1.2, March 7.

Drewry, M. and M. Callen, 2000: *TDRTB Metadata Ingest Collection*, Version 21, February 18.

Drewry, M. and M. Callen, 2000: *US National Weather Service Metadata Ingest Collection*, Version 1.1, January 28.

Drewry, M. and M. Callen, 2000: *GHRC Metadata Entry and Monitoring Collection*, Version 1.1, February 21.

Drewry, M. and M. Callen, 2000: *GHRC Order Monitoring Collection*, Version 1.1, February 21.

Callen, M., and M. Drewry, 2000: *GHRC Statistics Report Collection*, Version 1.1, May 3.

Callen, M., 2000: *IMS Guide / Filter Retrieval Collection*, Version 2.0, May 17-18.

Callen, M., 2000: *Anonymous FTP Summary and Statistics Collection*, Version 1.0, May 20.

Drewry, M., and M. Callen, 2000: *PM-ESIP Statistics Report Collection*, Version 1.1, June 30.

Appendix C:

Education Activities

Education Activities Year 1

1998 Groundwater Festival

On March 20th, 1200 fourth grade students and their teachers attended Alabama's First Annual Groundwater Festival. The event was hosted by UAH Earth System Science Laboratory. The purpose of the Festival was to educate the students as to where their drinking water comes from and how to protect it and keep it clean. The students participated in hands-on activities and were entertained by an environmental magician who performed water related magic tricks and illusions.

Globe Russia Workshop

On July 26 – August 1, 1998 a GLOBE (Global Learning and Observations to Benefit the Environment) Program joint Russian-American teacher workshop held on the campus of Rostov State University in Rostov-on-Don. The Marshall Space Flight Center Education Programs Office supports the GLOBE in Alabama franchise, which is lead by the University of Alabama in Huntsville (UAH). GLOBE students: make a core set of environmental observations at or near their schools; report their data through the Internet to a GLOBE data processing facility; receive and use global images created from worldwide GLOBE school data; and study environmental topics in their classrooms. Over 6,000 schools in 70 countries are participating in the GLOBE Program. GLOBE students have reported over one million science observations in the areas of atmosphere, hydrology, land cover/geology, and soils. These data are used by GLOBE students and scientists to support environmental research and other environmental science programs worldwide. The Rostov workshop was an international first of sorts. The GLOBE in Alabama franchise partnered with the GLOBE in Russia program to conduct the joint GLOBE teacher training. Previously, international GLOBE workshops have been held on a government-to-government level and have been strictly train-the-trainer workshops.

GLOBE Program in Alabama Teacher Training Workshops.

The Summer of 1998 saw the culmination of GLOBE workshops begun during the 1997-98 academic year. Seven weeks of 2.5 day workshops were conducted at the Huntsville/Madison County Botanical Gardens. Over 165 teachers were trained during these workshops which covered the soil and land cover/biology protocols of the GLOBE Program. The atmosphere, computer and hydrology protocol workshops were conducted during 2 days of in-service during the school year. In addition to the 2.5 day workshops, three week-long, full GLOBE workshops were also conducted. Two were conducted in Huntsville and the third was conducted in Russia. In all, over 210 teachers from 42 school systems across Alabama received GLOBE training in 1997-98.

Science Olympiad

March 14, 1998 held at UAH. Approximately 350 middle and high school students from 15 schools attend UAH's Fifth Annual Science Olympiad. Each teach participated in 23 science activities related to biology, math, engineering, optics, chemistry, physics, language arts, computer science, and environmental science. The top three middle school and high school teams advance to compete in the State Science Olympiad.

Education Activities Year 2

1999 Groundwater Festivals

The Earth System Science Center's Groundwater Festival program has seen much growth in the 1998-1999 year. Three Festivals were held for a total of 4,400 students from North Alabama. On May 12-13, 1999, 2600 fourth grade students and teachers attended Madison County's Second Annual Groundwater Festival at UAH. A Groundwater Festival was also held in Limestone County on May 10, 1999, for 650 fourth through sixth graders. On March 25, 1999, a joint Water Festival was held for 1,150 fourth grade students and teachers from Lauderdale and Colbert Counties. The purpose of the Festivals were to educate the students as to where their drinking water

comes from and how to protect it and keep it clean. The students participated in hands-on activities and were entertained by an environmental magician who performed water related magic tricks and illusions.

GLOBE Program in Alabama Teacher Training Workshops.

The 1998-99 academic year saw continued growth in the GLOBE Program in Alabama. New teacher training workshops were begun in Mobile, Baldwin, Montgomery, Tuscaloosa and Jefferson Counties. The GLOBE Program in Alabama continues to be acclaimed as one of the most outstanding of the 90+ franchise partners in the United States. The GLOBE program in Alabama now has over 400 trained teachers in over 250 schools in 48 schools systems across Alabama. In addition to conducting teacher training workshops, a GLOBE Teacher Mentoring Program was begun. Focusing on South Alabama and funded by the Alabama State Department of Education, the goal of this program is to provide continual contact with teachers as they implement the GLOBE Program in their schools. A new cadre of GLOBE trainers was also installed. These include individuals from the University of Alabama College of Education, the Jefferson County Board of Education, the University of South Alabama, Troy State University, the Tuscaloosa Children's Hands On Museum, University of Alabama in Tuscaloosa Arboretum and the NOAA - ADECA Weeks Bay Reserve in Baldwin County.

1999 Science Olympiad

UAH's Sixth Annual Science Olympiad was held on March 20, 1999 at UAH. Approximately 300 middle and high school students from 13 schools attended. Each team participated in 23 science activities related to biology, math, engineering, optics, chemistry, physics, language arts, computer science, and environmental science. The top three middle school and high school teams advanced to compete in the State Science Olympiad.

Education Activities Year 3

2000 Groundwater Festival – Year 3

The Earth System Science Center's Groundwater Festival program has seen some growth in the 1999-2000 year. Approximately 1,000 fourth graders participated in the Groundwater (Drinking Water) Festival held in Blount County, Alabama. The purpose of the Festivals was to educate the students as to where their drinking water comes from and how to protect it and keep it clean. The students participated in hands-on activities and were entertained by an environmental magician who performed water related magic tricks and illusions.

GLOBE Program in Alabama Teacher Training Workshops - Year 3

GLOBE in Alabama continued to expand across the state. Since the partnership's inception in January 1997, **350 (+38 in 2001)** schools, **657 (+66 in 2001)** teachers in 70 counties and 67 school systems have become involved. This representation includes both public and private K-12 institutions. In 2001, our emphasis was on reaching multiple teachers in a school, rather than single teachers per school. This resulted in a lower increase in overall numbers than the previous year. Though there are high-density pockets of GLOBE schools in the Mobile, Birmingham and Huntsville areas of Alabama, in the past year there has been an a great deal of expansion in the rural areas of the state as well. Over 43% are federally designated Title I schools, representing students who are participating in free or reduced-price lunch programs.

GLOBE Schools in Alabama
Mentor Regions in Color

The potential for students to be reached by the program is far more than the indicated number of teachers and their individual classes. The GLOBE trained teacher often returns to their

school and implements the program with the assistance of other teachers increasing the number of participants and program's impact. The level of implementation of the program is reliant upon the trained teacher and thus race and gender participation can only be estimates but from the inner city to rural small school systems, there seems to be equal distribution across gender and race of the students participating.

National GLOBE norms show the largest percentage of students involved is overwhelmingly in the middle school range, 2000 statistics for new teachers trained in Alabama show a similar distribution. For this analysis of the number of students touched, each GLOBE teacher grade level is assigned a number of students. Elementary teachers are given credit for serving 40 students while Middle and High school teachers are given credit for 80 students. It is understood this is an approximation since implementation varies between schools and across the State.

There are approximately 35,000 GLOBE students currently in schools throughout the state. Statewide, there are approximately 700,000 students in pre K-12.

2000 Science Olympiad

UAH's Eighth Annual Science Olympiad was held on February 26, 2000 at UAH. Approximately 285 middle and high school students from North Alabama18 schools attended. Each team participated in 23 science activities related to biology, math, engineering, optics, chemistry, physics, language arts, computer science, and environmental science. The top three middle school and high school teams advanced to compete in the State Science Olympiad.

Appendix D:

Students: Year 1 through 3

Year One
Graduate Research Assistants

Name	Affiliation	Research Area
Blair, Alys	University of Alabama in Huntsville	Thunder Storm Electricity
Callen, Mary	University of Alabama in Huntsville	Data Base Information Technology
Griffin, Dana	University of Alabama in Huntsville	Global Distribution of Water Vapor
Hisaki, Iwai	University of Alabama in Huntsville	Global Distribution of Water Vapor
Jin, Ying	University of Alabama in Huntsville	Remote Sensing Processing Software
*Leclair, Andre	University of Alabama in Huntsville	Developing an inversion model for remote sensing of Titan and Saturn atmosphere (Temperature, pressure profile and atmosphere component).
Lerner, Jeff	University of Alabama in Huntsville	Comparison of VAS and SSM/I Precipitable Water
Li, X	University of Alabama in Huntsville	Radiative Effects of Aerosols
Litten, Leslie	University of Alabama in Huntsville	Reconstruction of Sea Surface Temperatures in the Tropical Pacific
McDowell, Andrew	University of Alabama in Huntsville	Web Information Technology
Nair, U.	University of Alabama in Huntsville	Cumulus Cloud Fields, Modeling and Satellite Observations
Paech, Simon	University of Alabama in Huntsville	Case Study of the May 18, 1995 "Anderson Hills" Tornado
Ramachandran, Rahul	University of Alabama in Huntsville	NEXTRAD and LDAR Data Applications: Preparing for TRMM Data Analysis
Reid, John	University of Alabama in Huntsville	Lightning Spectrometer Calibration and Testing
Whitworth, Brandon	University of Alabama in Huntsville	GOES Data Analysis
Zhang, Jianglang	University of Alabama in Huntsville	Remote Sensing of Biomass Burning; Developing an inversion model for remote sensing of Titan and Saturn atmosphere (Temperature, pressure profile and atmosphere component).

Year Two
Graduate Research Assistants

Name	Affiliation	Research Area
Blair, Alys	University of Alabama in Huntsville	Thunder Storm Electricity
Callen, Mary	University of Alabama in Huntsville	Data Base Information Technology
Griffin, Dana	University of Alabama in Huntsville	Global Distribution of Water Vapor
Hisaki, Iwai	University of Alabama in Huntsville	Global Distribution of Water Vapor
Jin, Ying	University of Alabama in Huntsville	Remote Sensing Processing Software
Li, X	University of Alabama in Huntsville	Radiative Effects of Aerosols
Litten, Leslie	University of Alabama in Huntsville	Reconstruction of Sea Surface Temperatures in the Tropical Pacific
Nair, U.	University of Alabama in Huntsville	Cumulus Cloud Fields, Modeling and Satellite Observations
Zhang, Jianglang	University of Alabama in Huntsville	Remote Sensing of Biomass Burning; Developing an inversion model for remote sensing of Titan and Saturn atmosphere (Temperature, pressure profile and atmosphere component).

Year 3
Graduate Research Assistants

Name	Affiliation	Research Area
Blair, Alys	University of Alabama in Huntsville	Thunderstorm Electricity
Callen, Mary	University of Alabama in Huntsville	Data Base Information Technology
Decker, Ryan	University of Alabama in Huntsville	Modification of the Stable Nocturnal Boundary Layer By Clouds Over Heterogeneous Terrain: An Observational Study
Haines, Stephanie	University of Alabama in Huntsville	Inter-comparison of GOES-8 Images and Sounder Skin Temperature Retrievals
He, Hongli	University of Alabama in Huntsville	Satellite cloud climatology, remote sensing, radiative transfer
Hisaki, Iwai	University of Alabama in Huntsville	Global Distribution of Water Vapor
Laws, Kevin	University of Alabama in Huntsville	Global Distribution of Water Vapor
Litten, Leslie	University of Alabama in Huntsville	Reconstruction of Sea Surface Temperatures in the Tropical Pacific
Nair, U.	University of Alabama in Huntsville	Cumulus Cloud Fields, Modeling and Satellite Observations
Zeng, Jian	University of Alabama in Huntsville	Satellite cloud climatology, remote sensing, radiative transfer
Zhang, Jianglang	University of Alabama in Huntsville	Remote Sensing of Biomass Burning: Developing an inversion model for remote sensing of Titan and Saturn atmosphere (Temperature, pressure profile and atmosphere component).

*Please note, this is a representative list of graduate research assistants, and may not include every graduate research assistant.

Appendix E:

Seminars Year One through Three

Seminars: Year One

1997

October 1 — **Steve Lohmeier (Dynetics):** Classification Of Natural Targets Using Millimeter-Wave Polarimetric Radar Measurements

October 8 — **Kevin Knupp (UAH):** Utilization of Doppler Radar for Research in theAtmospheric Sciences

October 15 — **Kevin Doty (USRA):** Water Budget Studies With A Mesoscale PrimativeEquations Model With Convective Downdraft

October 22 — **Qing Han (UAH):** Towards Monitoring Aerosol Indirect Effects From Space

October 29 — **Don Johnson (Univ. of Wisconsin):** Uncertainty Of Climate Model Simulations In Relation To Hydrologic Processes, Aphysical Sources Of Entropy, And The Lorenz Energy Cycle.

November 5 — **Ron Welch, Kwo-Sen Kuo, Todd Berendes (UAH):** Evaluation Of Allgroithms For Classification Of AVHRR Local Area Coverage Cloud Imagery

November 12 — **Glenn Germany (UAH):** Global Auroral Imaging As A Remote Diagnostic Of Geospace

November 19 — **Jonathan Patz (Johns Hopkins):** Climate Change And The Spread Of Infectious Diseases

December 3 — **Jim Horwitz (UAH):** The Geospace Environment: Solar Wind Magnetosphere, And Auroras

December 4 — **Michael Box (Univ. of New South Wales/Australia):** Remote Sensing Of Aerosol Optical Properties Using Multi View Angle Satellite Observations

December 10 — **Robert Apodaca (Dynetics):** IR Radiometry

December 17 — **Jonathan Pliem (EPA):** Modeling And Field Measurements Of Surface Fluxes Of Heat, Moisture, And Pollutant Dry Depositions

1998

January 7 — **Gary Petti, Kevin Pence (National Weather Service-Birmingham):** Behind The Scene Operations At The Birmingham National Weather Service Office

January 14 — **No Seminar:** AMS Annual Meeting, Phoenix, AZ

January 21 — **Gary Jedlovec (MSFC):** Water Vapor Transport Index For Climate Variability Studies

January 28 — **Steve Goodman (MSFC):** Overview and Status of the Tropical Rainfall Measuring Mission

February 4 — **Bill Lapenta (MSFC):** Mesoscale Modeling Of Surface Features

February 5 — **Upton Hatch (Auburn):** Economic Value of Improved Weather Information in Agriculture

February 11 — **Albert Boehm (Nichols Research Corp.):** PCloudS: A Global Cloud Climatology

February 18 — **David Hathaway (MSFC):** Solar Physics, Solar Irradiance, And Effects On Earth's Atmosphere

February 25 — **Michael Kavaya (MSFC):** The SPARCLE Project: Coherent Doppler Lidar Tropospheric Wind Measurements From The Space Shuttle

February 26	**Andy Dessler (Univ. of Maryland):** Arctic Ozone Loss: How Close Are WeTo Forming An Arctic "Ozone Hole"?
March 4	**Aaron Song (UAH):** Simulating Some Large And Small Scale Evolutions During The 1995 Heatwave With An ECMWF/MM%/RAMS/LES Models System
March 11	**Dara Entekhabi (MIT):** Microwave Remote Sensing
March 18	**Howard Bluestein (Univ. of Oklahoma):** Airborne Doppler Radar Data Analysis And Interpretation
March 19	**Rick Knabb (FSU):** Numerical Simulations Of The Mesoscale Structure Within Eastern Pacific Tropical Plumes
March 25	**Shouping Wang (USRA):** Large Eddy Simulation Study Of Marine Boundary Layer Clouds
April 1	**Qi Mao (UAH/TVA):** On Model Output Statisitics (MOS) And Model Output) Calibration (MOC)
April 8	**Sundar Christopher (UAH):** Satellite Remote Sensing Of Biomass Burning
April 15	**Frank Binkowski (EPA):** Regional Particulate Model Development
April 22	**Ted Klimasewski (Jacksonville State Univ.):** Risk Analysis, Probability Forecasts, and TV Weather
April 29	**Ron Suggs (MSFC):** Derivations Of Land Surface Temperature From GOES
May 6	**Fong-Chiau Chang (UAH):** Validation Of Total Precipitable Water Data Sets
May 13	**Benjie Norris (UAH):** Estimates Of Sulfur Deposition In Wednesday Eastern U. S. for 1975, 1990, and 2010 From Atmospheric Emissions
May 20	**Mike Botts (UAH):** Advancements In Visualization Of Spatial-Temporal Data
May 27	**Frank Bowman (Vanderbilt):** Modeling Secondary Organic Aerosol
September 3	**Paul Krenhbiel (New Mexico Tech):** Lightning Observations in Oklahoma and New Mexico with a Deployable 3-D Lightning Location System
September 9	**Bill Koshak (MSFC):** Recent Advances in the Theory of Retrieving Lightning Locations from RF Arrival Time and Bearing Data
September 16	**Jim Cruise (UAH):** Macroscale Hydrologic Modeling of the Cumberland River Basin (Tenn/KY)
September 23	**Jeff Lerner (UAH):** Seasonal and Interannual Variations in Upper Tropospheric Humidity and Its Transport as Observed by Geostationary Satellite Measurements
September 30	**Pete Robertson (MSFC):** Tropical Oceanic Precipitation: System's Differences between Satellite Climatologies

Seminars: Year Two

1998

October 7 — **Roy Spencer (MSFC):** New Era in Global Temperature Measurements with AMSU (Advanced Microwave Sounding Unit)

October 14 — **Bill McCaul (USRA):** Landfalling Hurricanes: Observations and Opportunities

October 21 — **Dave Bowdle (UAH):** Aerosol Measurements and Modeling Inputs to Doppler Lidar Performance Simulations

October 28 — **Dave Emmitt (Simpson Weather Associates):** Lasers in Space: NASA's New Frontier in Atmospheric Research

November 4 — **Mike Newchurch (UAH):** Stratospheric Ozone Trends: Results from the IOC/SPARC Ozone Trends Assessment and the WMO/UNEP Assessment

November 10 — **Feodor Surkov (Rostov State University):** GIS-Project and Hydrology Modeling for a Small River in the Lower Don River Basin in Southern Russia

November 12 — **Helen Conover (UAH):** Promoting Science Data thru Innovative Information Systems

November 19 — **Josh Wurman (Univ. of Oklahoma):** Observations of Tornadoes and a Hurricane with the Doppler-On-Wheels

November 23 — **Tom Greenwald (Colorado State Univ.):** Remote Sensing of Cloud Liquid Water: An Overview

December 2 — **Robbie Hood (MSFC):** Overview of the Third Convection and Moisture Experiment (CAMEX-3)

December 9 — **Tommy Coleman and Andrew Manu (Alabama A & M):** Overview of HSCaRS Huntsville '98 Summer Field Experiment

December 16 — **Jere Justus(CSC):** New Findings About the Atmosphere of Mars from Pathfinder and Mars Global Surveyor

1999

January 6 — **Jason Ching (EPA):** Very High-resolution Modeling Of Urban Aerosols For Human Exposure

January 20 — **Teferi Tsegaye (Alabama A & M):** Spatial and Temporial Variability of Hydrolic Properties Under Different Tillage Management Practices

January 27 — **Roger Getz (Agricultural Weather Information Services, Inc.):** Transition from Public to Private Sector Opportunities in Meteorology

February 2 — **Peter J. Winzer (Technische Universiaet Wien – Vienna, Austria):** Telescope Arrays and Lidar

February 3 — **Ron Suggs (MSFC):** Satellite Derived Land Surface Temperature for Model Simulations

February 10 — **Boris Petrenko (USRA) and Roy W. Spencer (MSFC):** Low Dimensional Parameterization of the Kummerow's Microwave Radiative Transfer Model for the Atmosphere with Precipitation

February 11 — **B.J. Sohn (Seoul National University, Korea):** Optical Characteristics of Asian dust Aerosol from Ground-Based Solar Radiation and Satellite SeaWiFS Measurements in the Spring of 1998.

February 18 — **Paul Menzel (Univ. of Wisconsin):** Advances in Geosynchronous Observations of the Atmosphere

February 24 — **Gary Jedlovec (MSFC):** Monitoring Urban Growth with GOES Data

March 3	**Dale Quattrochi and Jeff Luvall (MSFC):** Project ATLANTA and the EPA Urban Heat Island Pilot Project: Remote Sensing Analysis of How the Urban Landscape Impacts Local and Regional Meteorology and Air Quality
March 4	**Student Seminars**
March 10	**Robert Harriss (Texas A & M):** Barriers and Bridges to Managing Carbon Metabolism in America
March 17	**Sasha Madronich (NCAR):** Tropospheric UV Radiation and Atmospheric Chemical Processes
March 24	**Qingyuan Han (UAH):** A New Approach for Monitoring Precipitation from Space Using GOES Data
March 31	**Tim Miller (MSFC):** Doppler Lidar Winds from Space
April 1	**James Nations (Conservation International):** Conflict and Conservation in the Maya Tropical Forest: Species, Refugees, and Remote Sensing in the Lowlands of Mexico, Guatemala, and Belize
April 7	**Kevin Knupp (UAH):** The UAH Mobile Integrated Profiling System: (Preliminary Measurements
April 8	**Jay Hnilo (Lawrence Livermore Nat. Lab.): .):** Research at Lawrence Livermore National Laboratory"s Program for Climate Model Diagnosis and Intercomparison
April 14	**John Christy (UAH):** Global Warming Issues: An Update
April 20	**Bryan Johnson (NOAA):** Ozonesonde Measurements At South Pole, Antarctica: Has The Ozone Hole Bottomed Out Yet?
April 21	**Ahmed Fahsi (Alabama A & M):** Spectral Attenuation of Vegetation Parameters (Biomass, Density) on the VIS/IR
April 28	**Narayan Rajbhandari (Alabama A & M):** Development and Verification of a Stochastic Model to Assess the Lag Effect of Precipitation on Soil Moisture
May 5	**Marius Schamschula (Alabama A & M):** Image Fusion Using Pulse Couple Neural Networks
May 12	**Tom Sever (MSFC):** New Discoveries in Archaeological Research from Remote Sensing
May 19	**Raman Inguva (Alabama A & M), Bill Crosson (USRA), and Marius Schamschula (Alabama A & M):** Assimilation of Remotely-Sensed Soil Moisture Estimates in a Distributed Surface Flux-Hydrology Model Using a Kalman Filter
May 26	**Youram Kaufman (NASA/GSFC):** Check-up of Planet Earth at the Turn of the Millennium—Anticipated New Phase in Earth Sciences
June 2	**Eric Smith (MSFC/GHCC):** Progress on the Proposed Global Precipitation Mission and Why I Am Here.
July 1	**Kirk Fuller (Colorado State University):** Applied Microparticle Optics and Radiometry
July 14	**B.J. Sohn (Seoul National University, Korea):** Water Vapor Retrieval from SSM/I and its Application to the Study of East Asian Summer Monsoon
September 1	**Raman Inguva (Alabama A&M) and Bill Crosson (USRA):** Assimilation of Remotely-Sensed Soil Moisture Estimates in a Distributed Surface Flux-hydrology Model Using A Kalman Filter
September 8	**Vandana Srivastava (USRA):** A View of Hurricane Juliette with Laser Radar

September 15 **Eric Smith (MSFC):** Progress on the Proposed Global Precipitation Mission: And Why I Am Here

September 22 **Stan Heckman (USRA):** The Mysteries of Lightning Processes

Seminars: Year Three

1999

October 6	Maury Estes (USRA): Using Urban Heat Island Information to Enhance Land Use/Development Planning
October 7	Connie Woodhouse (NOAA/NGDA): Paleoclimate Research on Droughts in the Central U.S. Over the Past 2000 Years
October 13	Mike Newchurch (UAH): Tropical Tropospheric Ozone Observations
October 18	Guy Brasseur (NCAR): Tropical Tropospheric Ozone Modeling
October 20	Tom Pierce (EPA): Lightning NOX (Visit Coordinator: Noor Gillani)
October 21	Ralph Kahn (Earth and Planetary Atmospheres Element Jet Propulsion Laboratory): What We Can Learn About Aerosols from Multi-Angle Remote Sensing Over Oceans
October 27	Toby Carlson (Penn. State Univ.): Diagnosis and Prediction of Urbanization Trends Using Remote Sensing and GIS
November 3	Bill Cooke (MSFC): November Leonid Meteoroid Shower, Origin and Overview, and Implications for Earth's Atmosphere
November 10	Doug Rickman (MSFC): Detection of Wind Patterns on Meter Scale in Crops
November 17	Bill Rossow (NASA/GISS): Systematic Effects on Climate of Small and Large-Scale Cloud Variations
November 24	HOLIDAY
December 1	Elaine Prins (NOAA/NESDIS): Monitoring of Biomass Burning Fires Using GOES-8
December 8	Udaysankar Nair (UAH): Impact of Land Use Change on Cumulus Cloud Development
December 15	Ashutosh Limaye (USRA): Macroscale Hydrology Modeling of Chattahoochee River Basin (Ala/Ga)
December 22	HOLIDAY
December 29	HOLIDAY

2000

January 5	Benjie Norris (UAH): Issues In Acid Deposition Model Development
January 19	Maurice Jarzembski (MSFC): Backscatter Studies Using the NASA/MSFC cw CO2 Doppler Lidar
January 26	Mike Botts (UAH): Space-Time Toolkit: Visual Integration of Dynamic GeoSpatial Data
February 2	Payson Sheets (Univ. of Colorado): Archaeological Applications of Remote Sensing in Costa Rica and El Salvador
February 9	Katherine O'Dell (UAH): Laser Doppler Velocimetry as a Low Altitude Wind Shear Detection Technique

February 17 Ron Suggs (MSFC): Overview of Induced Atmospheric Contamination on Spacecraft

February 23 Wade Batts (CSC): Day (or Two) in the Life of an Aerospace meteorologist: Needs, Issues, and Actions.

March 1 Kirk Fuller (UAH): A Hazy Picture of Global Warming

March 8 Stephen Smith (Tennessee Valley Energy Reform Collation): Bringing Green Power (Renewable Energy) to the Tennessee Valley

March 15 Student Seminar Presentations

March 22 Anthony Guillory (MSFC): Entrainment of Upper Level Dry Air into Hurricane Earl

March 29 SPRING BREAK – NO SEMINAR

April 12 Xiquan Dong (University of Utah): Boundary-Layer Stratus Cloud Properties Retrieved from Ground-Based Measurements

April 26 Boris Petrenko (USRA): The Beamfilling Algorithm for Retrieval of Hydrometer Profile Parameters

May 10 Barry Roberts (MSFC): Overview on New Automated Meteorological Profiling System (AMPS): Replacement Plans for Rawinsonde System

May 17 Mike Coffey (NCAR): FTIR Observations of Atmospheric Gases and Aerosols

May 31 Kenneth Schere (EPA): Regional/Urban Tropospheric Air Quality Modeling with US EPA's Models-3/CMAQ

September 6 Qi Mao (UAH): Influence Of Large-Scale Initial Oceanic Mixed Layer Depth On Tropical Cyclones

September 13 (CANCELLED – TO BE RESCHEDULED AT A LATER DATE) Robbie Hood (MSFC): CAMEX-Post Results And Future Plans

September 20 Jim Arnold (MSFC): Overview Of The NASA Earth Sciences Current And Planned Program

Appendix F:

Center for Applied Optics Projects

Year 2

Development of Diffractive Scanner and Low Mass Conventional Telescope, PI: Dr. Diane Chambers

Trade studies for 1-meter aperture lightweight telescope were continued over this period and its optical design and analysis were initiated. Novel lightweight materials are being evaluated with a concern towards thermalstability and manufacturability.

- Novel beam steering technologies have been investigated for application to a 1-meter aperture telescope. A diffractive optic concept has been developed and a test article is to be fabricated at UAH.
- The development of an autonomous operational capability for the system has begun. An automated interferometric concept is being considered for the telescope. These interfrometric techniques are capable of measuring the optical misalignment of selected critical components that may occur during the launch or the lidar operation when in orbit due to vibration and thermal variations. This is a major concern for large aperture, long life-time space-based lidar systems.
- The investigation of an integrated detector/amplifier technology was started and a monolithic optical heterodyne receiver concept based on a dual-detector configuration was selected for further design analysis. The possibility of including other receiver electronics on the same chip is also being considered.
- Several technical papers were presented at SPIE and OSA conferences.
- Technical briefings were made to GHCC.

LIDAR Feasibility Study
Funding Amount $20K
PI: Mr. Gary Spiers

A baseline coherent lidar instrument capable of meeting the sensitivity requirements on a single shot basis was derived. A coherent Doppler lidar to meet the requirements using multiple shot averaging was then derived. Theses instrument designs use the reference atmosphere profiles provided and use 833 km and 400 km orbit heights

A model of the incoherent lidar was developed. During a review of the prior work in the literature an incorrect assumption concerning etendue was identified in the papers of one of the main authors in this field. It should be noted that this issue will not invalidate the incoherent design presented as part of this study but will be an issue for some of the other designs that have been published. A second issue concerned the impact of the time lag during the round trip time and the potential for the spacecraft to change attitude during this time. This is a concern for the coherent designs but does not appear to have been addressed by the incoherent lidar community. The main issue here is that this will result in a return beam offset from the transmit beam by some angle, theta. This angularly offset must be compensated for if the return signal is to be efficiently coupled into the fiber typically used in these systems to link the collecting telescope to the receiver optics and clean up the mode. A preliminary attempt to quantify these concerns through the use of a finite difference split-step numerical simulation of optical propagation within the fiber (see attached figures) was conducted.

The results of these studies were presented at the Working Group on Space Based Lidar Winds.

NPOESS Study
PI: Mr. Gary Spiers

The NPOESS contractor library was searched for items of relevance to this task and the documents obtained subsequently reviewed. An analysis of the on-orbit stability requirements for coherent Doppler lidar from the NPOESS 833km was carried out using the tools developed during the SPARCLE project and provided to NPOESS. This analysis is attached (NPOESS Satellite Lidar Sensitivity Analyses.doc - 41 pages). Results were presented at the Working Group on Space Based Lidar Winds.

Step-Airedes
Funding Amount $6.7K
PI: Mr. Gary Spiers

Year 3
NPOESS Satellite Lidar Sensitivity Analyses Tutorial
833 km, 89 deg inclination orbit, 45 deg nadir instrument
Gary D. Spiers, Center for Applied Optics, University of Alabama in Huntsville

The equations in this document are in MAPLE, a symbolic mathematics package format. Define some constants:

$$r2d := 180\frac{1}{\pi}$$

$$d2r := \frac{1}{180}\pi$$

$$v\_c := .299792459010^{9}$$

$$G := .667259000010^{-10}$$

$$Me := .597900000010^{25}$$

where r2d and d2r are constants for converting between degrees and radians, v_c is the velocity of light in m/s , G is the Gravitational constant in N m^2/kg^2; and Me is the mass of the earth in kg. Now define the WGS84 ellipsoid parameters:

$$a := .637813701O^{7}$$

$$b := .635675231421O^{7}$$

$$We := .00007292115$$

$$ee := .0818191908426$$

$$ee2 := .00669437999013$$

where a and b are the semimajor (equatorial) and semiminor (polar) radii respectively, We is the angular velocity of the earth, ee and ee2 are the first eccentricity and its square respectively. Finally define the parameters for this analysis:

$$maxlat := 89$$

$$orbit1 := 833000$$

$$nadir1 := 45$$

where maxlat is the highest latitude that the orbit passes over, orbit1 is the orbit height with respect to the equatorial earth radius, a and nadir1 is the instrument nadir at the spacecraft. We now define a procedure to calculate the radius of the oblate earth with respect to the geodetic latitude. Note that the expression for calculating the geodetic latitude breaks down at the poles and so a check must be made for a latitude of Pi/2 radians.

```
Rlat := proc(lat)
global a, b;
   if lat = 1/2*Pi or lat = - 1/2*Pi then b
   else 1/(sqrt(1/a^2 + tan(lat)^2/b^2)*cos(lat))
   fi:
end;
```

This next procedure calculates the differential of the earth's radius as a function of latitude.

```
dRlat := proc(lat)
global a, b;
   sin(lat)/(cos(lat)^2*sqrt(1/a^2 + tan(lat)^2/b^2)) - 2* tan(lat)*(1 + tan(lat)^2)/
(cos(lat)*(1/a^2 + tan(lat)^2/b^2)^3*b^2)
end;
```

This procedure calculates the earth's rotational velocity at a latitude, lat :

```
Vlat := proc(lat)
global We, a, ee2;
   We*a*cos(lat)/sqrt((1 - ee2)*sin(lat)^2 + cos(lat)^2)
end;
```

Consider a satellite at some latitude, lat in an orbit of inclination, inc then the angle the satellite orbit makes to a meridian line at latitude, lat is:

```
orblat:=proc(lat,inc)
arcsin(cos(inc)/cos(lat)):
end;
```

Plot the angle between orbit and meridian as a function of latitude for the parameters above.

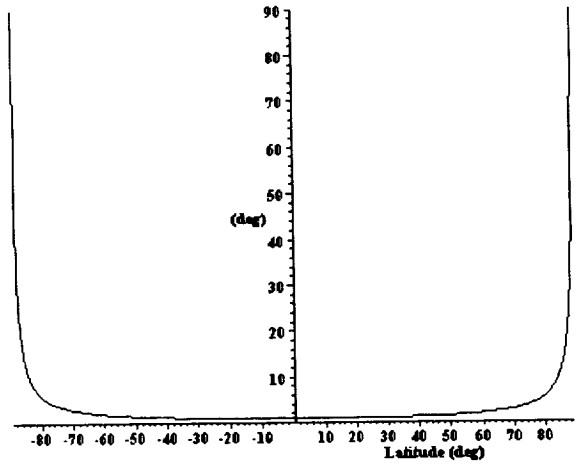

Figure 1: Angle between orbit and meridian.

We can also plot the rate of change of the angle between the orbit and meridian as a function of latitude.

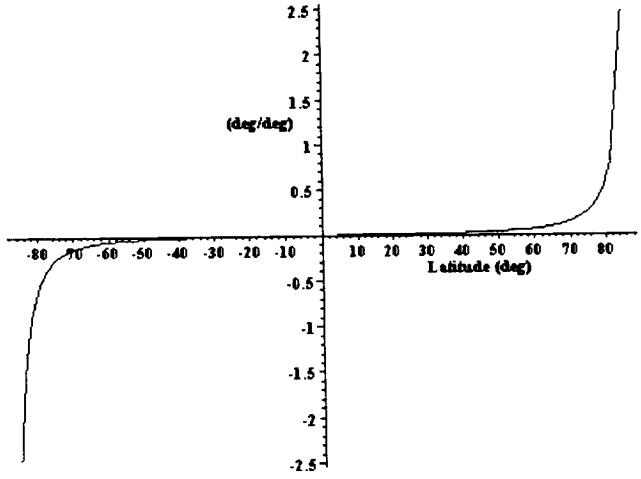

Figure 2: Rate of change of angle to local meridian.

Plot the change in WGS84 earth radius with respect to the equatorial radius as a function of latitude.

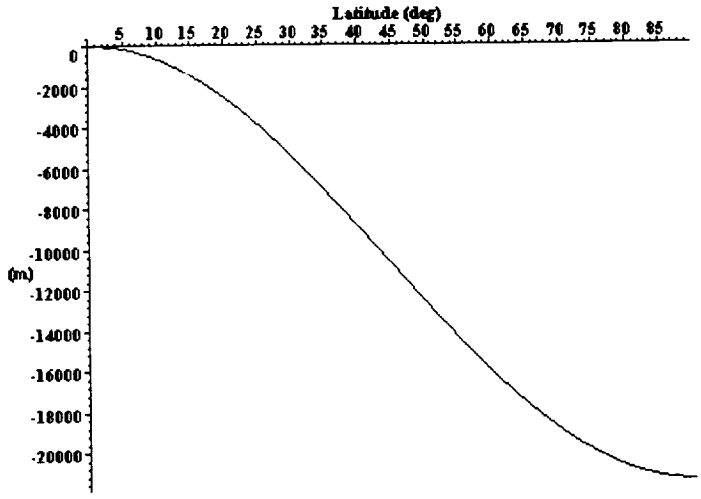

Figure 3: Variation in the earth's radius as a function of latitude.

This clearly shows the 20 km difference between the two radii. Plot the distance moved along the surface for one degree change in latitude.

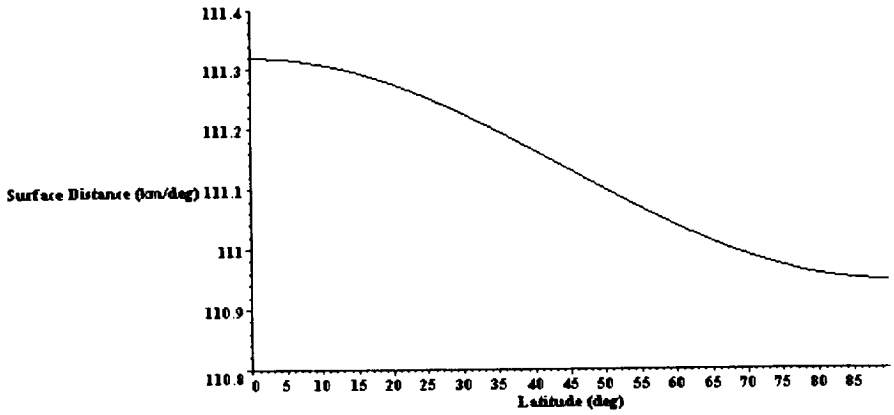

Figure 4: Latitude surface distance.

We can replot this as a delta change from the value at the equator.

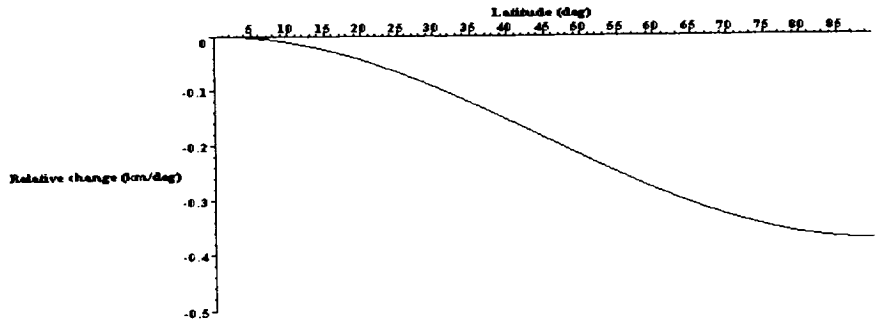

Figure 5: Delta change in Latitude surface distance.

The rate of change of the WGS84 ellipsoid radius is given by:

```
dRlat := proc(lat)
global a, b;
   sin(lat)/(cos(lat)^2*sqrt(1/a^2 + 1/(cos(lat)^2*b^2) - 1/b^2)) -
   sin(lat)/(cos(lat)^4*(1/a^2 + 1/(cos(lat)^2*b^2) - 1/b^2)^(3/2)*b^2 ):
end;
```

and we can also plot it:

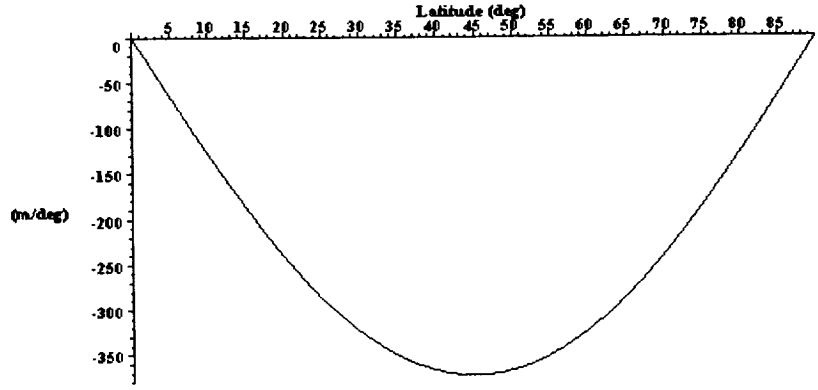

Figure 6: Rate of change of the WGS84 ellipsoid radius.

If we plot the integral of the rate of change of the WGS84 ellipsoid with latitude we should get back to the initial plot.

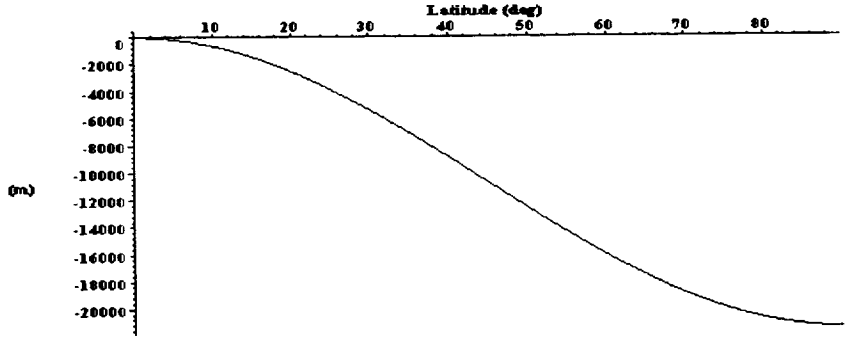

Figure 7: Integral of dWGS84/dlat as a fn of lat (sanity check).

A satellite in a circular orbit around the earth with an orbit radius of (orbh + a), where orbh is the height of the orbit above the equator, has a velocity given by:

```
vsat:=proc(orbh)
 global a,b,G,Me;
 sqrt(G*Me/(orbh+a));
end;
```

The following plot shows the variation in velocity over the orbit heights within 50 km of the nominal orbit height.

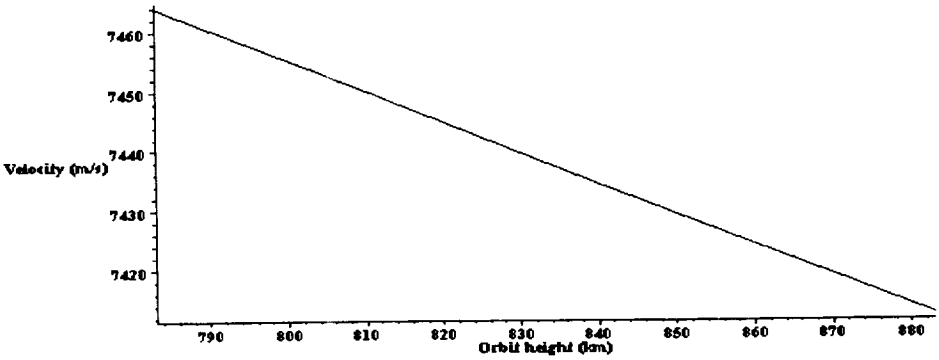

Figure 8: Satellite Velocity.

We can replot this as a change in satellite velocity relative to the nominal orbit height.

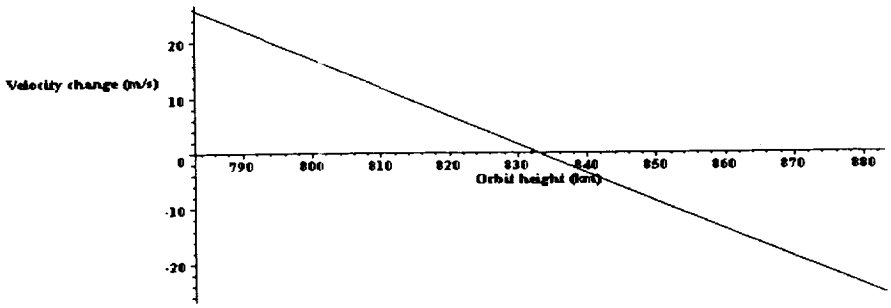

Figure 9: Change in Satellite Velocity.

The sensitivity of the satellite velocity to changes in orbit height can be determined by plotting the differential with respect to the orbit height.

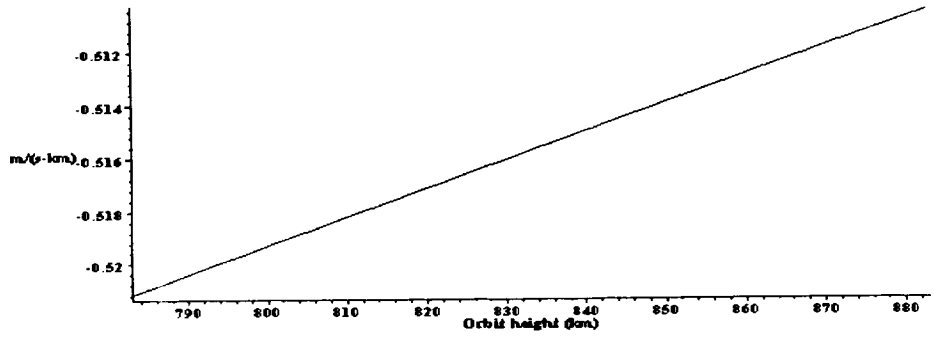

Figure 10: Rate of change in satellite velocity vs. orbit height.

The time for one orbit is simply given by:

```
torbit:=proc(orbh)
 global a,b;
 2*Pi*(orbh+a)/vsat(orbh);
end;
```

and the variation in orbit period over the orbit heights of interest is shown in the following plot:

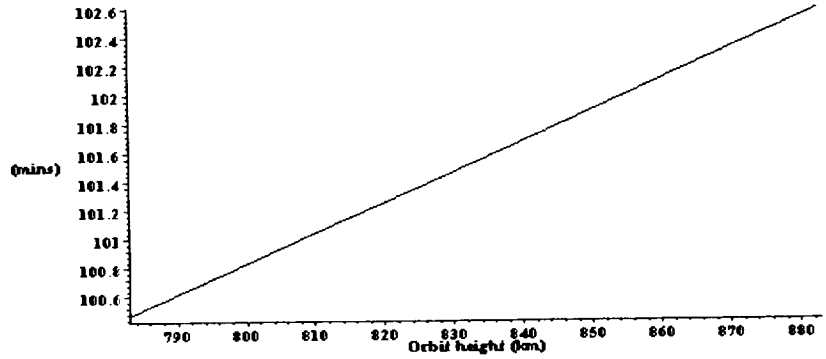

Figure 11: Orbit Period.

We can modify this to show a delta change with respect to the lowest orbit height.

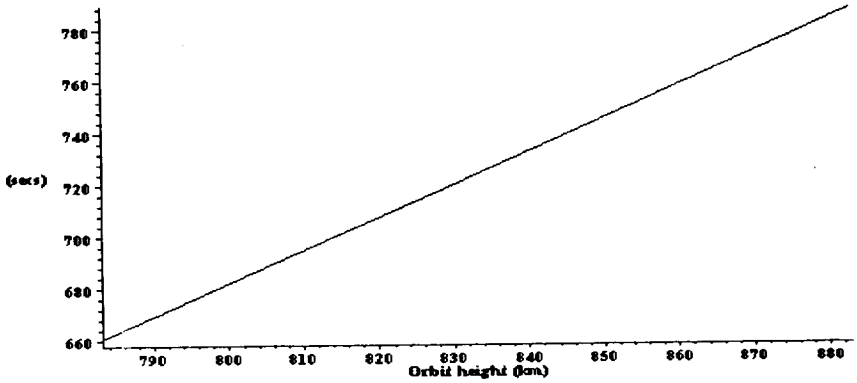

Figure 12: Change in orbit period with orbit height.

For the orbit conditions specified at the beginning of this document the component of the satellite velocity parallel to the local line of meridian at a given latitude is:

```
vlat:=proc(lat,orbh,inc)
 global a,b;
 vsat(orbh)*cos(orblat(lat,inc));
end;
```

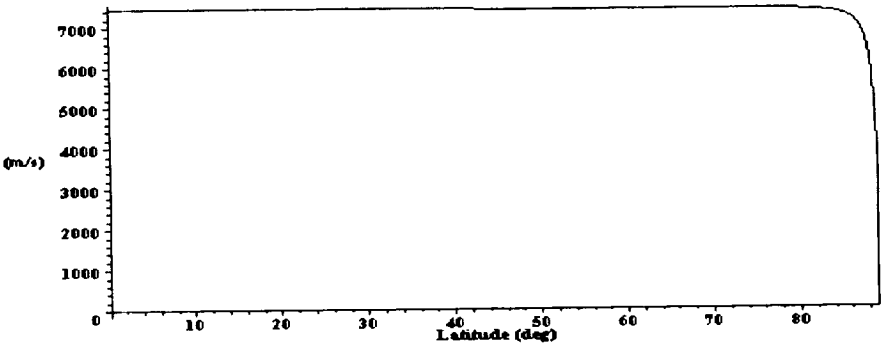

Figure 13: Satellite velocity parallel to lines of meridian.

Similarly the component of the satellite velocity parallel to the lines of latitude at a given latitude is:

```
vlong:=proc(lat,orbh,inc)
```

```
 global a,b;
  vsat(orbh)*sin(orblat(lat,inc));
end;
```

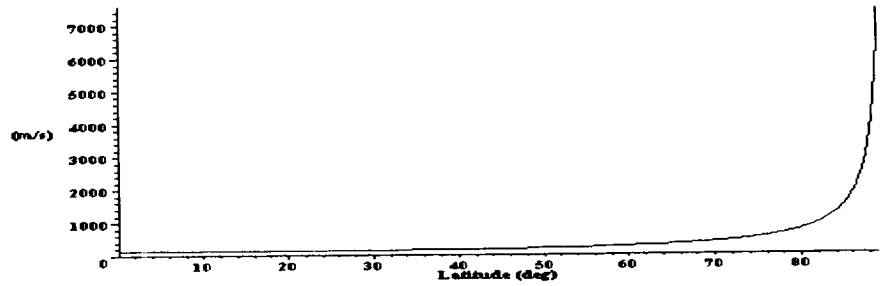

Figure 14: Satellite velocity parallel to lines of latitude.

Recombining these we should get a constant satellite velocity independent of latitude:

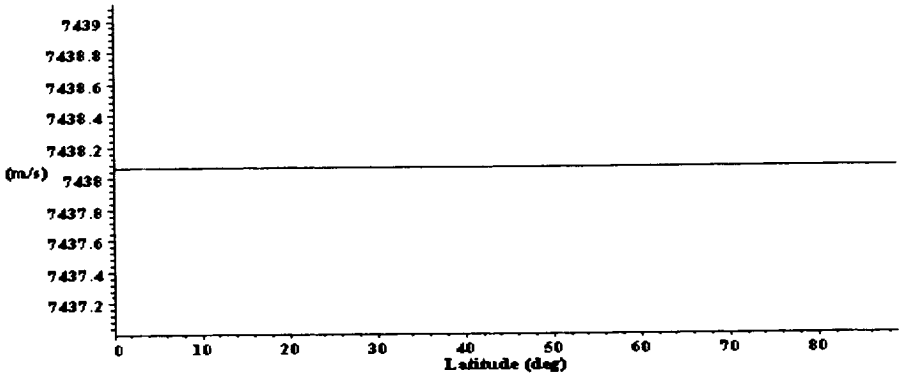

Figure 15: Sqrt(Vlong^2+Vlat^2) (sanity/numerics check).

Once we know the component of the velocity along the lines of longitude we can determine the rate of change of latitude as a function of latitude for any given orbit.

```
 global a,b;
  vlat(lat,orbh,inc)/(orbh+a)*r2d.
end;
dlatdt:=proc(lat,orbh,inc)
```

For the orbit under consideration this gives:

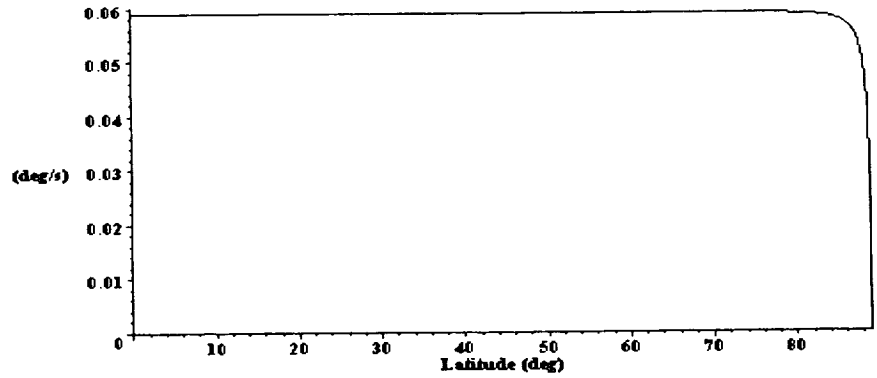

Figure 16: Rate of change of latitude.

We can then combine this with the WGS84 ellipsoid radius to get the time rate of change of the Earth's radius as a function of latitude for this orbit configuration.

```
dRlatdt:=proc(lat,orbh,inc)
 global a,b;
  dlatdt(lat,orbh,inc)*dRlat(lat)*d2r;
end;
```

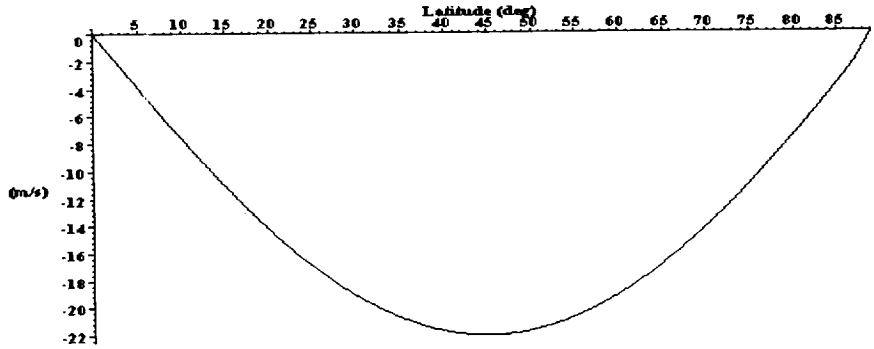

Figure 17: Rate of change of the Earth's radius.

We can look at the earth's rotational velocity as a function of latitude:

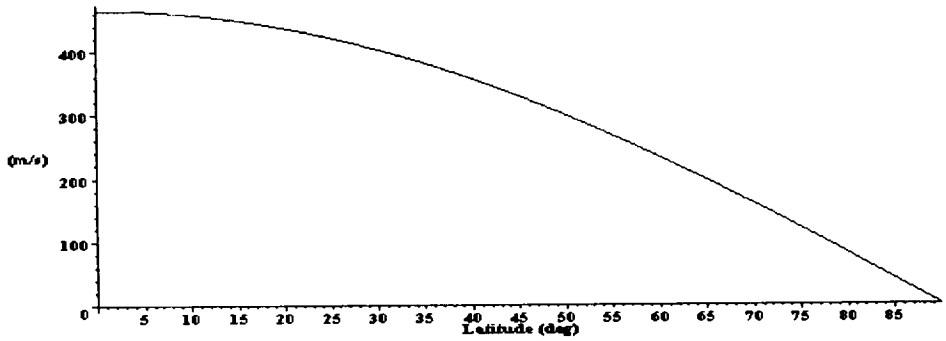

Figure 18: Earth's rotational velocity at the WGS84 ellipsoid radius.

and the rate of change of the earth's rotational velocity with latitude:

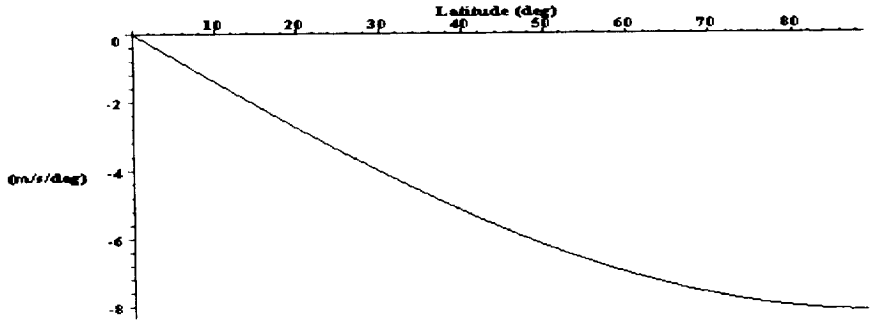

Figure 19: Rate of change of Earth's rotational velocity with latitude.

The nadir angle at a target height, alt above the ground is given by:

```
nadalt:=proc(orbh,nadir,alt,lat)
  global a;
```

```
 arcsin((orbh+a)*sin(nadir)/(Rlat(lat)+alt));
end;
```

where nadir is the nadir angle at the spacecraft. We can then plot the change in nadir angle at the earth's surface, for the current orbit height and nadir angle as a function of latitude.

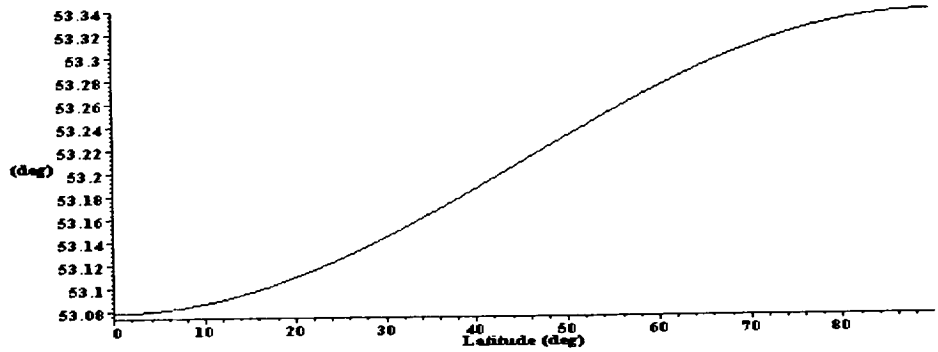

Figure 20: Nadir angle at the earth's surface.

As previously we can show the change in degrees with respect to the nadir angle at the surface near the equator.

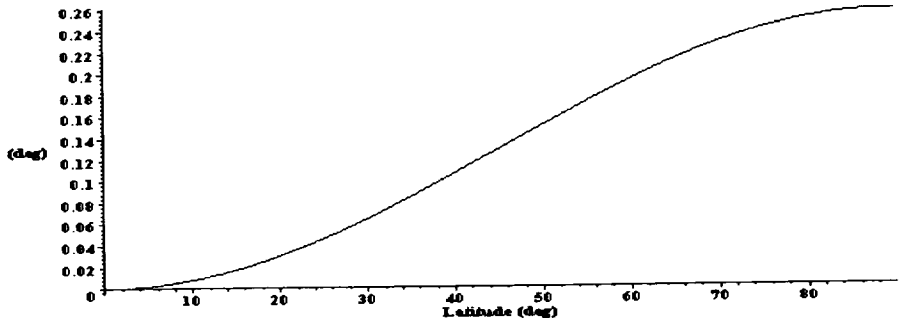

Figure 21: Variation of the nadir angle at the earth's surface.

and replot this in milliradians.

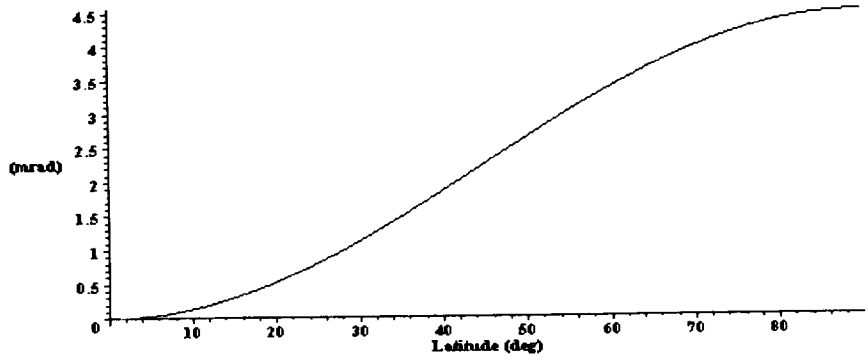

Figure 22: Variation of the nadir angle at the earth's surface.

We can also determine the nadir angle at a given target altitude. The following plot is for a latitude of 45 deg.

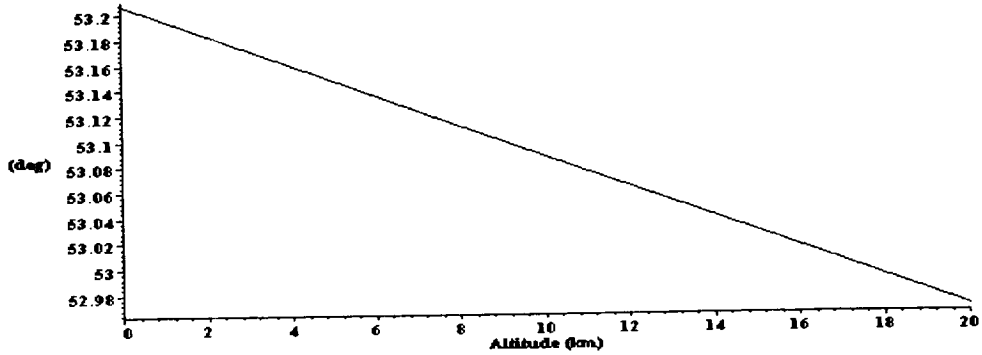

Figure 23: Nadir angle at a given altitude above the surface.

We can combine the altitude and latitude dependencies of the nadir angle at the target:

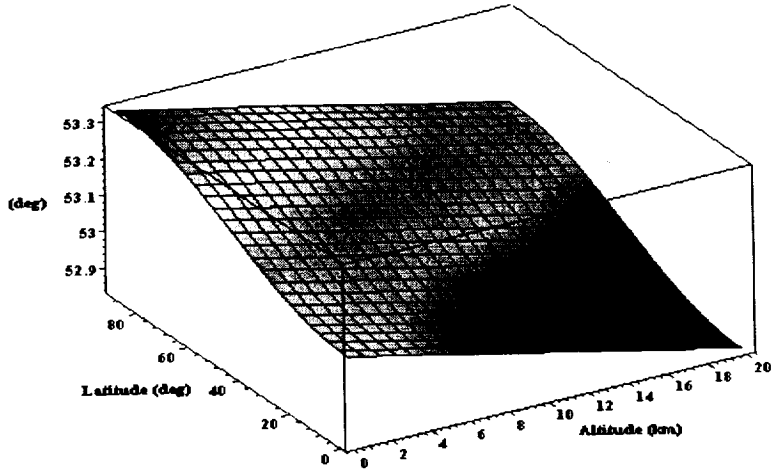

Figure 24: Variation of nadir angle with altitude and latitude.

The range from the lidar to a target at an altitude, alt is given by:

```
Range:=proc(orbh,nadir,alt,lat)
  sqrt((orbh+a)^2+(Rlat(lat)+alt)^2-2*(orbh+a)*(Rlat(lat)+alt)*cos(nadalt(orbh,nadir,alt,lat)-nadir)):
end;
```

We can plot this as a function of latitude and target altitude:

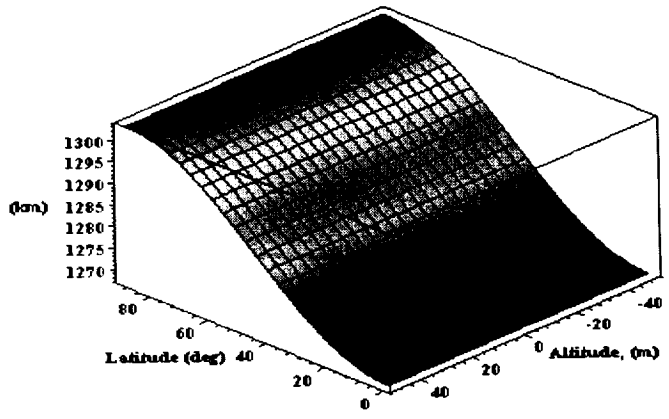

Figure 25: Range to altitude (with respect to WGS84).

For the orbit conditions documented earlier we can determine the sensitivity of the range to a given altitude by plotting the range as a function of altitude. For the plot shown, a latitude of 45 degrees was used as this is the latitude at which the range is most sensitive to changes in latitude.

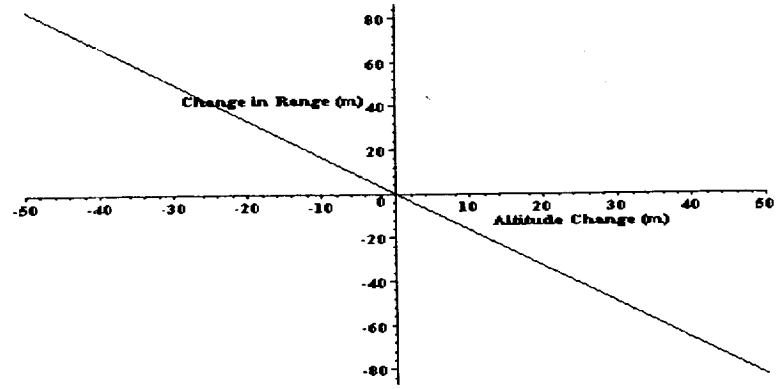

Figure 26: Variation in range as a function of target altitude.

Similarly we can plot the range dependence on variations in orbit height:

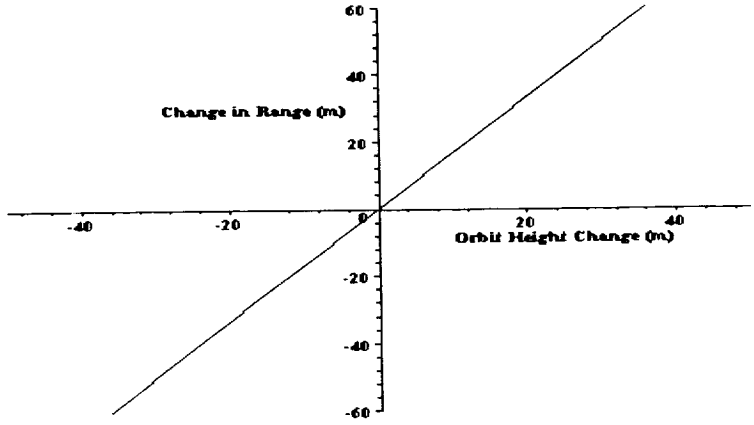

Figure 27: Variation in range as a function of orbit height change.

on variations in nadir angle:

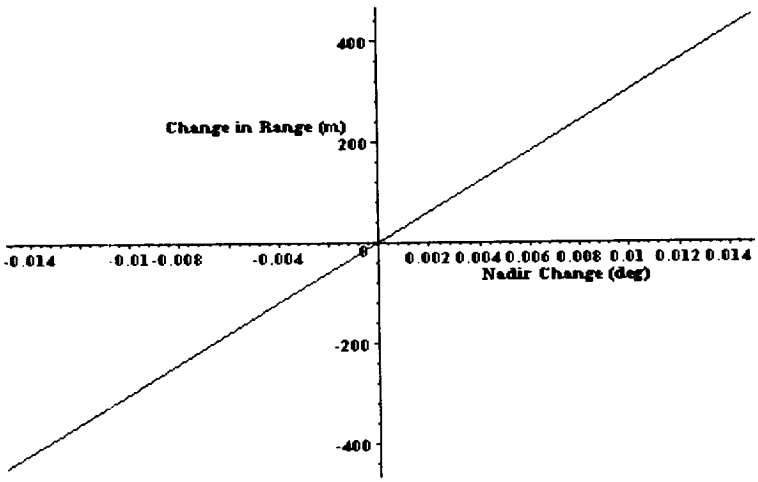

Figure 28: Variation in range as a function of nadir change.

and finally on variations in latitude:

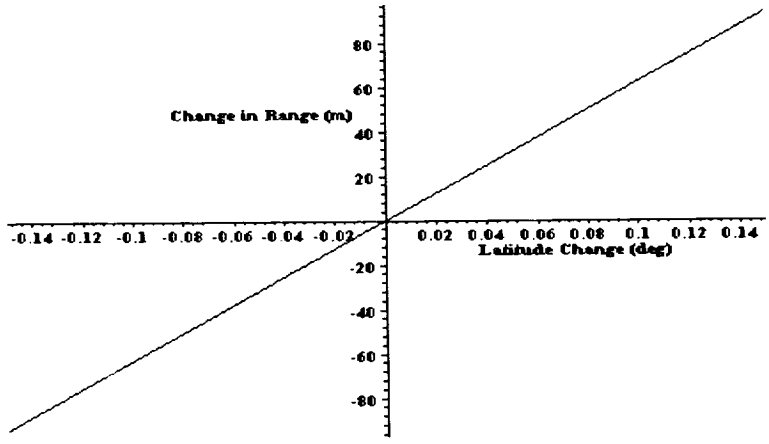

Figure 29: Variation in range as a function of latitude change at a nominal 45 deg latitude.

To determine the range from the lidar to a target we measure the round trip time of flight and calculate the range.

```
t_rtrp:=proc(orbh,nadir,alt,lat)
  2*Range(orbh,nadir,alt,lat)/v_c;
end;
```

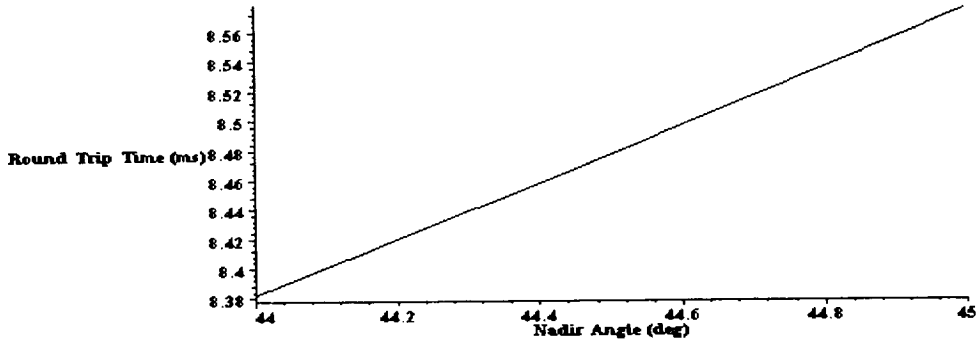

Figure 30: Round trip time variation with nadir angle.

We can plot the round trip time as a function of orbit height and nadir angle to determine the range of round trip times we can anticipate seeing:

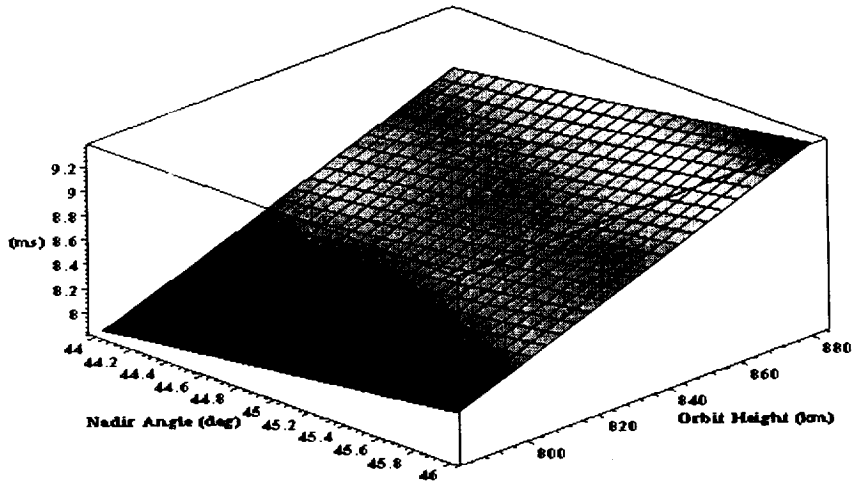

Figure 31: Lidar signal round trip time.

During the round trip time the spacecraft continues to rotate about the planet. This rotation results in a tipping of the nadir angle during the round trip time that translates into a misalignment angle between the transmit and receive optical paths. The round trip time depends on the nadir angle and therefore the nadir tipping angle, nadirtip, given by:

```
nadirtip:=proc(orbh,nadir,alt,lat)
 global a;
 vsat(orbh)*t_rtrp(orbh,nadir,alt,lat)/(orbh+a);
end;
```

has a dependence on nadir angle and this is shown in the following plot.

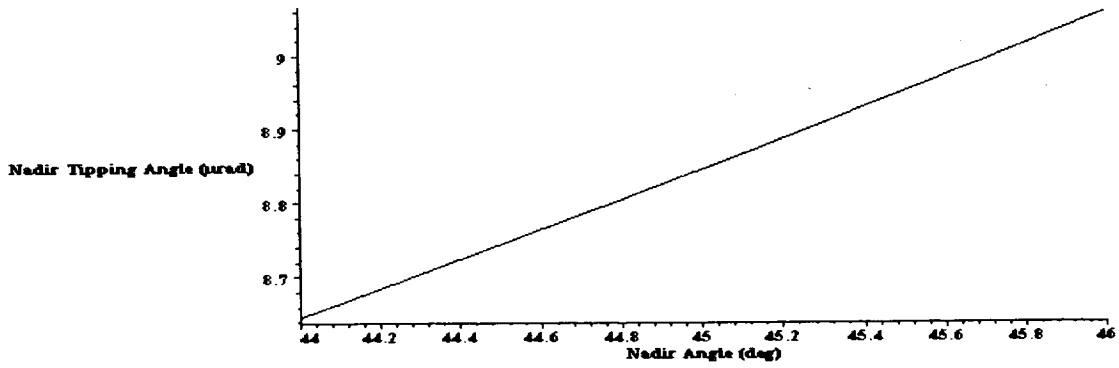

Figure 32: Nadir tipping angle dependence on nadir angle.

We can see that this is a weak dependence. The dependence on orbit height is much stronger as the next plot shows:

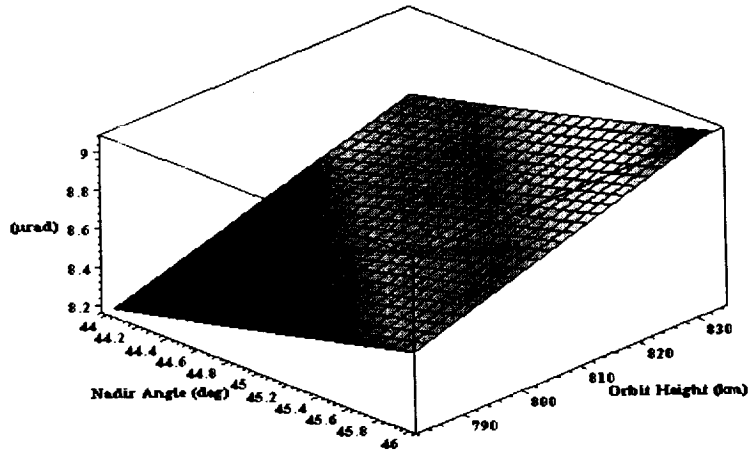

Figure 33: Nadir Tipping Angle.

The orbital velocity, in m/s, of a satellite at the orbit height documented earlier is ~7438 m/s. The line of sight velocity seen by the satellite is a function of the target, satellite and earth rotation velocities and is given by:

```
los_vel:=proc(nadir,az,alt,inc,orbh,lat,trgta,vtrgtv,htrgtv,hsatv,vsatv)
 htrgtv*cos(az+orblat(lat,inc)-trgta)*sin(nadalt(orbh,nadir,alt,lat))+
 vtrgtv*cos(nadalt(orbh,nadir,alt,lat))+hsatv*cos(az)*sin(nadir)+
 vsatv*cos(nadir)+Vlat(lat)*sin(orblat(lat,inc)+az)*sin(nadalt(orbh,nadir,alt,lat)):
end;
```

where az, trgta, vtrgtv, htrgtv, hsatv, vsatv are the azimuth angle of the line of sight with respect to the velocity direction, the azimuthal angle the target velocity makes with respect to the local meridian, the target vertical and horizontal velocities and the satellite horizontal and target velocities respectively. For the orbit and lidar parameters listed at the start of this document the line of sight velocity due to the line of sight components of the satellite and earth rotation velocities only (0 target velocity) as a function of azimuth is shown in the following figure for a lidar over the earth's equator .

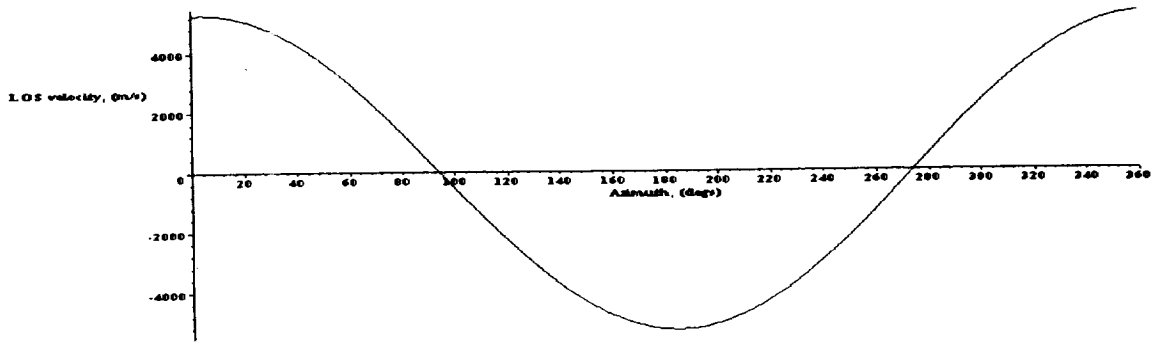

Figure 34: LOS velocity as a function of azimuth.

Expanding the region around the first 0 m/s point enables the gradient to be determined.

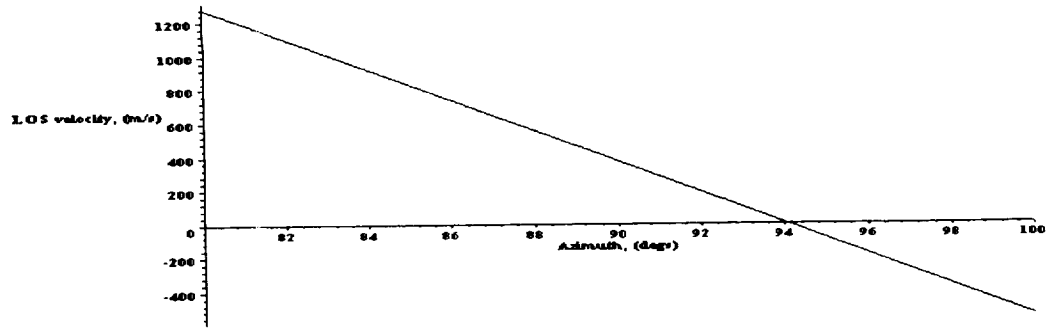

Figure 35: LOS velocity as a function of azimuth.

Alternatively plotting the differential of the line of sight velocity with respect to the azimuth angle enables the maximum rate of change to be determined:

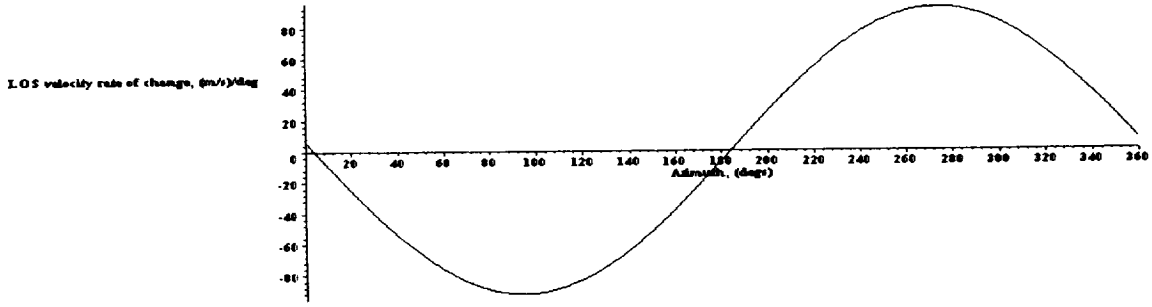

Figure 36: Rate of change of LOS velocity as a function of azimuth.

The line of sight velocity is dominated by the spacecraft velocity, if this is removed then we can see the dependence on the earth's rotational velocity:

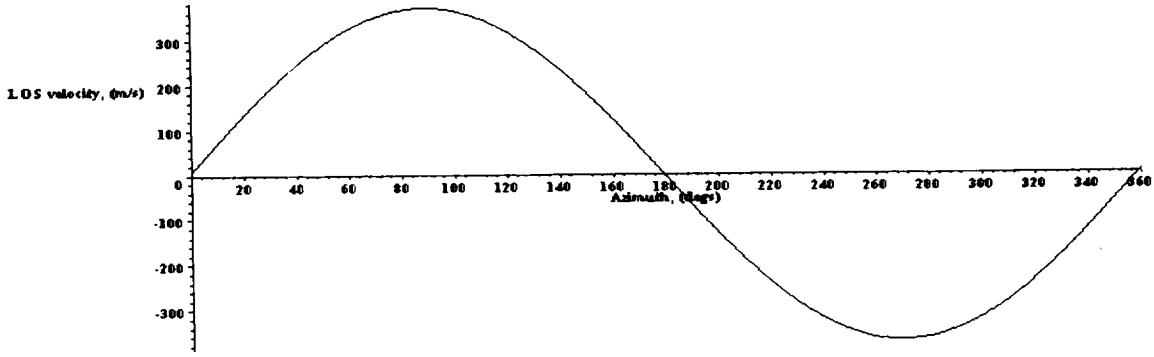

Figure 37: Earth rotation component of the LOS velocity as a function of azimuth.

This clearly shows the much smaller magnitude of the earth's rotational contribution. Again we can determine the maximum rate of change with azimuth by plotting the differential with respect to the azimuth angle:

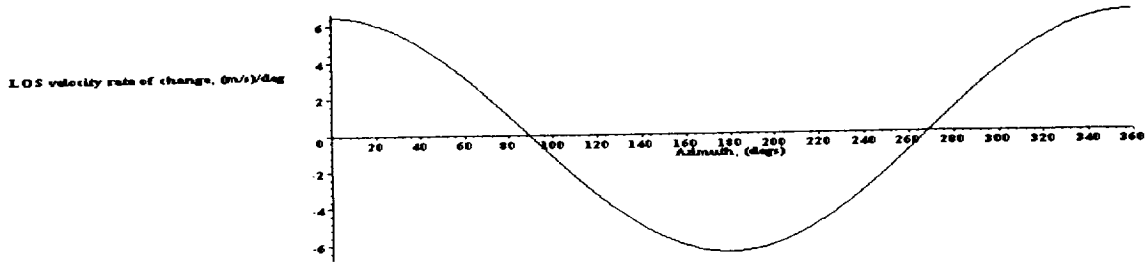

Figure 38: Rate of change of the Earth rotation component of the LOS velocity as a function of azimuth.

As a sanity check we can also remove the earth's rotational velocity such that only the satellite's orbital velocity contributes to the line of sight. This should result in the absolute value of the line of sight velocity being a maximum at 0and 360 deg azimuth and 0 m/s at 90 and 270 deg. azimuth.

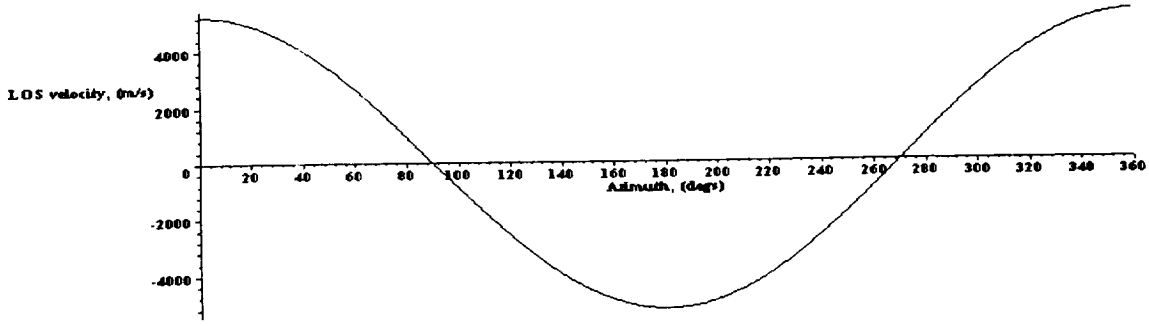

Figure 39: Satellite velocity component of the LOS velocity as a function of azimuth.

This plot provides the result expected. The line of sight velocity also depends on the nadir angle. All subsequent plots of line of sight velocity in this document include components due to the satellite and earth rotation but a 0 m/s target velocity unless otherwise stated. The following plot shows the line of sight velocity dependence on both nadir and azimuth angle:

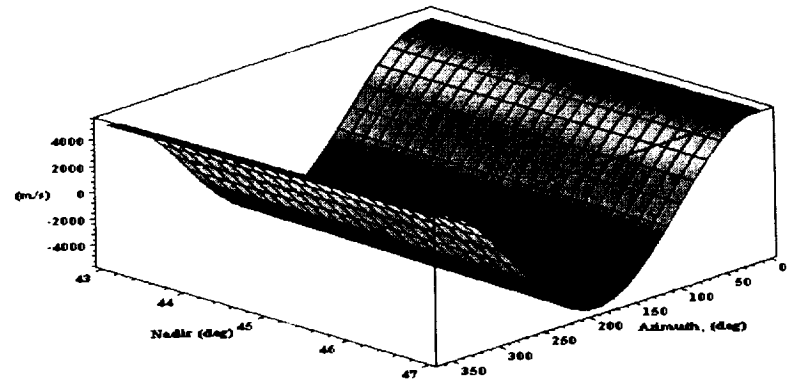

Figure 40: LOS velocity as a function of azimuth and nadir angles.

Clearly the azimuthal dependence dominates over the restricted range of nadir angles plotted. The dependence on nadir only becomes clearly visible when a much wider range of nadir angles is considered:

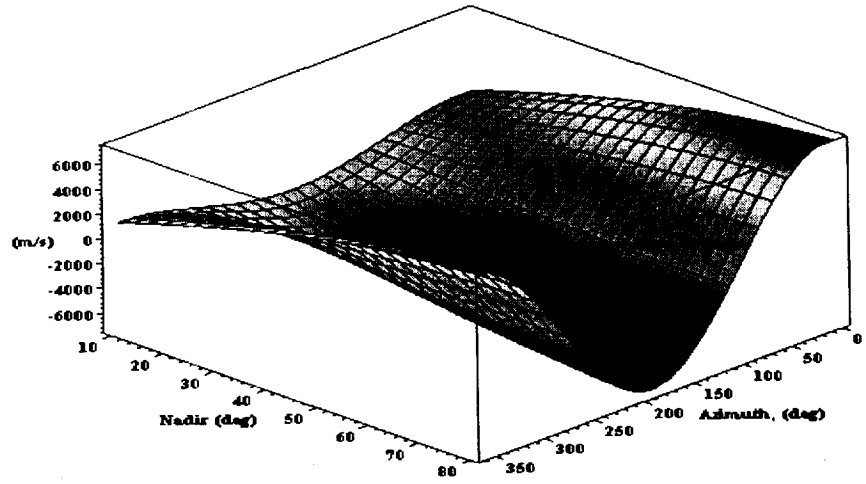

Figure 41: LOS velocity as a function of azimuth and nadir angles.

Alternatively the dependence of the line of sight velocity on nadir angle can be obtained by plotting the differential with respect to the nadir angle:

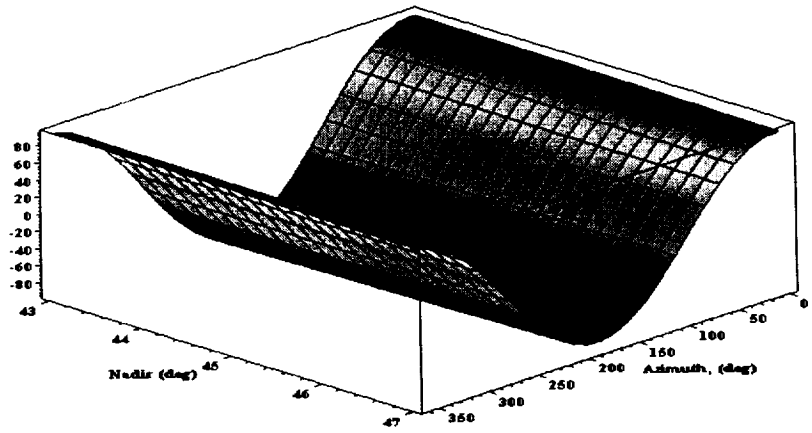

Figure 42: Rate of change of LOS velocity ((m/s)/deg-nadir) with nadir angle.

We can see that the rate of change of the line of sight velocity with nadir angle varies between about ± 90 m/s/deg depending on the azimuth angle as expected. The following plot for an azimuth angle of 0 deg clearly shows the gradient as a function of nadir angle:

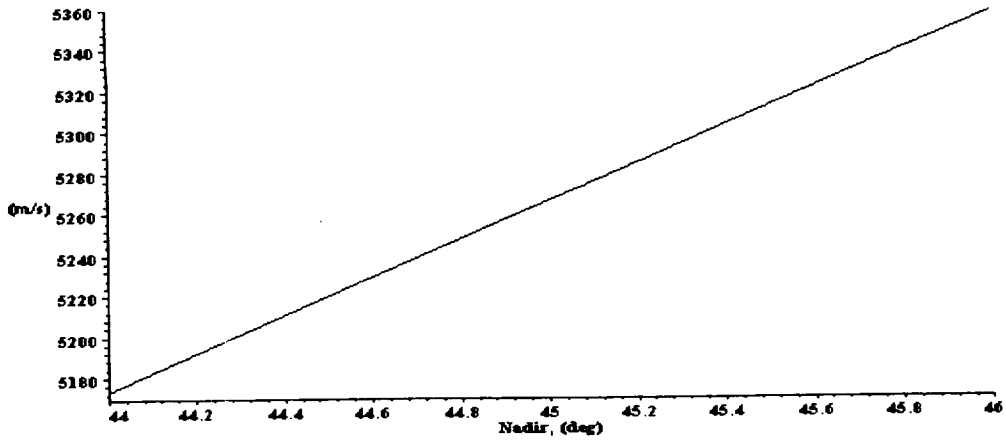

Figure 43: Change of LOS velocity with respect to the value at the nominal nadir angle.

Similarly the following plot shows the variation in the LOS velocity as a function of nadir relative to the LOS velocity at the nominal nadir angle for three azimuth angles of 0 , 45 and 90 degrees respectively.

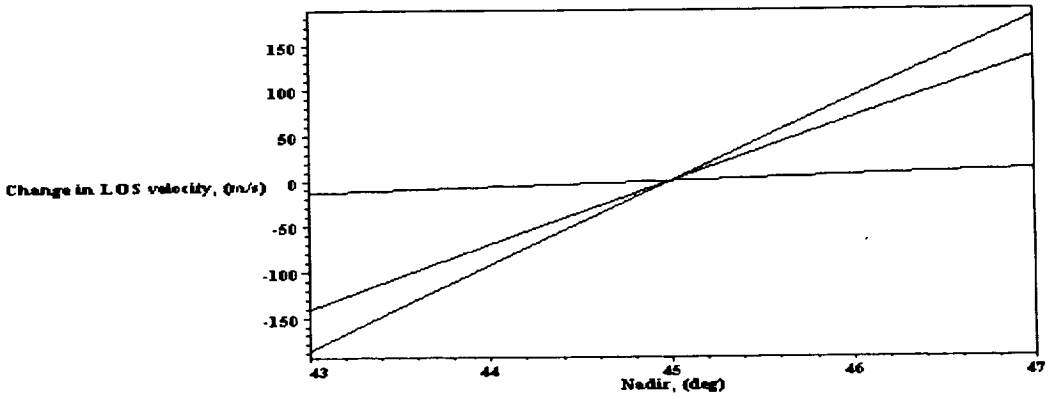

Figure 44: Change of LOS velocity with respect to the value at the nominal nadir angle.

Plotting the change relative to the value at the nominal nadir angle makes the dependence on nadir and azimuth angle easier to see:

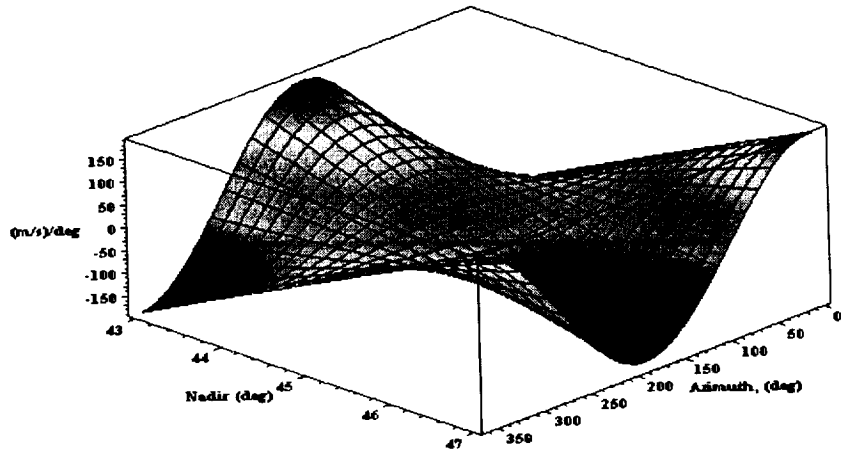

Figure 45: Change of LOS velocity with respect to the value at the nominal nadir angle.

Finally, as a consistency check if we plot the differential of Figure 45 with respect to the nadir angle we should get back to Figure 42.

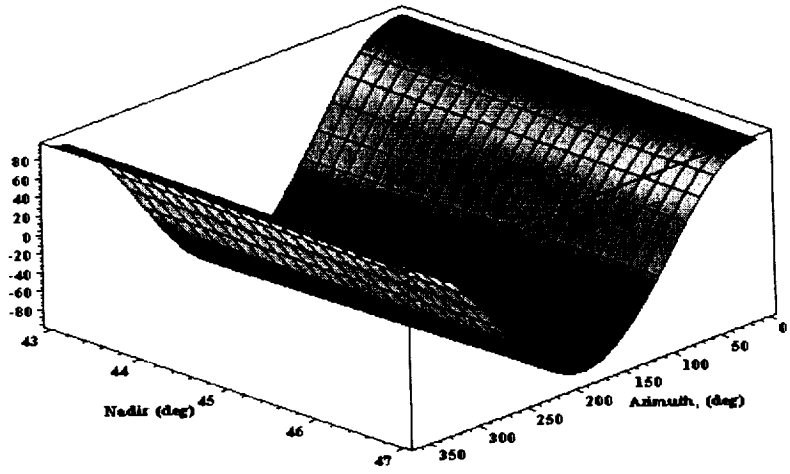

Figure 46: Rate of change of LOS velocity ((m/s)/deg-nadir) with nadir angle.

We can find the dependence on latitude by subtracting the value at the equator from the value at some other latitude.

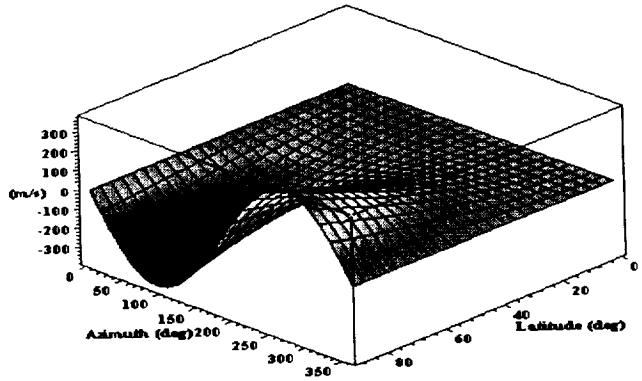

Figure 47: Relative change of LOS velocity as a function of latitude.

What this figure shows is that as the instrument moves to higher or lower latitudes with respect to the equator the component of the line of sight velocity due to the earth's rotation at a given azimuth changes. This occurs because the angle the orbit makes to the local meridian changes as a function of latitude. Plotting the differential of Figure 47 with respect to latitude enables the increase in slope to be determined.

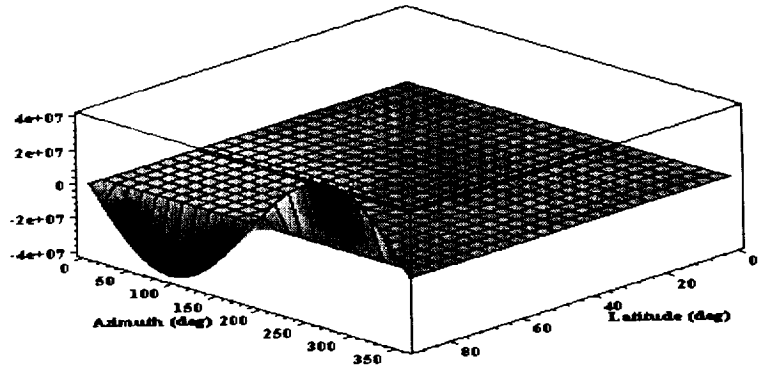

Figure 48: Rate of change of LOS velocity ((m/s)/deg-latitude) as a function of latitude.

Figure 48 clearly shows the rapid increase in the sensitivity to latitude at the highest latitudes. The plot clearly shows the difficulty the numeric routines have near the maximum latitude where the rate of change of line of sight velocity with latitude approaches ± infinity depending on the azimuth angle. We can replot this on a logarithmic scale, using the absolute value of the slope, to get a clearer view of the rate of change and also limit the plot to a latitude slightly below the maximum value. The following plot is for a maximum latitude of 0.001 deg below the true maximum.

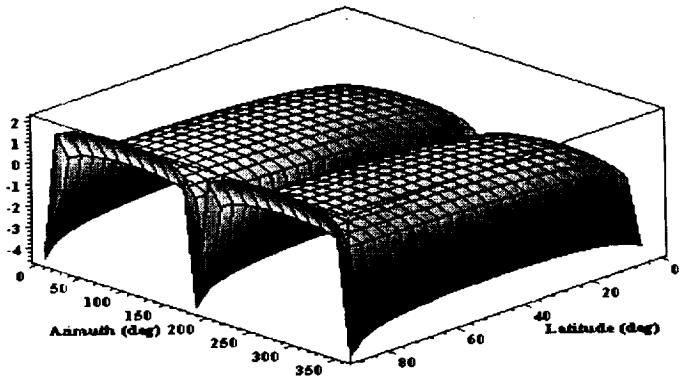

Figure 49: Rate of change of LOS velocity (m/s)/deg-latitude as a function of latitude (log z-axis).

Finally we can plot just the higher latitude portion of this plot:

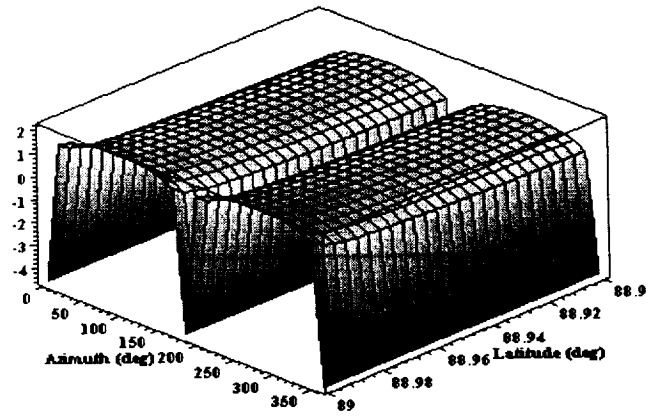

Figure 50: Rate of change of LOS velocity ((m/s)/deg-latitude) as a function of latitude (log z-axis).

The dependence of the line of sight velocity on orbit inclination is shown below:

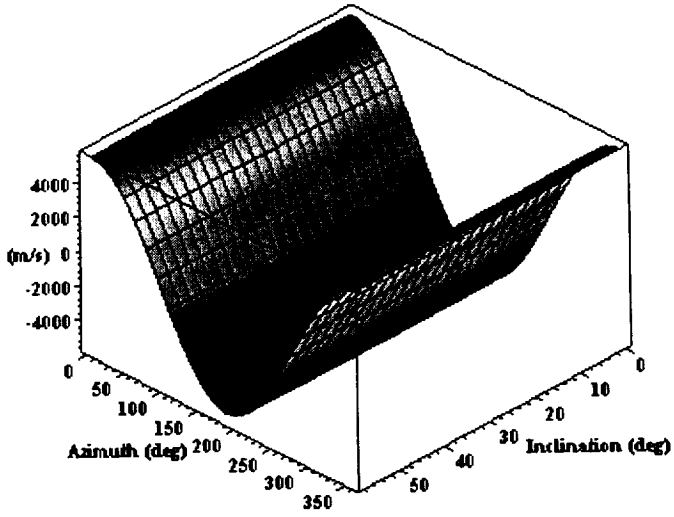

Figure 51: LOS velocity as a function of orbit inclination.

The dependence on azimuth angle is clearly dominant again and we can plot the differential with respect to the inclination angle to more clearly show the dependence on inclination angle.

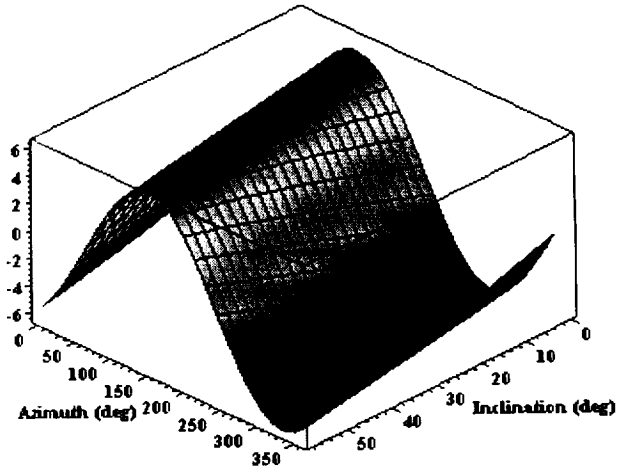

Figure 52: Rate of change of LOS velocity ((m/s/deg-inclination) with orbit inclination.

Figure 8 showed the satellite velocity as a function of orbit height. The line of sight velocity dependence on orbit height for an azimuth angle of 0 deg will simply be a component of this that depends on the nadir angle. Although the line of sight velocity component contains a contribution from the earth's rotational velocity this is so much smaller than the satellite velocity that it will not be visible in the plot.

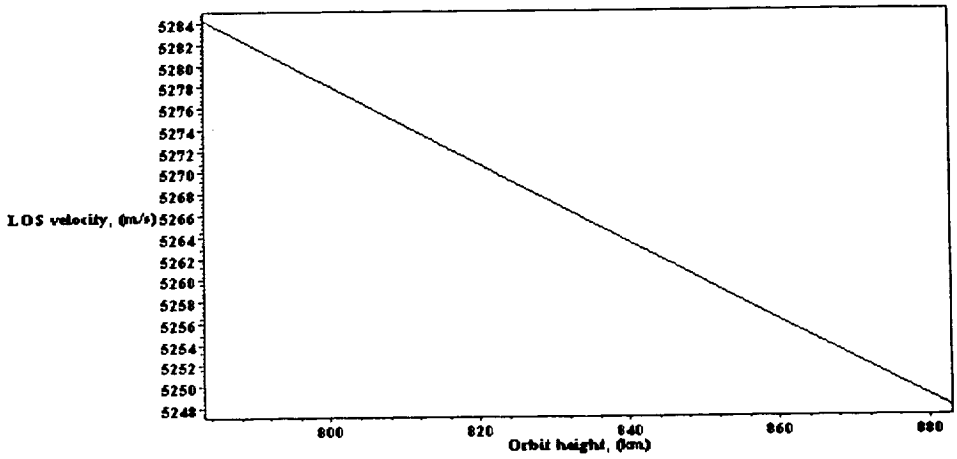

Figure 53: LOS velocity as a function of orbit height.

Plotting the differential with respect to the orbit height permits the sensitivity to be easily determined.

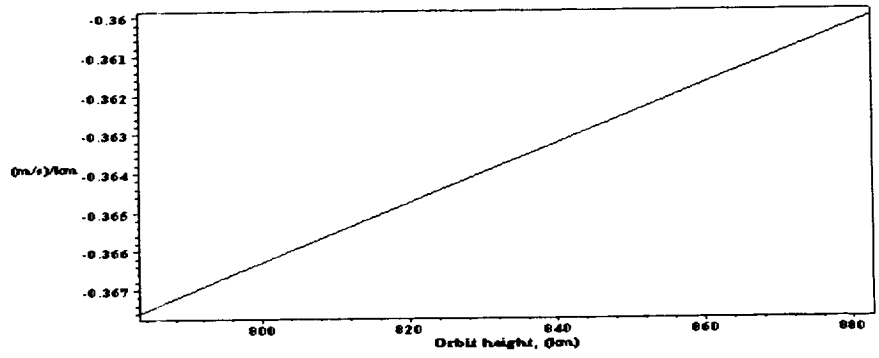

Figure 54: Rate of change of LOS velocity with orbit height.

Figure 54 assumes an azimuth angle of 0 deg which corresponds to maximising the magnitude of the line of sight component of the spacecraft velocity. At other azimuth angles the dependence will be weaker and this is shown in the following 3D plot.

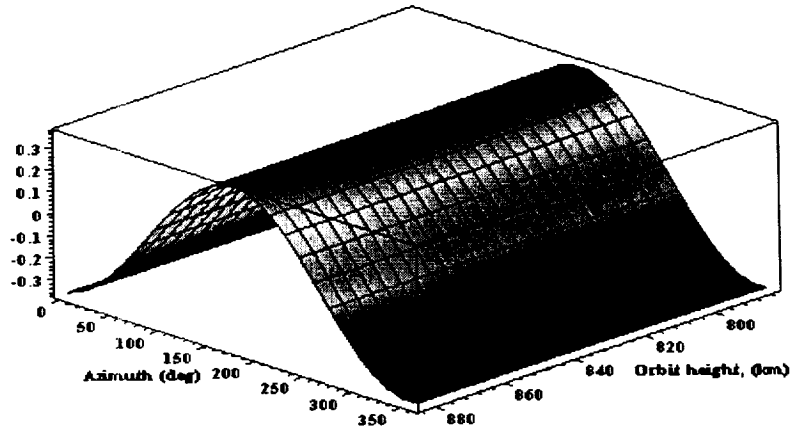

Figure 55: Rate of change of LOS velocity ((m/s)/km-orbh) with orbit height.

The nadir angle at the target varies as a function of the altitude of the target and so the line of sight velocity has a weak dependence on the target latitude. This is shown below for an azimuth angle of 0 degrees.

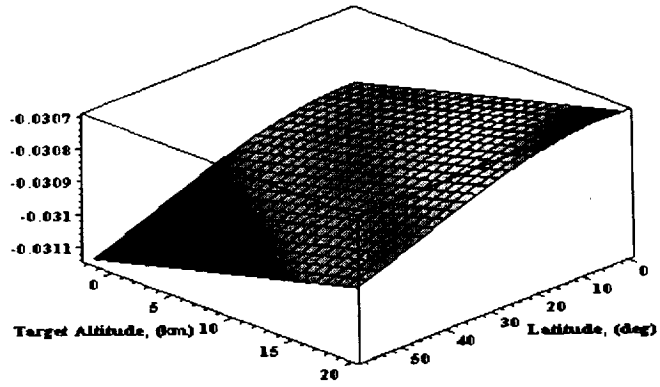

Figure 56: Rate of change of LOS velocity ((m/s)/km-altitude) with target altitude.

For a fixed azimuth angle the line of sight velocity should be simply proportional to the satellite horizontal and vertical velocities with the constant of proportionality being simply the sine and cosine of the nadir angle respectively. Plotting the differential of the line of sight velocity with respect to the satellite velocity should therefore obtain sin(nadir) and cos(nadir) for the horizontal and vertical velocities respectively.

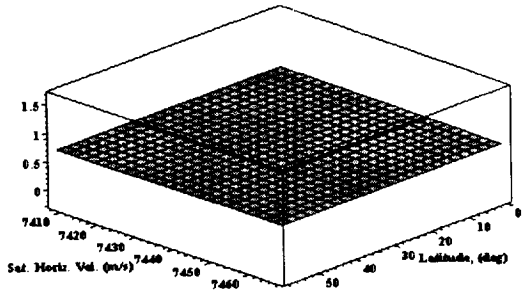

Figure 57: Rate of change of LOS velocity with satellite horizontal velocity.

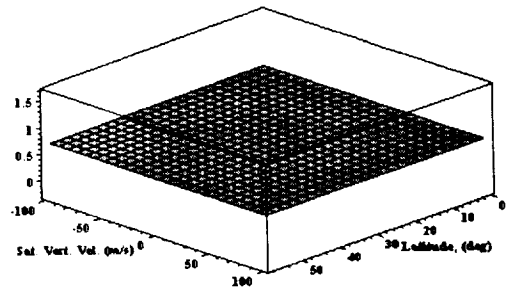

Figure 58 Rate of change of LOS velocity with satellite vertical velocity.

This provides the anticipated result. Plotting as a function of latitude ensures that there are no WGS84 related dependencies. As indicated previously the line of sight velocity includes a component due to the earth's rotational velocity (Figure 37). The earth's rotational velocity also depends on the latitude (Figure 18) as does the nadir angle at the surface (Figure 20). These dependencies combine to create a complex surface that must be accounted for in order to correctly determine the target velocity independent of the latitude and azimuth angle.

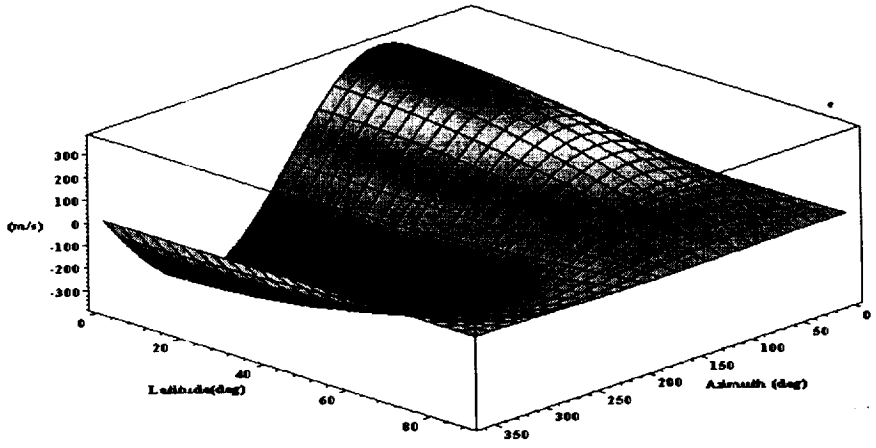

Figure 59: LOS velocity due to earth rotation.

We can plot the differential with respect to the azimuth angle and latitude respectively to determine the sensitivities.

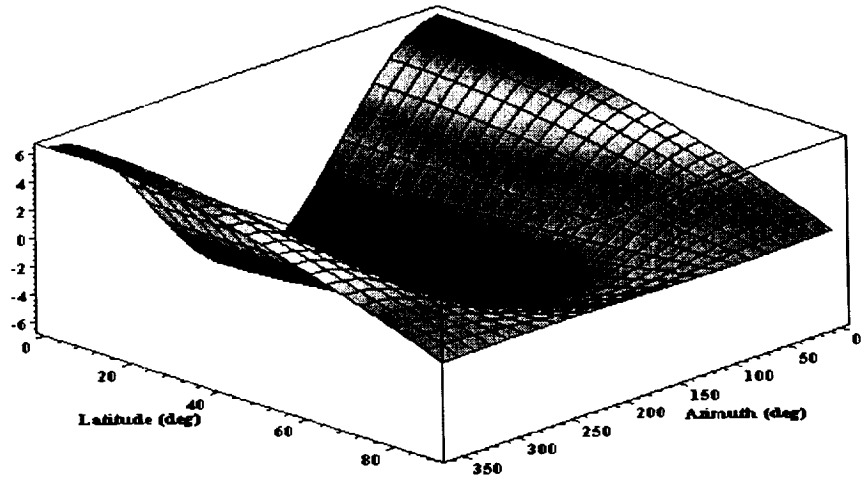

Figure 60: Rate of change of line of sight component of the earth's rotational velocity ((m/s)/deg-azimuth) with azimuth.

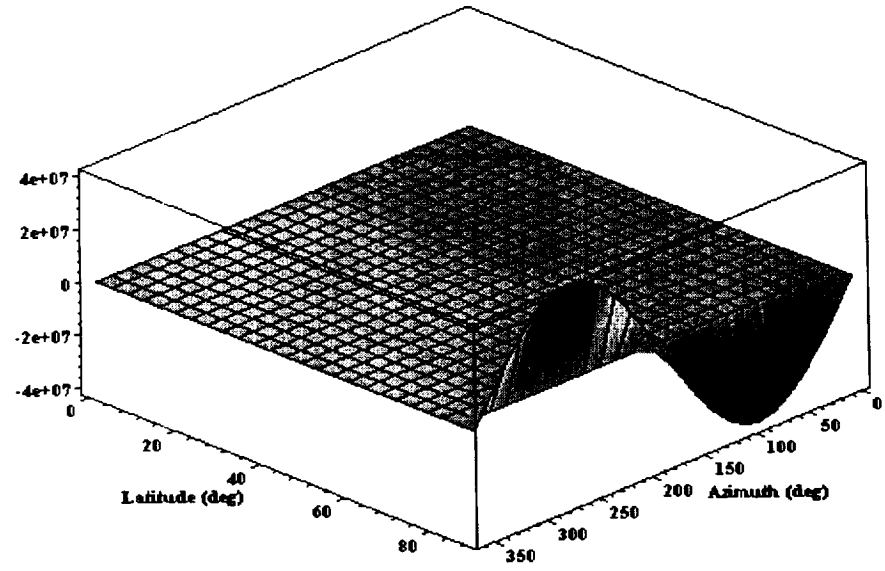

Figure 61: Rate of change of line of sight component of the earth's rotational velocity ((m/s)/deg-latitude) with latitude.

The rate of change of the line of sight component of the earth's rotational velocity with latitude (Figure 61) should be the same as for the rate of change of the total line of sight velocity (Figure 48).

We now consider the frequencies seen by the lidar. The local oscillator frequency is given by:

```
lo_f:=proc(lambda)
 global v_c:
 v_c/lambda;
end;
```

where lambda; is the wavelength and v_c is the velocity of light. In order to reduce the detector bandwidth we want to tune one of the lasers to track the anticipated Doppler shift from the line of sight velocities due to the spacecraft and earth rotation velocities. The Doppler shift tuning function is given by:

```
tune_f:=proc(n,az,alt,inc,orbh,lat,hsatv,vsatv,lambda)
 (hsatv*cos(az)*sin(n)+vsatv*cos(n)+Vlat(lat)*sin(orblat(lat,inc)+az)*
 sin(nadalt(orbh,n,alt,lat)))*2/lambda:
end;
```

If we consider the case where the outgoing laser pulse is tuned then the master oscillator tuning function is given by:

```
mo_f:=proc(n,az,alt,inc,orbh,lat,hsatv,vsatv,lambda,offset_f,deadband,qswitchf)
 global d2r;
 local a,b,c;
 b:=tune_f(n,az,alt,inc,orbh,lat,hsatv,vsatv,lambda)+qswitchf;
 if (evalf(az<90*d2r) and evalf(abs(b+offset_f)<deadband)) then a:=b+offset_f;
 elif (evalf(az>=90*d2r) and evalf(az<=270*d2r) and evalf(abs(b-offset_f) >= deadband) ) then
  a:=b-offset_f;
 else a:=b+offset_f
 fi;
 lo_f(lambda)-a;
end;
```

where offset_f is the desired offset frequency on the atmospheric signal detector for a target velocity of 0 m/s, deadband is the deadband desired to avoid operating the electronics too close to D.C. and qswitchf is the frequency offset that the slave oscillator

q-switch introduces. The deadband is primarily required to ensure that the MO/LO offset frequency can be accurately measured. We can plot the master oscillator tuning as a function of azimuth angle for a latitude of 45 deg, a wavelength of 2.051 μm, an offset frequency of 250 MHz, a deadband of 100 MHz and a q-switch frequency shift of 50 MHz.

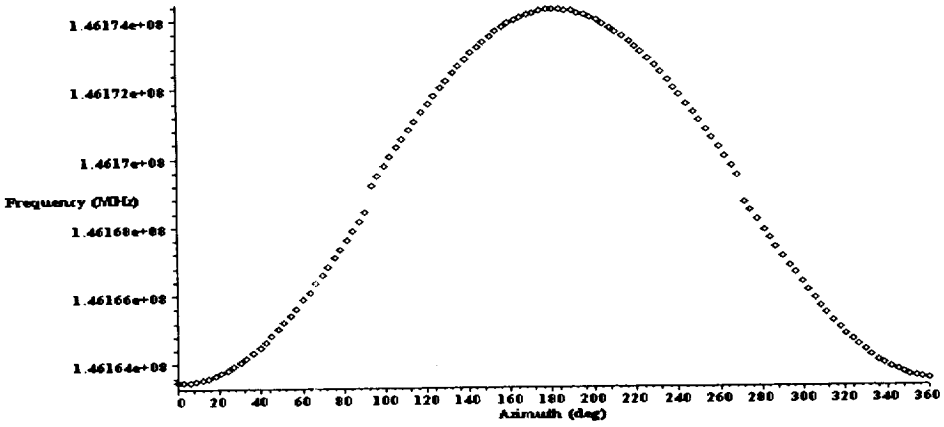

Figure 62: Master oscillator tuning.

The plot clearly shows the frequency hop in the tuning curve that is required to meet the deadband requirements. The slave oscillator output frequency is simply the master oscillator frequency combined with the slave oscillator frequency shift.

```
Slave_f:=proc(n,az,alt,inc,orbh,lat,hsatv,vsatv,lambda,offset_f,deadband,qswitchf)
  mo_f(n,az,alt,inc,orbh,lat,hsatv,vsatv,lambda,offset_f,deadband,qswitchf)+qswitchf;
end;
```

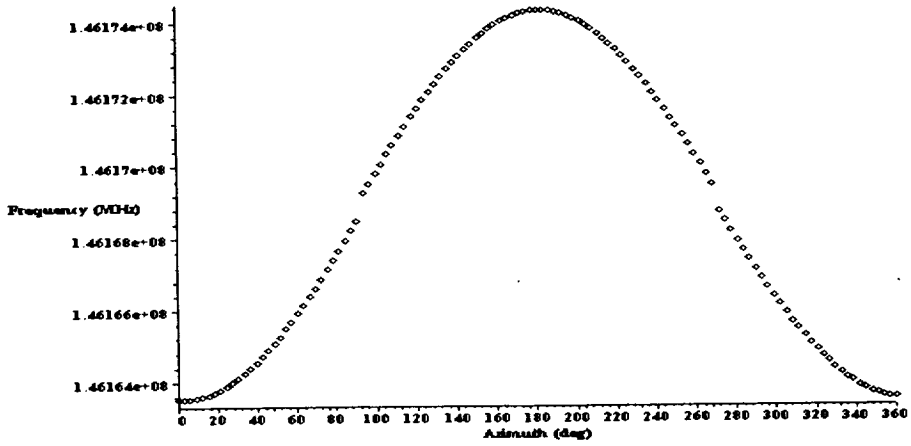

Figure 63: Slave oscillator frequency.

The slave oscillator frequency is Doppler shifted.

```
Doppler_f:=proc(n,az,alt,inc,orbh,lat,trgta,vtrgtv,htrgtv,hsatv,vsatv,lambda,offset_f,deadband,qswitchf)
 global v_c;
 los_vel(n,az,alt,inc,orbh,lat,trgta,vtrgtv,htrgtv,hsatv,vsatv)*2*
 Slave_f(n,az,alt,inc,orbh,lat,hsatv,vsatv,lambda,offset_f,deadband,qswitchf)/v_c;
end;
```

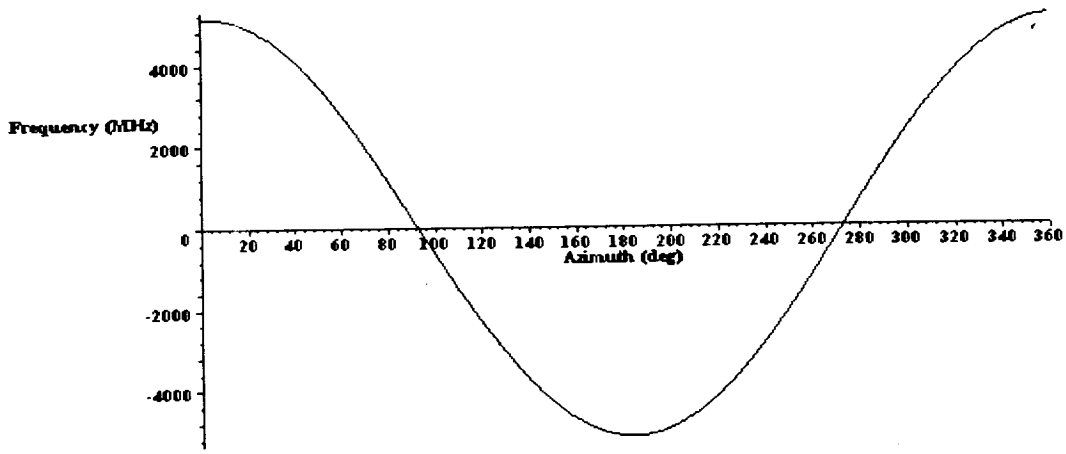

Figure 64: Doppler frequency shift.

One of the detectors monitors the offset frequency between the master oscillator and the local oscillator. This detector sees the full bandwidth of possible signals and is the one that requires the deadband frequency to ensure adequate measurement of the MO/LO offset frequency. The MO/LO frequency difference is given by:

```
molo_f:=proc(n,az,alt,inc,orbh,lat,hsatv,vsatv,lambda,offset_f,deadband,qswitchf)
 lo_f(lambda)-mo_f(n,az,alt,inc,orbh,lat,hsatv,vsatv,lambda,offset_f,deadband,qswitchf);
end;
```

The return signal is mixed with the local oscillator on the signal detector and the return signal/LO frequency difference is given by:

```
det_f:=proc(n,az,alt,inc,orbh,lat,trgta,vtrgtv,htrgtv,hsatv,vsatv,lambda,offset_f,deadband,qswitchf)
 Slave_f(n,az,alt,inc,orbh,lat,hsatv,vsatv,lambda,offset_f,deadband,qswitchf)+
 Doppler_f(n,az,alt,inc,orbh,lat,trgta,vtrgtv,htrgtv,hsatv,vsatv,lambda,offset_f,deadband,qswitchf)-
 lo_f(lambda);
end;
```

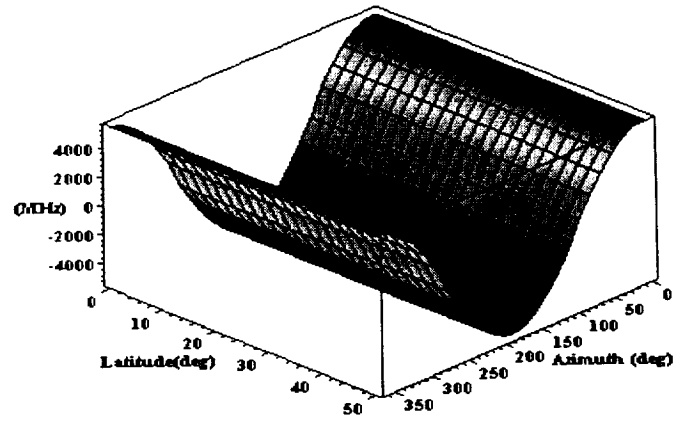

Figure 65: LO/MO frequency difference.

Note that the plot above is discontinuous about 0 MHz due to the frequency jump that is introduced by the tuning algorithm however this discontinuity does not show up in the plot because of the plotting routine. In order to clearly show the discontinuity we can plot a slice through the above plot at a fixed latitude value (45 deg).

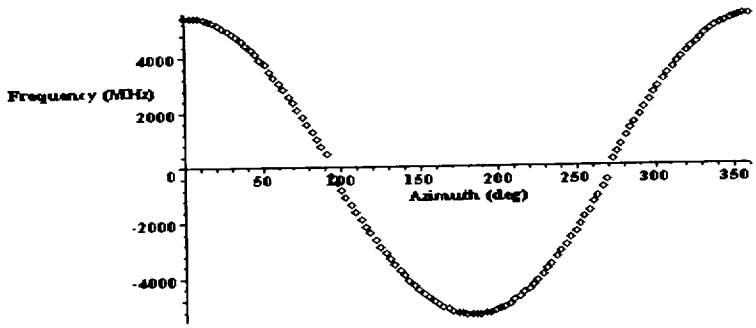

Figure 66: LO/MO frequency difference.

The frequencies from the MO/LO detector are simply given by:

```
molodet_f:=proc(nadir,az,alt,inc,orbh,lat,hsatv,vsatv,lambda,offset_f,deadband,qswitchf)
 abs(molo_f(nadir,az,alt,inc,orbh,lat,hsatv,vsatv,lambda,offset_f,deadband,qswitchf));
end;
```

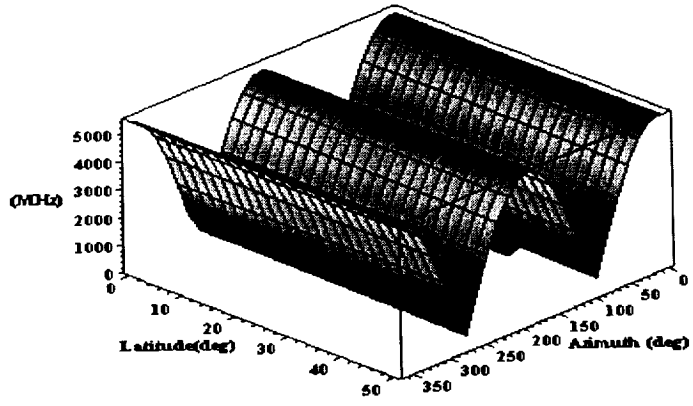

Figure 67: LO/MO detector frequency.

The minimum frequency in this plot is 100.9 MHz which is greater than the deadband frequency desired. Thus the algorithm correctly maintains the deadband requirements on the MO/LO detector. The Q-switch introduces a frequency offset of the slave oscillator frequency with respect to the master oscillator frequency. Taking the beat frequency between the two should result in the Q-switch frequency shift independent of azimuth angle or latitude.

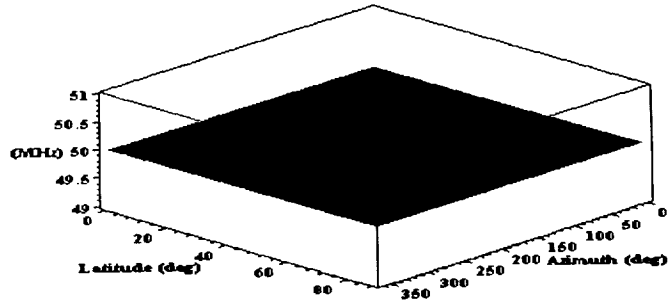

Figure 68: MO/SO frequency difference.

This figure clearly shows that the MO/SO frequency difference is independent of the azimuth angle and latitude. The following figure shows the actual frequency transmitted as a function of azimuth angle and latitude.

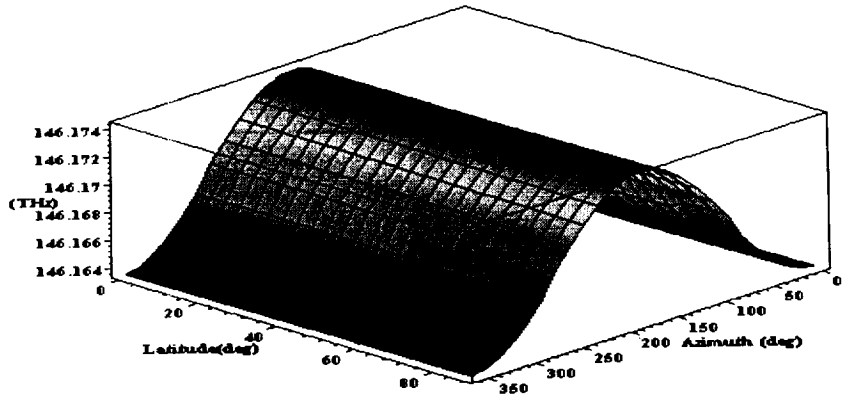

Figure 69: Outgoing slave oscillator frequency.

The transmitted frequency is Doppler shifted by the line of sight components of the satellite, earth rotation and target velocities and returns to the spacecraft where it is mixed with the local oscillator. The frequency difference between the local oscillator and the return signal is:

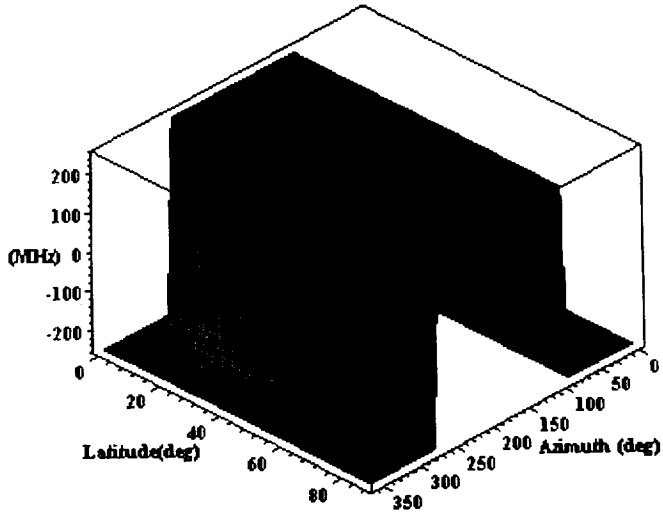

Figure 70: Return signal/LO frequency difference.

Figure 70 clearly shows the signal center frequency hop from -(Offset frequency) to +(Offset frequency) as the tuning algorithm accounts for the MO/LO detector deadband requirements. The frequencies actually seen on the signal detector are the absolute values of Figure 70:

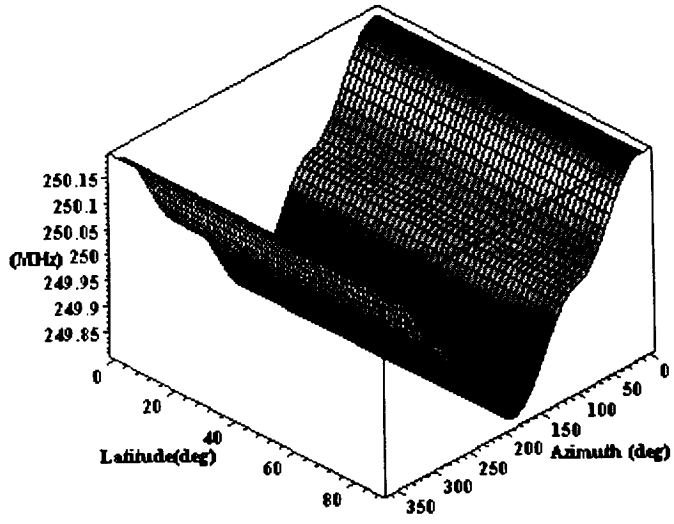

Figure 71: Signal detector frequency.

We can see from this figure that the signal floor is not completely flat but varies by ~± 0.2 MHz. This occurs because the Doppler frequency shift for tuning the MO is calculated from the center frequency of the laser but the actual Doppler frequency shift seen is the shift for a frequency of (center frequency of the laser +calculated offset) and this means there is a small error attributable to the method by which the offset is determined. This error, if not accounted for, introduces the small frequency/velocity error seen in Figure 71. The following figure shows the absolute value of this offset error as a function of azimuth and latitude relative to the 'ideal' value. Knowing this effect it is possible to remove it in post-processing.

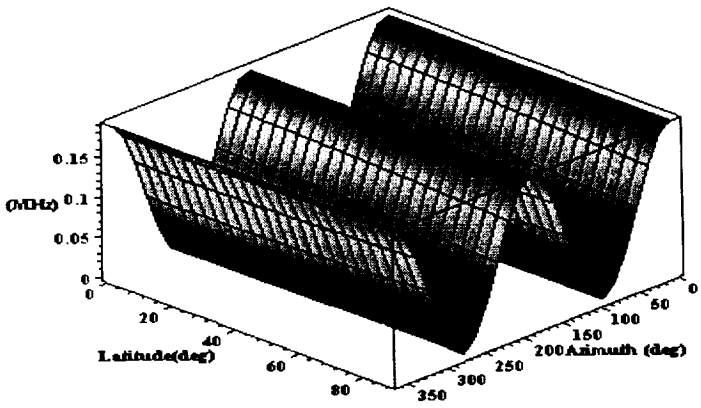

Figure 72: Magnitude of the uncompensated Doppler frequency.

We can plot a series of views of the frequency on the detector as a function of latitude and azimuth for target horizontal velocities of -100 m/s, -50 m/s, 0 m/s, +50 m/s and 100 m/s. This first series of plots is for the velocity always being aligned to the azimuth angle. This ensures that the maximum component of the target velocity is always seen and should result in a frequency independent of latitude and azimuth except for the difference due to maintaining the deadband on the MO/LO detector. Note that there appears to be steps in the following plots in the region around azimuth angles of 90 - 100 degrees. This is an artifact of the plotting grid used - at higher grid resolutions these artifacts disappear. Figure 70 shows how these plots appear with higher resolution plotting grids.

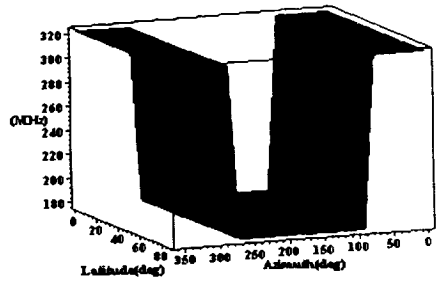

Figure 73: Target velocity of -100m/s.

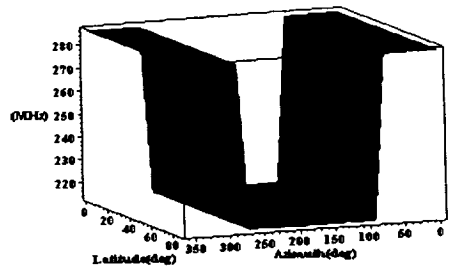

Figure 74: Target velocity of -50m/s.

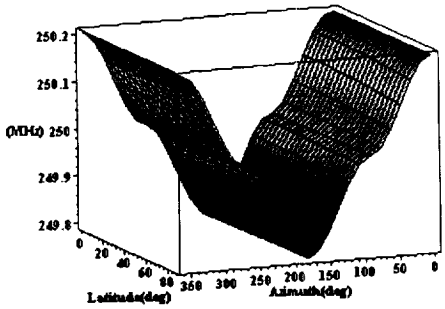

Figure 75: Target velocity of 0m/s.

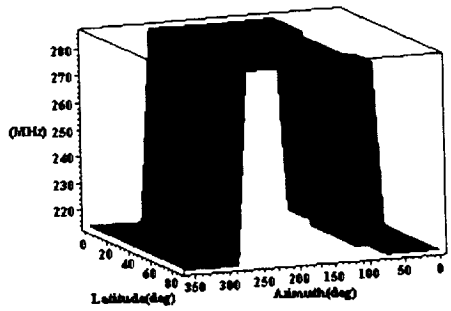

Figure 76: Target velocity of 50m/s.

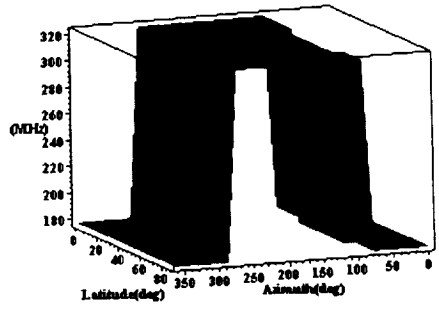

Figure 77: Target velocity of 100m/s.

Figures 73 - 77: Frequency on the detector for target horizontal velocities of -100,-50,0,50,100 m/s into the line of sight.

This set of plots shows that as the target velocity varies between the minimum and maximum velocities the signal frequency is independent of the latitude and azimuth angle and depends only on the magnitude of the target velocity. The clear separation of the two portions of the signal ensures that in post-processing it will be clearly distinguishable where the frequency hop required to maintain the deadband occurred. For comparison purposes the next set of plots is for the same target velocities except that the target velocity is always oriented at a fixed angle, parallel to the lines of latitude. In this case the line of sight component of the target velocity will have an azimuthal dependence. Note that there appears to be steps in the following plots in the region around azimuth angles of 90 - 100 degrees. As in the prior plots this is an artifact of the plotting grid used - at higher grid resolutions these artifacts disappear.

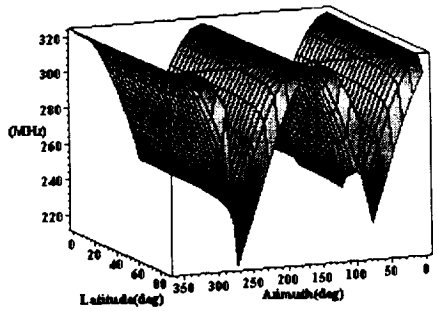

Figure 78: Target velocity of -100m/s.

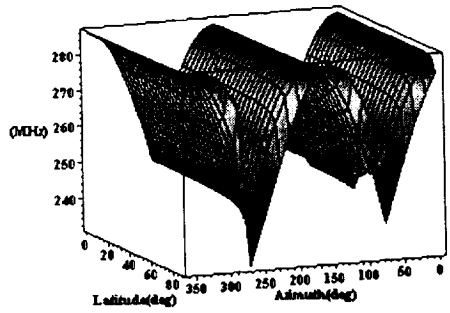

Figure 79: Target velocity of -50m/s.

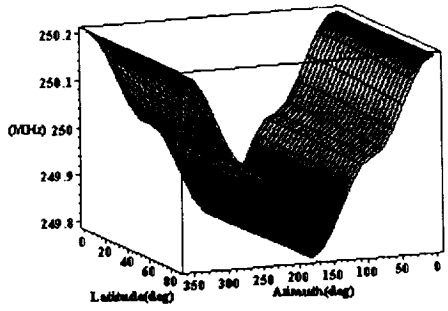

Figure 80: Target velocity of 0m/s.

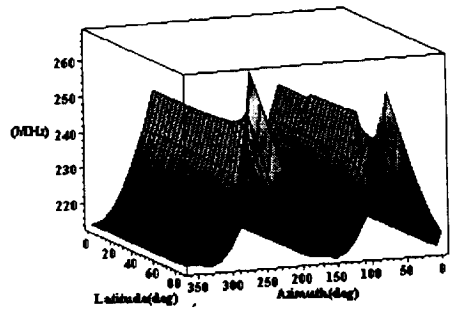

Figure 81: Target velocity of 50m/s.

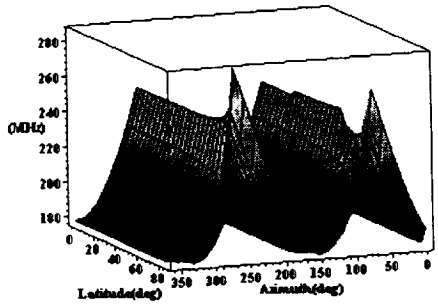

Figure 82: Target velocity of 100m/s.

Figures 78 - 82: Frequency on the detector for target horizontal velocities of -100,-50,0,50,100 m/s parallel to the lines of latitude.

Results from the model of optical propagation within a multi-mode fiber.

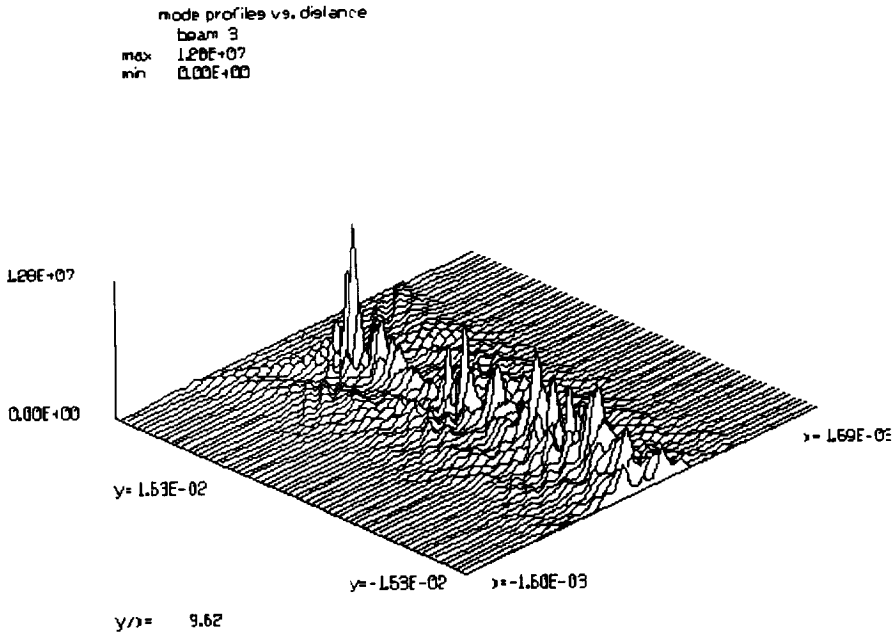

This image shows the mode propagation within a multi-mode fiber. The beam is input on the left with uniform intensity but random phase noise and as it propagates within the fiber the light becomes "guided" within the central core of the fiber. The model currently supports the propagation of about 100 superimposed modes. This plot represents 512 propagation steps (every third step is plotted) and represents propagation of ~300 microns into the fiber.

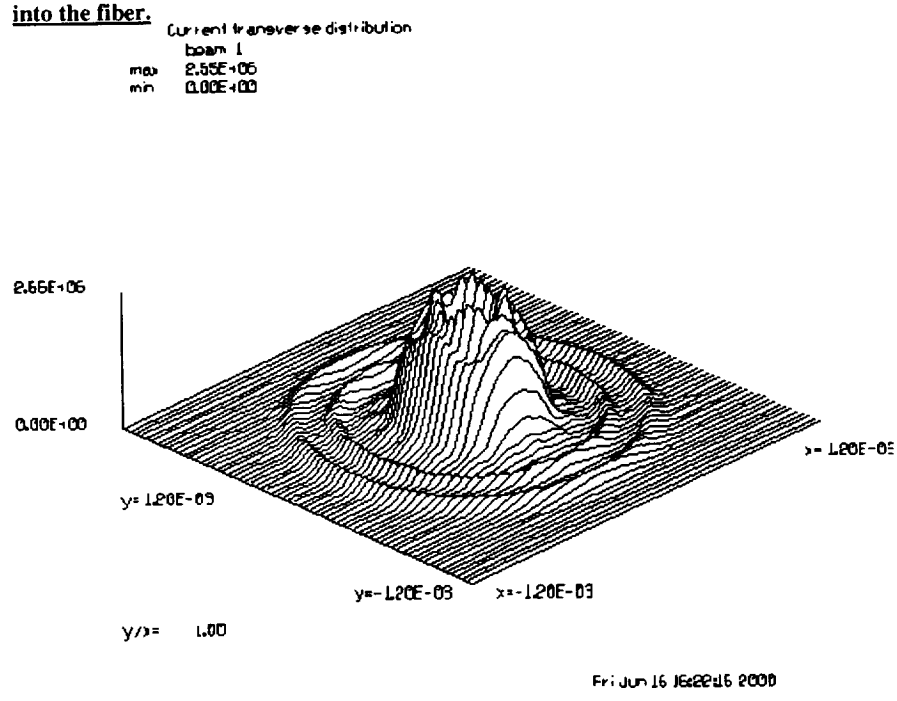

This shows the transverse intensity profile of the beam at the end of the propagation shown above.

DEVELOPMENT OF
SOLID STATE COHERENT LIDAR TECHNOLOGIES

CONTRACT No. NCC8-141

Period:

September 30, 1999 - September 29, 2000

Submitted To:

NASA/MSFC
Marshall Space Flight Center, AL 35812

Prepared By:

Farzin Amzajerdian

March 11, 2002

Center For Applied Optics
University Of Alabama In Huntsville
Huntsville, Al 35899

ACKNOWLEDGMENTS

The author wishes to acknowledge Dr. Bruce Peters, Thomas Papetti, Darrell Engelhaupt, Timothy Blackwell, Diana Chambers, and Deborah R. Bailey for significantly contributing to this work. The author would also like to acknowledge the other members of The Center for Applied Optics at UAH, in particular, Dr. John O. Dimmock and Freya W. Bailey for their support and valuable assistance.

Introduction

The primary motivation for developing CDWL technology is to enable global space-based measurements of tropospheric vector wind profiles for NASA's Earth Science Enterprise (ESE). These tropospheric wind profiles would greatly enhance scientific understanding of the Earth-atmosphere system, atmospheric processes and dynamics, weather, and climate. Another strong motivation for this technology is the requirement of the National Polar-orbiting Operational Environmental Satellite System (NPOESS) Integrated Program Office (IPO) for operational measurements of tropospheric winds ["Unaccommodated Environmental Data Records: Technology Status and Promising Technological Areas," National Polar-orbiting Operational Environmental Satellite System (NPOESS) Integrated Program Office (IPO), 28 June 1996]. NASA is a partner in the IPO with the DOD and the DOC, and is charged with developing needed technology. The IPO has identified tropospheric winds as the most important currently unaccommodated measurement. NOAA, a part of the DOC, would utilize the operational wind measurements to dramatically improve weather forecasting.

Currently available and planned sensors provide only extremely sparse coverage of the tropospheric winds over the oceans and in the Southern Hemisphere. When the wind measurement requirements and the practicalities of space-based sensors are jointly examined, coherent Doppler wind lidar becomes the most promising candidate technology and technique for providing the measurements. Some of these joint requirements and practical considerations are low velocity error, good horizontal and vertical resolution, very low bias, complete low-to-high wind speed capability, conical scan capability, eyesafe laser beam, small size and mass, and minimum electrical power needs.

Secondary motivations are numerous. Applicability of the CDWL technology and technique to NASA's Aeronautics and Space Transportation Technology Enterprise (ASTTE) is planned in the next five years for the aeronautic applications of in-flight winds and Clear Air Turbulence (CAT) detection, and ascent and descent detection of wind shear. The ASTTE may also desire launch and landing wind measurements for Reusable Launch Vehicle (RLV) safety, and object range and velocity measurements for space Automatic Rendezvous & Docking (AR&C) maneuvers. The CDWL technology and technique will also assist NASA's Space Science Enterprise (SSE) by enabling both orbiting and surface based wind measurements of other solar system bodies in the future.

Lightweight Telescope

As part of this activity, a new fabrication technique was developed that will allow for an ultra-lightweight, thermally-stable, telescope capable of scanning the lidar beam and meeting the stringent coherent lidar performance requirements. This fabrication approach is based on electroplating and electroless coating methods that can be utilized to form the material into nickel shells for use as optical components.

Coherent lidars are sensitive to aberrations in the outgoing laser radiation and optical distortions added to the received signal, all of which unacceptably lowers the signal-to-noise ratio (SNR) of the instrument jeopardizing the precision of the measurements made. The telescope required is challenging to build because it has a large field of view requiring diffraction limited performance throughout; low surface scatter from the mirrors and minimal

backscatter towards the detector; highly reflective coatings on the mirrors for the infrared laser; compact optical path to minimize misalignments; and limited reflections to disrupt the beam polarization. To maintain operation on orbit, the telescope should be athermal (uniform coefficient of thermal expansion). To maintain optical alignment between the time it is assembled (under a 1-g environment) and when it reaches orbit (under a μ-g environment) the telescope material needs to have high stiffness (high microyield) and minimal self-weight deflection. Metal mirrors with all of these attributes and without the weight can be fabricated using a novel approach developed by the CAO called LOMASS - Lightweight Optics using Metal Alloy Shells and Surfaces.

In the LOMASS process, illustrated in Figure 1, nested groups of metal shells supply structural support to the thin metal surface that serves as the precision mirror to form a three dimensional shell structure that is rigid yet lightweight. The shells and optical surfaces are formed by either electrochemical deposition or plasma depositing metals, typically nickel or aluminum alloys, to coat a near net shape mandrel, often aluminum, to create as continuous and homogeneous a shell structure over the mandrel as possible. Further structural support is given to the thin shell through a series of lightweight same metal inserts that provide cross bracing within the shell without adversely affecting the quality of the optical surface or adding significantly to the weight. The final figuring of the mirror is accomplished through the use of traditional and readily available commercial optical figuring processes such as diamond turning or polishing. The expense in precision machining is incurred only on the final part and not the mandrel so the process is competitive in cost. Once fabrication, stress relief, and thermal treatments are completed, the mandrel is dissolved leaving a thin metal shell that is self-supporting and which contains a high quality optical surface. The approach includes some unique processing steps in applying the metal shell to minimize the buildup of stress in the shell so that the separation from the mandrel does not cause the shell to distort.

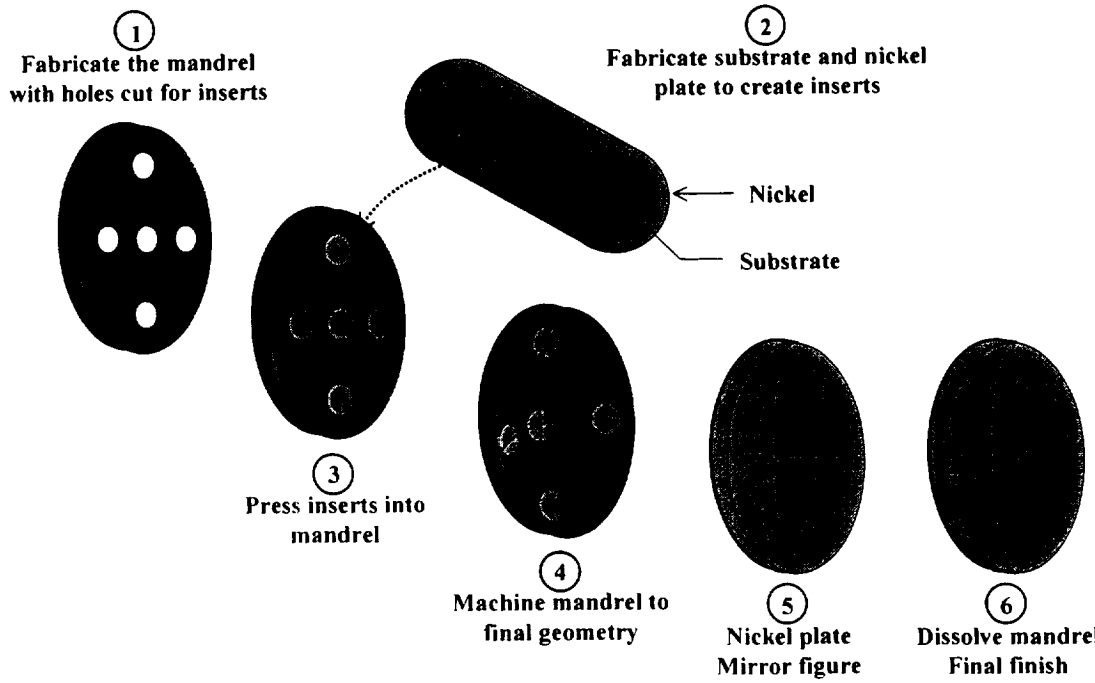

Figure 1 illustrates theLOMASS fabrication process

To maintain operation on orbit where the telescope will likely see colder temperatures than when it was originally aligned, the telescope should be athermal (uniform coefficient of thermal expansion). In this way, it will experience insignificant differential changes in the presence of temperature excursions and thermal gradients so that complex on-orbit realignment systems are eliminated or at least simplified. To maintain optical alignment between the time it is assembled (under a 1-g environment) and when it reaches orbit (under a μ-g environment) the telescope material needs to have high stiffness (high microyield) and minimal self-weight deflection. Aluminum is not stiff enough and has heightened sensitivity to thermal gradients and it is difficult to procure high purity aluminum billets from which to make mirrors. Invar and similar materials are too heavy and therefore unacceptable for space applications. Beryllium, Silicon Carbide, and composites have shown promise for this type of application and could be suitable for space; but they are relatively expensive, require special material handling, and cannot be readily machined using conventional practices. An alternative is to use a metal that has very high microyield and great ultimate strength for the mirrors such that it can maintain its surface figure under the high stress of space launch and during thermal cycles. One such material is Phosphor Nickel. Because of its high modulus of elasticity it can carry relatively large loads and stresses with minimal deformation and the material has excellent thermal properties (low coefficient of thermal expansion, high thermal conductivity, and high thermal capacitance to dampen out transient thermal effects). Furthermore, its relatively high hardness makes it suitable to diamond turn and easy to polish which is important for optics.

The problem with using nickel has been that large billets of the high strength, pure alloy material are difficult to come by and expensive. Therefore, nickel is commonly used as a thin layer, applied by electrolyses nickel coating or electroplating, over other base metals. The nickel then becomes the optical surface that is supported by the base metal beneath. This is commonly done to fabricate quality mirrors where an aluminum substrate is rough machined to near final surface geometry and figure and then coated with nickel. The thin nickel layer bonds well to the aluminum and can be easily diamond turned or polished to achieve the high surface quality desired. The drawback to this approach is that the large aluminum substrate adds a great deal of mass to the optic and the strength of the nickel material are not exploited because it is too thin. Even though the nickel layer is thin, there still remains a significant difference between the coefficient of thermal expansion of the aluminum base and the nickel layer that could cause displacement or distortion of the optical surface. This also increases the potential buildup of stress in the part as the device is cooled after deployment to orbit and reaches the coldness of space. Thicker layers of nickel applied to the base metal could alleviate some of these problems; but it is difficult to achieve good uniformity from the nickel coating processes. Without material homogeneity, the material could develop even worse stress within the nickel causing it to debond from the substrate and fail.

Figures 2 and 3 show two sample pieces, a 10 cm pathfinder and a 25 cm demonstration mirror mandrel, fabricated under this task.

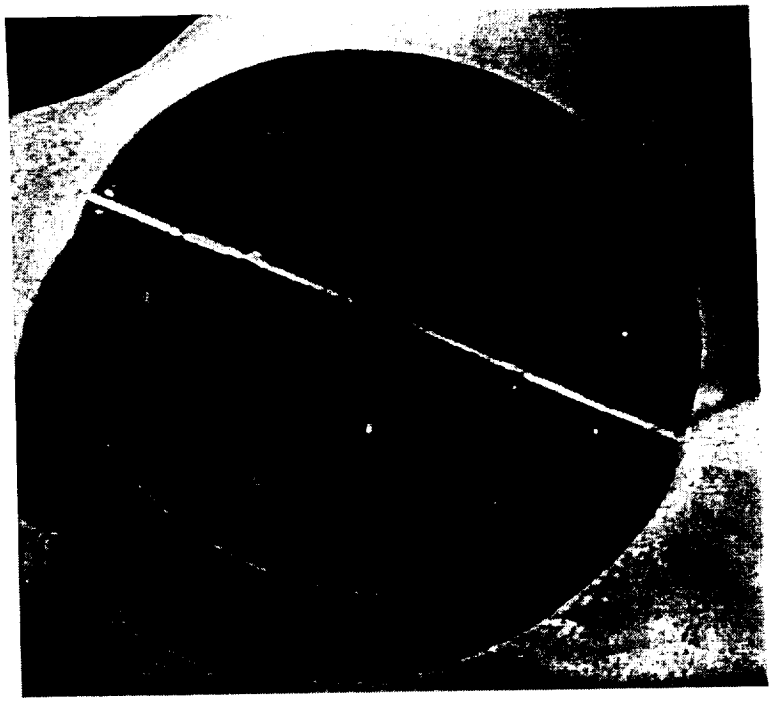

Figure 2. 10cm Mirror Pathfinder

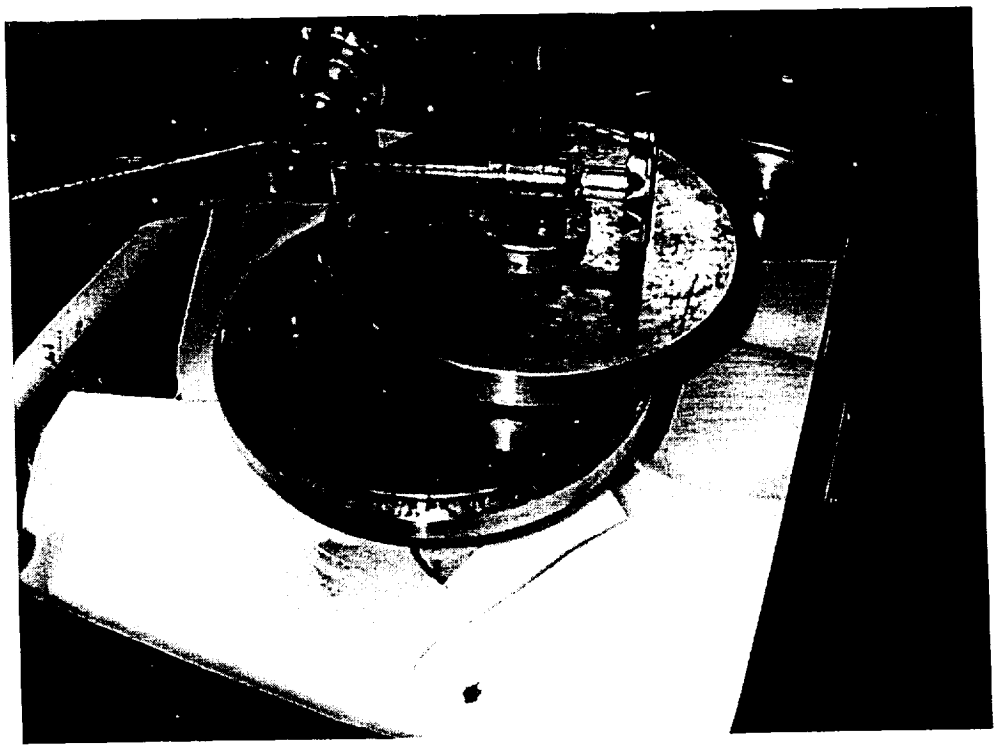

Figure 3. Back side of 25cm Mirror being lapped.

Lidar Receiver

Many coherent lidar applications continue to demand higher levels of sensitivity while imposing stringent power and size constraints. Therefore, optimization of the lidar heterodyne photoreciever is one of the critical steps in ensuring full utilization of limited resources to achieve the required sensititivity. Many earlier works have identified and investigated the critical photoreceiver parameters, such as the detector's nonlinearity, series resistance, parasitic capacitance and inductance, and the preamplifier feedback loading. But, the combined effect of the critical detector and preamplifier parameters, that can play an important role in performance of heterodyne photoreceivers, particularly for wider bandwidths applications, has not been fully investigated. Furthermore, simple expressions for defining the optimum photoreceiver parameters and predicting its performance were never derived.

This paper describes the derivation of the analytical formulations that can accurately predict the performance of heterodyne photoreceivers. The derived formulations include a closed-form expression for the optimum local oscillator power as a function of the detector and the preamplifier characteristics parameters. Using these derived expressions, the optimum designs of several heterodyne receiver configurations, suitable for coherent lidars operating at 2 microns wavelength, have been analyzed. This paper also presents and discusses representative results of these analyses based on actual measured InGaAs detector parameters.

Photoreceiver Model

The performance of any heterodyne photoreceiver is established by the operating and intrinsic parameters of its detection device and its interfacing preamplifier. Figure 1 shows a typical heterodyne photoreceiver topology where the detector output current is amplified by a transimpedance amplifier. As explained by Morikuni, et al.[1], the performance of photoreceivers is best described by their Transimpedance Transfer Function (TTF) as opposed to the standard transfer function defined by the circuit response to a rectangular pulse input. The TTF simply relates the output voltage of the detector preamplifier to the current generated by the detector upon illumination of an optical radiation for a given circuit topology. Since the TTF is signal-independent, it provides more accurate noise formulations for analyses of photorecievers.

Using the topology of figure 4, the TTF was obtained and written in a form suitable for analysis and optimization of heterodyne phototrecievers:

$$H_T(\omega) = \frac{v_{out}}{i_{in}} = \frac{-A_0 R_f}{B + j\omega C + (j\omega)^2 D}$$

where A_0 is the amplifier DC open-loop gain, and

$$B = 1 + A_0$$

$$C = R_f(C_{in} + C_d + (1 + A_0)C_f) + R_s C_d + 1 \quad \omega 0$$

$$D = R_f R_s C_d(C_{in} + (1 + A_0)C_f) + R_f(C_{in} + C_d + C_f) \quad \omega 0 + R_s C_d \quad \omega 0$$

R_f and C_f are the feedback resistance and capacitance, C_{in} is the amplifier input capacitance and C_d is the detector junction capacitance.

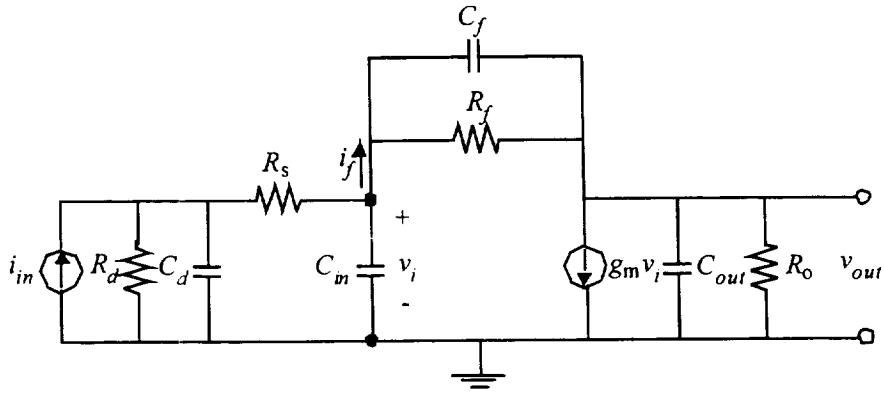

Figure 4. Optical Heterodyne Receiver Topology.

Signal To Noise Ratio

Including the detector non-linearity, the detector DC output in response to an optical power can be written as:

$$I_d = \rho P_{in} - \rho\alpha P_{in}^2$$

where P_{in} is the incident optical power, I_d is the detector output current, ρ and α are the detector responsivity and non-linearity coefficients. The heterodyne signal power is then given by[2]

$$\langle i_s^2 \rangle = 2F_0[\rho(1-2\alpha P_{LO})]^2 P_{LO} P_s$$

where F_0 accounts for the signal power reduction due to speckle, turbulence, atmospheric transmission, misalignment and other systematic losses.

The major noise sources for a heterodyne receiver are the detector shot noise, dark current noise, amplifier input noise voltage and input noise current, and amplifier feedback resistor thermal noise. Using the TTF given earlier, the total noise power referred to the photoreceiver input wase obtained.

Using the expressions for the signal and noise powers, the receiver Signal-to-Noise Ratio (SNR) can be simplified and written in the following form.

$$\frac{S}{N} = \frac{2\rho^2(1-2\alpha P_{LO})^2 P_{LO} P_s F_0}{\left(2e\rho(1-\alpha P_{LO})P_{LO} + 2eI_d + \frac{4KT_e}{R_f} + \langle i^2_{N_{amp}} \rangle\right)\left(\frac{B}{4C}\right)}$$

Optimum Local Oscillator Power Level

The optimum local oscillator power can be obtained by setting the derivative of the SNR equation to zero and solve for P_{LO}, that is[2]

$$\frac{d(S/N)}{dP_{LO}} = 0$$

After some tedious algebraic manipulations, the optimum local oscillator power was obtained in closed and simple form, given by:

$$(P_{LO})_{opt} = \frac{1}{2\alpha} - \frac{1}{2\alpha}\left(1 + \frac{2\alpha N}{e\rho}\right)^{1/2}\left[\cos\left(\frac{1}{3}\text{atan}\sqrt{\frac{2\alpha N}{e\rho}}\right) - \sqrt{3}\sin\left(\frac{1}{3}\text{atan}\sqrt{\frac{2\alpha N}{e\rho}}\right)\right]$$

Where

$$N = 2eI_d + \frac{4KT_e}{R_f} + \langle i^2_{N_{amp}} \rangle$$

This expression provides an easy tool for specifying the optimum local oscillator power provided knowledge of the detector responsivity and non-linearity parameters and the preamplifier noise characteristics. Figure 5 illustrates the dependence of the optimum local oscillator power on the detector non-linearity and the preamplifier noise power using a responsivity of 1.5 A/W that is typical for InGaAs detectors. As can be seen from this plot, the dependence of the optimum local oscillator power level on the detector non-linearity increases with the preamplifier noise power.

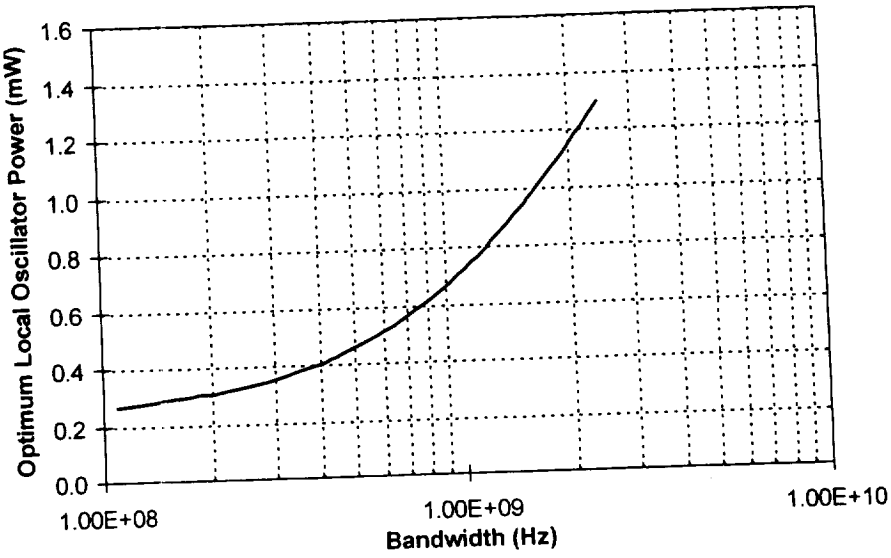

Figure 7. Optimum local oscillator power as a function of operating bandwidth.

Ground-based Coherent Doppler Lidar Experiments

These experiments were performed using a Pulsed Coherent Lidar developed for MSFC by Coherent Technologies Inc. and US Air Force. This lidar is a relatively high power solid state system suitable for both ground-based and airborne measurements (see Figure 8). This system uses a flash lamp-pumped Tm:YAG laser as the transmitter and a diode-pumped continuous wave (CW) laser as the master oscillator (MO). The lidar signal detector is a room-temperature InGaAs detector with a quantum efficiency of about 80%. This lidar system has been successfully used in several airborne measurement campaigns onboard an Air Force C-141 aircraft. The lidar major specifications are summarized in table 1.

Table-1. Pulsed Coherent Doppler Lidar Specifications

Operating Wavelength	2.018 μm
Lasing Material	Tm:YAG
Transmitter Laser Pump	Flash Lamp
Pulse energy Laser	48 mJ
Pulse Repetition Rate	7 Hz
Pulse Width	550 nsec
Clear Aperture Diameter	10 cm
Lidar Transceiver Dimensions	1.07(L) x 0.61(W) x 0.18 (H) m^3

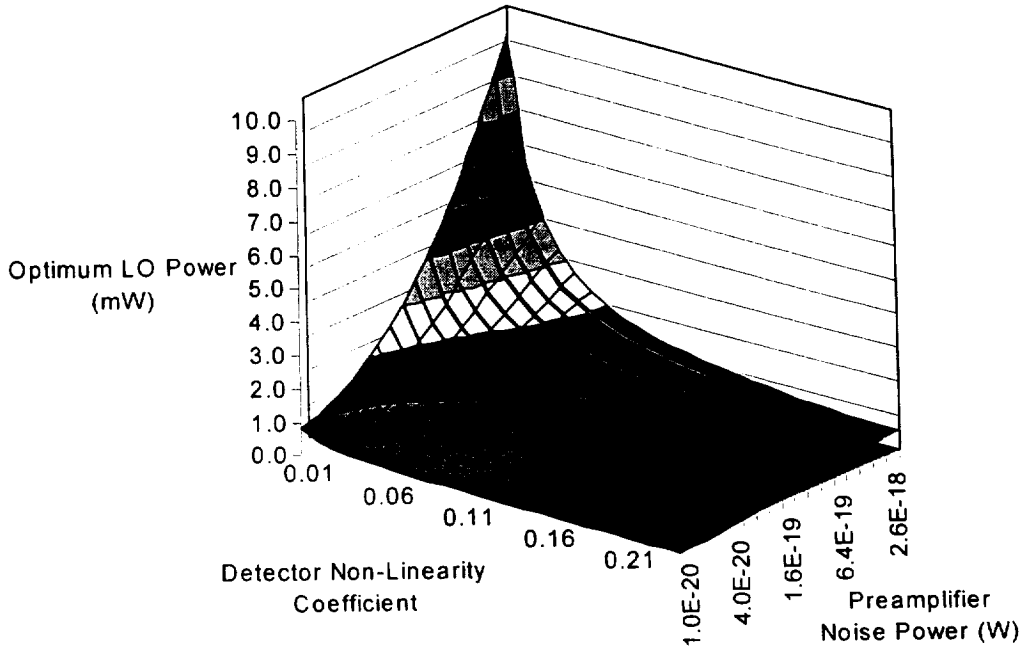

Figure 5. Optimum local oscillator power dependence on detector non-linearity and preamplifier noise power.

Figure 6 shows the responsivity and non-linear behavior of an InGaAs detector, with an active area diameter of 75 microns, at 2 microns wavelength[3]. Figure 7 shows the optimum local oscillator power of a heterodyne photoreceiver, using the detector of Figure 6, as a function of operating bandwidth. This example uses a MESFET transimpedance preamplifier for which its feedback resistance is adjusted in accordance with the receiver bandwidth. Figure 7 shows the strong dependence of the optimum local oscillator power on the operating bandwidth. It also indicates that excessive local oscillator power, particularly for narrower bandwidth applications, can significantly reduce the receiver's sensitivity.

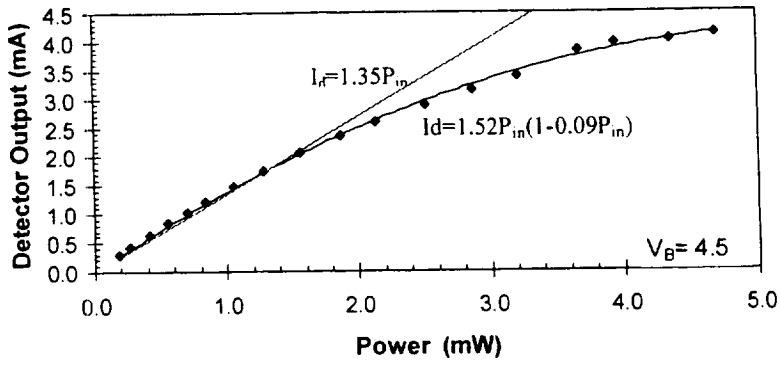

Figure 6. Responsivity of an InGaAs detector at 2 microns wavelength.

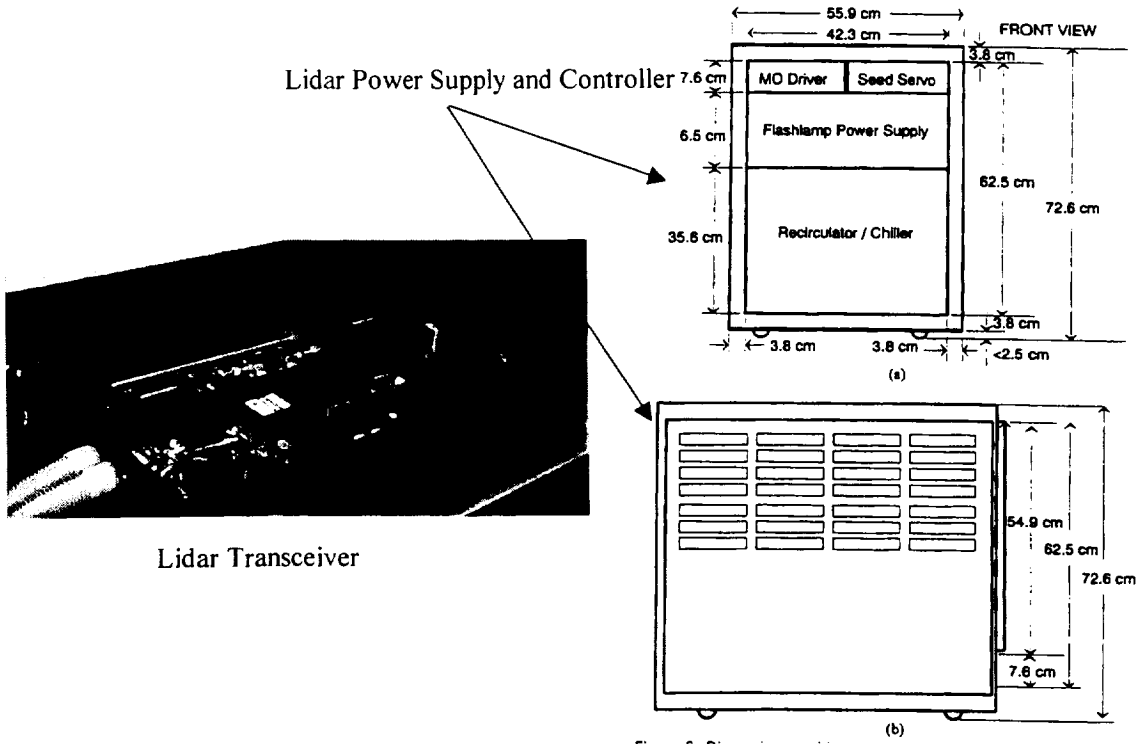

Figure 8. MSFC Pulsed Coherent Doppler Lidar System

Figures 9 and 10 show an example of measurements performed at Wilson Dam.

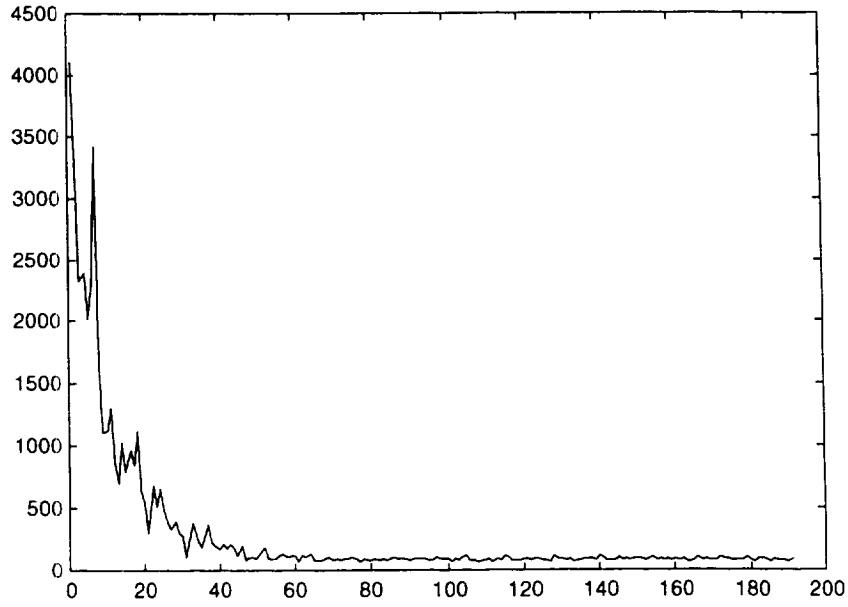

Figure 9. Amplitude vs. Range.

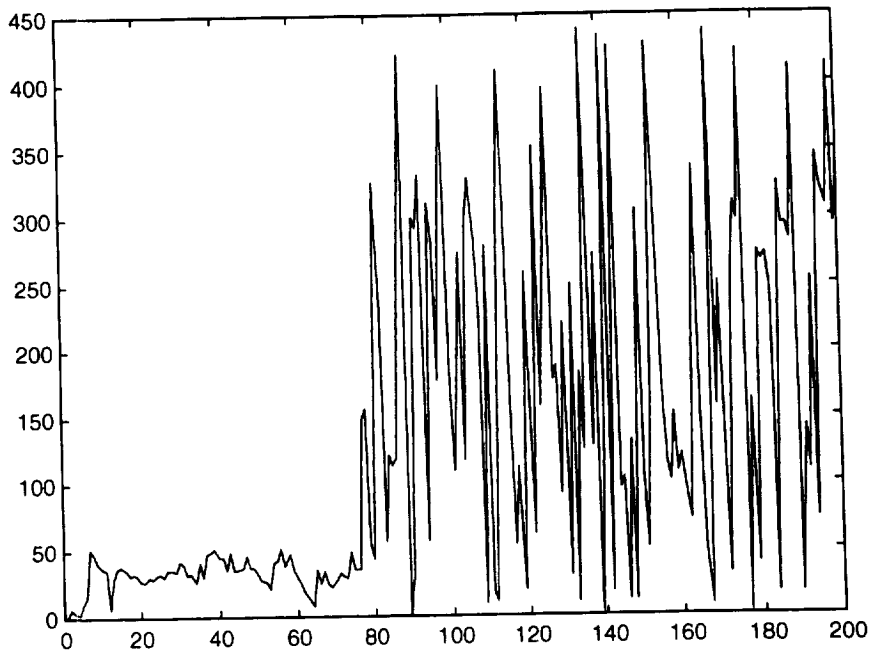

Figure 10. Frequency vs. Range

Diffractive Scanner

Under this task task, improvements were made in the plasma etching chemistry of TiO2 that greatly reduced process time and improved results. Based on suggestions in recent literature, a new gas was introduced into the etching plasma in varying concentrations and pressures until a desirable process was achieved. The new process resulting from this chemistry yielded straight, vertical sidewalls on our gratings rather than the slanted, trapezoidal shape obtained previously. More importantly, the time to complete an etch was reduced by a factor of 15; this implies a reduction in process time from 5 hours to 20 minutes for etching a 1 micron thick TiO2 grating. This improvement will allow a greater number of samples to be processed through the laboratory in order to meet our grating layer alignment goals. We continued to work toward improving our grating layer alignment tolerance by gathering more statistics on systematic biases introduced during the process and by further stabilizing the laser used in measuring the layer offsets. There is a need for continued work in this area. We also continued to characterize deposition parameters for our homogeneous layer material by examining the effect of environmental conditions, such as relative humidity and temperature, on the consistency of deposition.

The diffractive scanner task was focused on fabrication and testing of two-layer Stratified Volume Diffractive Optical Elements (SVDOE). Several demonstration elements were processed through the laboratory and, subsequently, SEM micrographs have been obtained to allow measurement of geometry of the elements. One of these micrographs is shown in the figure below. The lower-most layer is a glass substrate followed by a TiO2 grating, a

homogeneous layer, a second TiO2 grating with an offset, a homogeneous cover layer and then air. Roughness seen on the face of the element occurs during cleaving.

Measurements of the grating dimensions made from these micrographs allow calculation of theoretical performance of the element, which is then compared with actual performance data measured in the laboratory. Comparison between predicted and actual performance shows good agreement.

Further examination of fabrication processes and parameters revealed that the alignment tolerance between layers could be relaxed by approximately a factor of three (e.g. 35nm to 100nm allowed error) while maintaining the same high diffraction efficiency. While this tolerance is still stringent, 100nm can be achieved much more readily than 35nm.

APPENDIX

Lightweight lidar telescopes for space applications

B. R. Peters,* P. J. Reardon, F. Amzajerdian, T. S. Blackwell

Center for Applied Optics
The University of Alabama in Huntsville
Huntsville, Alabama 35899

ABSTRACT

NASA is intent on exploiting the unique perspective of space-based remote optical instruments to observe and study large-scale environmental processes. Emphasis on smaller and more affordable missions continues to force the remote sensing instruments to find innovative ways to reduce the size, weight, and cost of the sensor package. This is a challenge because many of the proposed instruments incorporate a high quality meter-class telescope that can be a significant driver of total instrument costs. While various methods for telescope weight reduction have been achieved, many of the current approaches rely on exotic materials and specialized manufacturing techniques that limit availability or substantially increase costs. A competitive lightweight telescope technology that is especially well suited to space-based coherent Doppler wind lidar has been developed through a collaborative effort involving NASA Marshall Space Flight Center (MSFC) through the Global Hydrology and Climate Center (GHCC) and the University of Alabama in Huntsville (UAH) at the Center for Applied Optics (CAO). The new lightweight optics using metal alloy shells and surfaces (LOMASS) fabrication approach is suitable for high quality metal mirrors and meter-class telescopes. Compared to alternative materials and fabrication methods the new approach promises to reduce the areal density of a meter-class telescope to less than 15-kg/m^2; deliver a minimum λ/10-RMS surface optical quality; while using commercial materials and equipment to lower procurement costs. The final optical figure and finish is put into the mirrors through conventional diamond turning and polishing techniques. This approach is especially advantageous for a coherent lidar instrument because the reduced telescope weight permits the rotation of the telescope to scan the beam without requiring heavy wedges or additional large mirrors. Ongoing investigations and preliminary results show promise for the LOMASS approach to be successful in demonstrating a novel alternative approach to fabricating lightweight mirrors with performance parameters comparable with the Space Readiness Coherent Lidar Experiment (SPARCLE). Development and process characterization is continuing with the design and fabrication of mirrors for a 25-cm telescope suitable for a lidar instrument.

Keywords: lidar, telescope, lightweight optics, mirrors

1. INTRODUCTION

Ongoing interdisciplinary investigations into atmospheric climate processes and prediction rely on data from various satellite instruments, data from other sources, and a variety of models to construct an integrated view of atmospheric climate over the Earth. Improving climate models is critical to the increased understanding of global climate and the prediction of future climate changes. Topics of interest include the role of circulation, clouds, radiation, water vapor, and precipitation in climate change, and the role of ocean-atmosphere interactions in the energy and water cycles. The surface climate of the Earth is strongly influenced by the amount and distribution of water vapor, liquid water, and ice suspended in the atmosphere. The processes that control water in the atmosphere are very complex and extend across a wide range of spatial scales from the few centimeter scale of turbulence in the boundary layer to the tens of thousands that characterize the scale of global atmospheric circulation systems. While existing data sets have been used whenever available in the development and testing of models, additional quality data over substantial spatial scales is needed to improve the models.

Currently, no one sensor platform can adequately obtain all the data needed to address this broad range of scales so it becomes necessary to synthesize data from a variety of different sensor platforms at a number of different locations. The prevalence of water instead of land covering the surface of the Earth complicates the logistics associated with using ground-based systems to monitor global atmosphere. While airborne sensors can alleviate some of these problems by providing

* Further corresponding author information –
Dr. Bruce R. Peters: Email: petersb@email.uah.edu; WWW: http://www.uah.edu/cao/;
Tel: 256-824-2526; Fax: 256-824-6618.

mobile platforms that can range over much of the earth, local weather, loitering time, and operations costs can limit their use. The access of space-based sensors to the global atmosphere is not as limiting since satellites can theoretically gain access to any portion of the atmosphere to provide long-term monitoring of atmospheric phenomena. A further advantage to satellite sensors is that the satellite provides a unique viewpoint since it is above the atmosphere looking down and can thereby provided easy access to the upper levels of the atmosphere. An integrated, multisensor-based, worldwide observation system is desired to obtain the needed data to better anchor the climate models. Towards this end, the National Aeronautic and Space Administration (NASA) has taken the lead in developing and demonstrating continuous long-term global observations of the land surface, biosphere, solid Earth, atmosphere, and oceans from low Earth orbit for a minimum of fifteen years. The concept is to incorporate several space-based instruments and integrate the data with ground-based and airborne measurements to provide the scientific basis for understanding the Earth's climate system and its variations. This paper outlines the investigations into the development of one sensor that could be included in a worldwide observation system – a coherent Doppler wind lidar (CDWL).

2. COHERENT DOPPLER WIND LIDAR INSTRUMENT

Despite many of the challenges mentioned above, the measurement of global atmospheric wind velocities, from ground to upper atmosphere, remains one of the fundamental data sets necessary to advance the understanding and forecasting of weather.[1] As stated earlier, logistics and instrumentation limitations conspire to limit the ability to obtain data on a globally relevant scale with sufficient precision to support climate modeling. These limitations can be overcome by employing a space-based measurement platform, specifically a coherent Doppler wind lidar. CDWL for horizontal wind velocity measurements relies on the backscatter from aerosols in the atmosphere to derive a velocity map of the horizontal winds at a given height within the troposphere. The Space Readiness Coherent Lidar Experiment (SPARCLE) was designed to be a first step towards demonstrating the feasibility of measuring troposphere wind velocities using the space shuttle in lieu of a satellite.[2] The project has since been cancelled but the technology development is continuing.

The use of coherent Doppler lidar for determining wind velocity has long been recognized as a viable approach.[3,4] The CDWL employs heterodyne detection to increase signal-to-noise (SNR) and thereby increase sensitivity by overcoming the noise problems inherent in incoherent lidar systems.[5] In operation, a short laser pulse is transmitted from the instrument into the atmosphere. The photons scattered off of the aerosol particles within the atmosphere are collected by the same telescope and focused onto a detector. The return signal is Doppler shifted due to the combination of the spacecraft motion and the relative velocity of the aerosols and winds. The signal is mixed with the frequency stable reference beam on the detector and the velocity bias of the spacecraft is removed to determine the wind velocity. By scanning the laser beam about the nadir of the spacecraft, different lines-of-sight (such as looking forward and backward relative to the ground path of the satellite) for the same volume of atmosphere will permit the calculation of the horizontal wind vectors. The velocity vectors will be accurate provided the signal produced from the aerosol scattering is representative of the velocities within the sample volume, if the sample volume is small in size, and if the instrument performance uncertainties are sufficiently low.

A CO_2 laser Doppler wind lidar measurement capability was demonstrated as early as 1968 and lidar remains the only space-based instrument capable of measuring troposphere wind velocities.[6] MSFC conducted a series of studies to develop instrument designs utilizing both CO_2 and solid state laser technology with an emphasis on spacecraft adaptation and reducing system cost.[7,8] While technologically feasible, the drawbacks to utilizing CO_2 lasers, such as greater mass, volume, power requirements and cost, limited the development of a space-based system. However, with the advent of solid state laser technology beginning in the 1980's, a space-based wind velocity instrument became attractive.[9,10] The CDWL profiling instrument first described in 1996[11] has further evolved into the instrument used in SPARCLE. This instrument has become the baseline for future comparisons with regards to mass, volume, and performance.

As envisioned, the SPARCLE instrument is a compact and relatively low power, solid state coherent lidar that was conceived to be a compromise between current technological limitations and science goals. The instrument consists of a solid state laser transceiver, a beam expanding telescope and beam scanning optics, a support structure, a thermal subsystem, and a computer based data management and control subsystem. It was to be packaged into several pressurized Hitch Hiker (HH) canisters with an "optics can" and several supporting "electronics cans" (Figure 1). The standard canisters have a 50-cm internal diameter and a nominal usable experiment length of 71 cm. If additional volume is needed within the canister, the HH Program office has canister extensions to increase the can length in regular increments. The optics can contains the actual instrument sensing hardware such as the laser transceiver, the telescope, and beam scanning optics (Figure 2). The laser subsystem will function at 2.06 μm with 100 mJ of energy per pulse at 6 Hz pulse repetition rate. In this configuration, the laser will deliver a total optical power of 600 mW.[12] The output laser beam is expanded by an off-axis, afocal telescope

directed out through a window towards the atmosphere at a 30° nadir angle. The beam is scanned in a conical fashion, and the telescope collects the back scattered photons from the atmosphere and focuses it onto a detector. The instrument optical design allows for achieving the stringent wavefront qualities and optical performance within the tight physical constraints. The optomechanical design of the instrument is driven by the precision and accuracy required from the wind velocity measurements which demands achieving and maintaining the required optical alignment (pointing) through out a range of operational scenarios and environments and within the HH physical constraints.

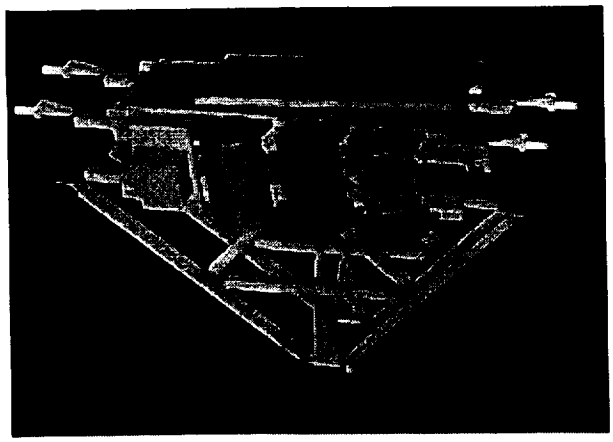

Figure 1. SPARCLE Instrument Configuration

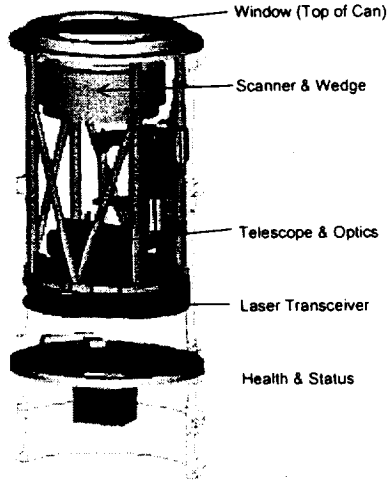

Figure 2. SPARCLE Optical System

3. TELESCOPE

Performance requirements for the SPARCLE telescope (Figure 3) optical quality are driven by the desire to maintain a minimal coherent laser radar signal to noise limit, withstand the thermal cycling and operate within the environment, and to survive launch loads by maintaining alignment. To meet the signal to noise requirements, the telescope must minimize optical aberrations in order to project the outgoing pulse from space through the troposphere with the best possible beam profile. Studies show that, although all aberrations reduce the lidar performance, small amounts (½ wave PV) of spherical aberration will produce approximately 50% reduction in heterodyne efficiency[13]. In addition to the overall wavefront quality requirements, spatial polarization efficiency and optical transmission are of great concern due to the tenuous return signal from atmospheric aerosols. The thermal environment is fluctuating in a regular fashion throughout the mission as the shuttle encounters heating and cooling due to sun exposure and shade behind the Earth. Although the telescope is designed to maintain its wavefront quality over a large static temperature range, it remains sensitive to thermal gradients.

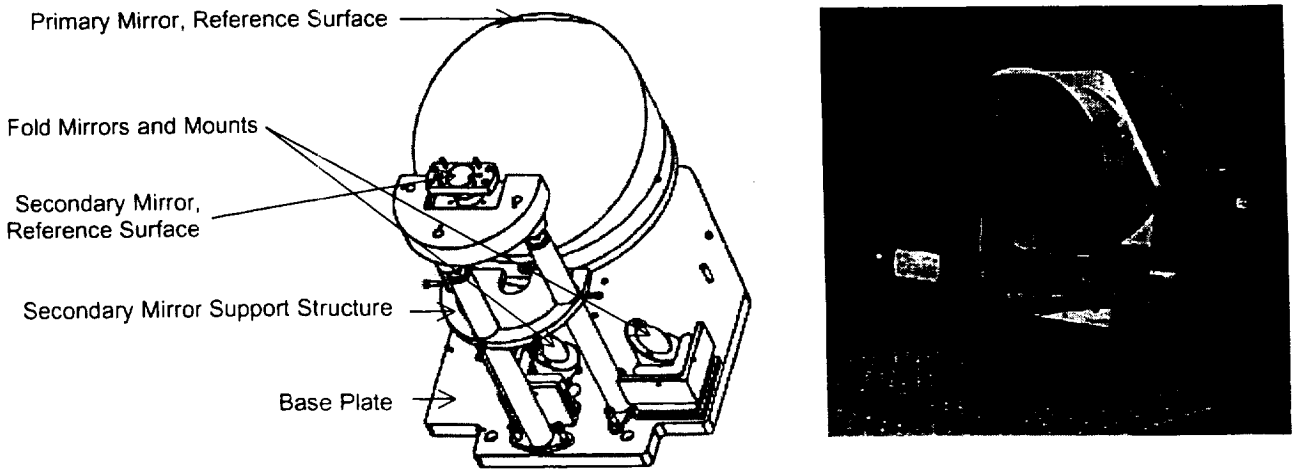

Figure 3. SPARCLE telescope showing the components and the structure.

The telescope mirrors incorporate a number of alignment reference surfaces including flats on both the primary mirror and the secondary mirror. The reference flat surfaces are for alignment of the relative tilts between the two elements. The primary mirror has a 7.0mm wide flat reference surface on the edge of its optical surface and three mounting pads, with optical-grade surfaces, on the reverse side. All four of the primary's reference surfaces are diamond turned to be parallel to each other and perpendicular to the virtual axis of the mirror's parabola. The secondary mirror also has reference flat surfaces on the front and backside of the mirror. The primary mirror and the secondary support posts are mounted to an optical baseplate. The top surface of the optical baseplate is diamond turned to generate a large flat optical surface to serve as a datum plane and to further reduce any distortion that can result from attaching the primary mirror and the secondary mirror support posts to the baseplate. The backside of the optical baseplate also has three flat and parallel pads for mounting to the lidar transceiver without distorting the telescope alignment. Location and alignment of the transceiver beam to the telescope is achieved through two mirror tip-tilt-stages and a linear stage on one mirror that together deliver stages 5 degrees of freedom.

The telescope and support structure was fabricated from 6061-T6 Aluminum alloy to make the telescope athermal. The two mirrors were rough machined, thermally cycled to remove stress and to stabilize the blanks before diamond turning the optical surfaces. The aspheric surfaces were machined into the blanks using conventional SPDT technology in the Aluminum and then the surfaces were electroless nickel plated and turned to the final surface figure. Post polishing was used to remove the diamond tooling marks and lower scattering by decreasing RMS surface roughness. The completed telescope is shown in Figure 3.

The assembled telescope is designed as a compact 38 x 32 x 33 cm volume, 25X angular magnification afocal beam expander. The telescope is designed to have a full field of view of 80 micro-radians and a primary mirror aperture of 25 cm is an off-axis parabola of f-number 0.6. The optical spacing between the primary and secondary mirror is 22.5 cm de-centered by 15 cm. with a 23-cm obscuration free aperture exiting the primary mirror. The secondary mirror is a convex paraboloid with a useable 6-mm aperture having a full 32-mm physical aperture. While the telescope was designed to be relatively low weight, there was no radical weight reduction measures taken to reduce the overall mass. This was deemed to be the lowest risk approach since UAH had experience in the fabrication of similar mirrors and structures. The result was an essentially solid aluminum primary mirror, baseplate, secondary mirror, and structure. The total weight of the assembled telescope was approximately 20 kg.

4. LIGHTWEIGHT TELESCOPE

With the subsequent cancellation of SPARCLE, the urgency in flying was somewhat reduced so the science requirements could be re-evaluated and the instrument design revisited along with necessary technology developments. As stated earlier, the SPARCLE instrument was a compromise and a successful SPARCLE mission would not have provided the technology needed for the future missions. A global troposphere wind roadmap was developed that outlined the CDWL instrument that was desired. Strongly influencing CDWL instrument performance were the requirements of the National Polar-orbiting Operational Environmental Satellite System (NPOESS) Integrated Program Office (IPO) for operational measurements of troposphere winds. As a partner in IPO, NASA with the Department of Defense (DOD) and the Department of Commerce (DOC), was charged with developing the CDWL instrument and the needed technology. It was obvious that a scaled up version of SPARCLE's telescope was not a viable approach.

SPARCLE was planning on using a silicon wedge to deflect the outgoing lidar beam. Rotation of the wedge will provide the conical scanning pattern that is needed. The outgoing lidar beam diameter will likely be 50 cm for a future NASA science mission, and 100 cm for the NPOESS operational mission. It is believed that employing a rotating wedge for these larger diameter beams will present several problems for future space-based lidar missions where the desired aperture is 50 cm and larger. One concern is that the wedge materials with suitable refractive index, such as Silicon, are crystalline and, consequently, must be grown. The final boule must be large enough to allow the optical blank to be cut in the desired orientation and must be free from optical imperfections. Another concern associated with a large aperture wedge is the ability to polish the surfaces to the required optical quality while maintaining the exact wedge angle. In addition, the optomechanical aspects of rotating such a large, asymmetric mass become difficult. Therefore, alternative concepts for beam scanning were explored.

One approach amongst many was to utilize a rotating telescope. For this embodiment to succeed, the weight of the telescope had to be kept to a minimum to permit the rapid step and stare with its quick stating and stopping of the rotation to occur without unduly taxing the rotation motor. However, a rotating telescope would need to have a primary of significant size near the diameter of the desired outgoing beam and this was to be in the 50-100 cm range. Therefore, the mass of the telescope

had to be reduced for three reasons. The telescope weight needed to be minimized to permit the scanning of such a large primary mirror and its significant inertia to allow step-stare operation. A reduction in weight would reduce the load on the scanning motor and permit lower power requirements, less thermal load (a smaller scanner motor), and greater procurement options. Also, a lighter but structurally stiff telescope would permit faster motion with less deceleration time to come to a stop without ringing. Finally, a lighter telescope would fit within the constraints of the satellite bus for NPOESS and therefore permit easier integration.

The instrument cost is usually directly related to instrument performance and the high quality, meter-class telescope can be a significant driver of total instrument costs. Lowering unit costs through production of many units (mass production) does not apply to space-based optical instruments because each instrument has specialized optical performance parameters that require different component designs and the quantities required are usually too low to benefit from economies of scale. There is also a direct cost associated with launching the significant mass/volume of a telescope. Telescope weight reduction is achievable but the current approaches tend to rely on exotic materials and specialized manufacturing techniques.[14,15,16] However, these materials typically have higher costs such as: more nonrecurring engineering, specialized tooling, and added handling costs (material quality, availability, waste disposal, etc.). Therefore, the cost of fabrication will rise along with an increase in technical risk that could negate the cost savings from the weight reduction. A remote sensing instrument with a meter-class telescope must be both lightweight, and economical to fabricate.

Ultimately, the telescope must have low surface scatter from the mirrors and minimal backscatter towards the detector; highly reflective coatings on the mirrors for the infrared laser; compact optical path to minimize misalignments; and limited reflections to disrupt the beam polarization. To maintain operation on orbit, the telescope should be athermal (uniform coefficient of thermal expansion). To maintain optical alignment between the time it is assembled (under a 1-g environment) and when it reaches orbit (under a μ-g environment) the telescope material needs to have high stiffness (high microyield) and minimal self-weight deflection. Metal mirrors with all of these attributes and without the weight can be fabricated using a novel approach developed by the CAO called LOMASS - Lightweight Optics using Metal Alloy Shells and Surfaces.

In the LOMASS process, nested groups of metal shells supply structural support to the thin metal surface that serves as the precision mirror to form a three dimensional shell structure that is rigid yet lightweight. The shells and optical surfaces are formed by either electrochemical deposition, typically nickel, to coat a near net shape mandrel, often aluminum, to create as continuous and homogeneous a shell structure over the mandrel as possible. Metal plating processes over aluminum mandrels are well accepted by industry and NASA.[17] Nickel's relatively high hardness makes it suitable to diamond turn and easy to polish and it has excellent microyield properties. UAH and NASA-MSFC have extensive experience in developing and applying nickel coatings and creating nickel shells for use in x-ray telescopes. The chemical properties of the nickel alloy can be tailored to the requirements of the part to help control strength, rigidity, ease of machining, and hardness. The object is to balance the proportions of the various elements in the nickel alloy (phosphor and others) such that the metal achieves a glassy-like behavior with high microyield strength but without becoming so hard that machining and finishing become a problem. While the highest microyield nickels also have the highest hardness values and are difficult to cut with anything other than diamond or specialty tools, there are alloys with similar compositions that achieve adequate strength and are significantly easier to machine using conventional steel tools. The latter is the alloys selected for telescope applications described in this paper in order to minimize the fabrication costs by avoiding the need for expensive exotic tooling..

The nickel is applied in essentially a stress free state and at greater thickness than typically used in x-ray mirror fabrication. This is necessary so that the thin shell will be rigid enough to support itself, the anticipated launch loads, and still maintain the optical quality. Second, the nickel shell created over the mandrel is far more complex in structure than a x-ray mirror shell. The shell relies on three dimensional surfaces or membranes to create structural stability rather than bulk material. For this reason, thin shells are harder to design and more complex to analyze, hence the reliance on computer analysis tools as the only means to optimize a thin shell mirror.

Once fabrication, stress relief, and thermal treatments are completed, the mandrel is dissolved leaving a thin metal shell that is self-supporting and which contains a high quality optical surface. The approach includes some unique processing steps in applying the metal shell to minimize the buildup of stress in the shell so that the separation from the mandrel does not cause the shell to distort. The final figuring of the mirror is accomplished through the use of traditional and readily available commercial optical figuring processes such as diamond turning or polishing (Figure 4). The flat was generated and measured to be ~1 wave flat across the 100 mm aperture at 632 nm wavelength. The error in surface figure was attributed to a vibration set up in the turning of the thin shell. The vibration was dampened through the filling of the cavity with a wax that supported the surface and dampened vibration. Once the wax was removed, the surface remained relatively unchanged. Subsequent test

articles employing this process to stabilize the surface during diamond turning and polishing have yielded sub-wavelength quality flats. The expense in precision machining is incurred only on the final part and not the mandrel so the process is competitive in cost.

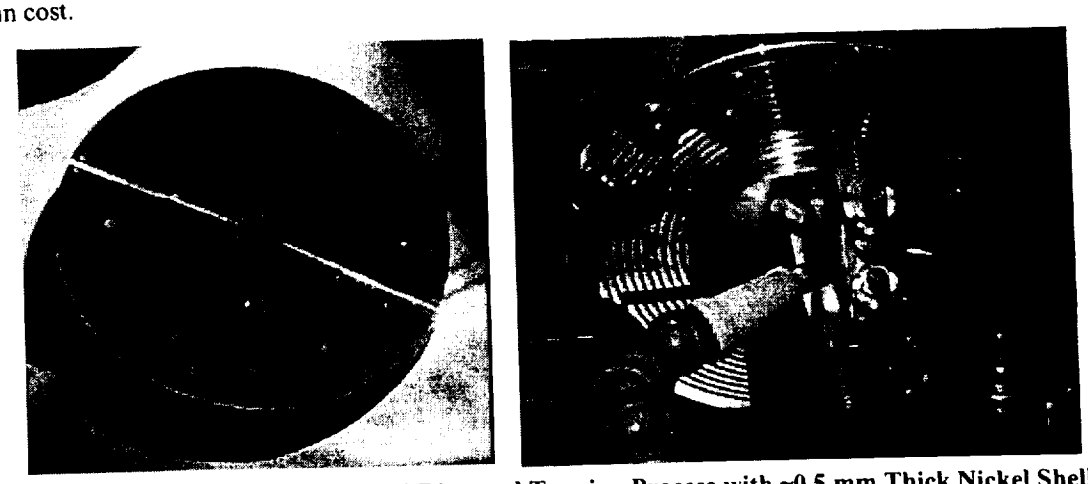

Figure 4. LOMASS Test Article and Diamond Turning Process with ~0.5 mm Thick Nickel Shell

Initial development and some sample small scale proof-of-concept parts (Figure 4) have already been fabricated to support the GHCC coherent wind lidar technology development. The initial results showed some difficulties in getting the nickel to adhere to both the aluminum mandrel and the nickel coated inserts. The chemical activation process used for the aluminum was less effective in allowing the nickel to adhere to the nickel inserts. This has since been addressed by interposing an intermediate metallic coating over the assembled mandrel (aluminum and nickel) that enhances the adherence of the nickel to itself while providing adequate adherence to the aluminum yet permitting easy separation later on. An initial laboratory demonstration telescope is presently under development that includes a 25-cm primary mirror. The lightweight rotating telescope concept which includes the demonstration primary mirror is shown in Figure 5. The primary under development is an on-axis paraboloid and its optical performance is designed to equal the SPARCLE baseline design except for the central obscuration. It is significant to note that the new primary should weigh only 10% as much as the previous SPARCLE primary while maintaining optical performance.

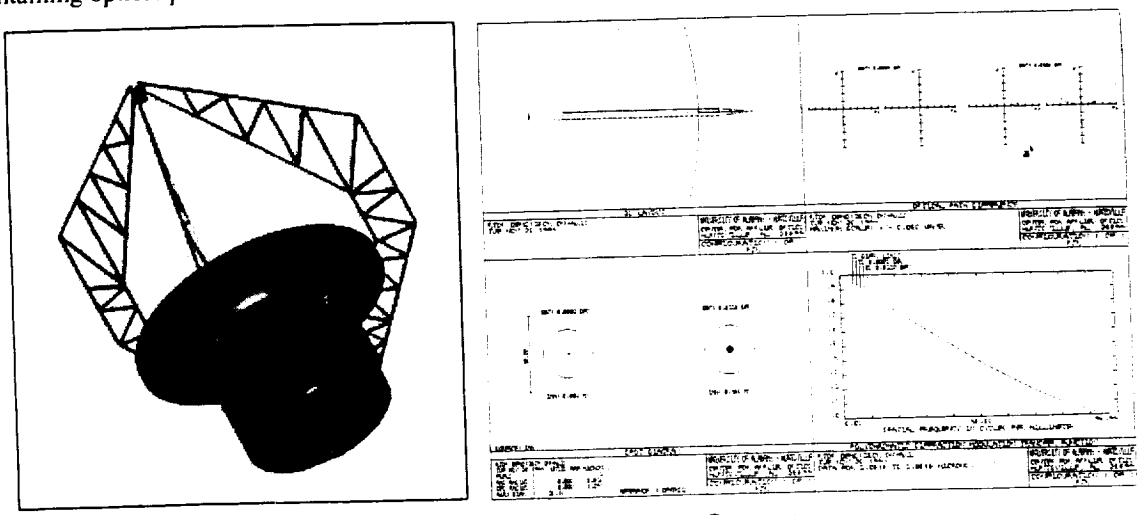

Figure 5. LOMASS Telescope Concept

5. SUMMARY

The LOMASS approach shows promise as a method for fabricating meter-class mirrors that are lightweight and of suitable optical quality for telescope applications. Initial test articles have demonstrated the capabilities of the process and larger mirrors are under development. The approach relies on industry accepted processes to minimize costs and ease fabrication. Since the mandrel does not require any special manufacturing processes, it can be fabricated at relatively low cost and

through a variety of commercial sources. The expertise is required in the selection of the proper nickel alloy and the application of the nickel layer. Success at this step is very dependent on the stability and fidelity of the nickel coating process. Once coated, the part can once again be treated as a conventional metal mirror and finished as desired using diamond turning and optical polishing techniques. Continuing development will proceed towards fabricating larger mirrors.

6. ACKNOWLEDGEMENT

This work was supported by NASA Marshall Space Flight Center Global Hydrology and Climate Center through a Cooperative Agreement with The University of Alabama in Huntsville at The Center for Applied Optics.

7. REFERENCES

1. R. Atlas, " Atmospheric observations and experiments to assess their usefulness in data assimilation," J. Meteor. Soc. Japan, Vol. 75, pp. 111-130 (1997).
2. M.J. Kavaya and G.D. Emmitt, "The space readiness coherent lidar experiment (SPARCLE) space shuttle mission," Proc. of the SPIE Laser Radar Technology and Applications III Conference, Vol. 3380 (1998).
3. R.T. Menzies and R.M. Hardesty, "Coherent doppler lidar for measurements of wind fields," Proc. IEEE, Vol. 77, pp. 449-462 (1989).
4. M. Huffaker and R.M. Hardesty, "Remote sensing of atmospheric wind velocities using solid state and CO2 coherent laser systems," Proc. IEEE, Vol. 84, No. 2, pp. 181-204 (1996).
5. M.J. Kavaya, S.W. Henderson and C.P. Hale, "Solid-state progress supports coherent laser-radar technology," Laser Focus World, August, pp. 83-93 (1989).
6. W.E. Baker, et.al., "Lidar-measured winds from space: a key component for weather and climate prediction," Bulletin of the American Meteorological Society, Vol. 76, No. 6, pp. 869-888 (1995).
7. R.G. Beranek, et.al., "Laser atmospheric wind sounder (LAWS)," Proc. of the SPIE Laser Applications in Meteorology and Earth and Atmospheric Remote Sensing, Vol. 1062, pp. 234-248 (1989).
8. M.J. Kavaya, et.al., Direct global measurements of tropospheric winds employing a simplified coherent laser radar using fully scaleable technology and technique," Proc. of the SPIE Space Instrumentation and Dual-Use Technologies Conference, Vol. 2214, pp. 237-249 (1994).
9. M.J. Kavaya, et.al., "Remote wind profiling with a solid-state Nd:YAG coherent lidar system," Optics Letters, Vol. 14, No. 15, pp. 776-778 (1989).
10. S.W. Henderson, et.al., "Eye-safe coherent laser radar system at 2.1-micron using Tm,Ho:YAG lasers," Optics Letters, Vol. 16, No. 10, pp. 773-7758 (1991).
11. M.J. Kavaya, "Novel technology for satellite based wind sensing," Proc. of the 1996 AIAA Space Programs and Technologies Conference, AIAA 96-4276 (1996).
12. U.N. Singh, et.al., "Injection seeded, room temperature, diode pumped, Ho,Tm:YLF laser with output energy of 600 mJ at 10 Hz," Proc. of the Advanced Solid State Lasers Conference, OSA AWC1, pp. 322-324 (1998).
13. Gary D. Spiers, The effect of optical aberrations on the performance of a coherent Doppler lidar. Proceedings of the Tenth Biennial Coherent Laser Radar Technology and Applications Conference (1999).
14. P. C. Chen, T. T. Saha, A. M. Smith, and R. Romero, "Progress in very lightweight optics using graphite fiber composite materials," *Opt. Eng.* 37, 666-676 (1998).
15. M. Anapol, L. Gardner, T. Tucker, and R. Koczor, "Lightweight 0.5 m silicon carbide telescope for a geo-stationary earth observatory mission," Proc. SPIE Vol. 2543, 164-172, 1995.
16. Y. W. Hsu and R. A. Johnson, "Design and Analysis of one meter beryllium space telescope," Proc. SPIE Vol. 2543, 244-257, 1995.
17. D. L. Hibbard, "Electrochemically deposited nickel alloys with controlled thermal expansion for optical applications," Proc. SPIE Vol. 2543, 236-243, 1995.

1. R. Atlas, " Atmospheric observations and experiments to assess their usefulness in data assimilation," J. Meteor. Soc. Japan, Vol. 75, pp. 111-130 (1997).
2. M.J. Kavaya and G.D. Emmitt, "The space readiness coherent lidar experiment (SPARCLE) space shuttle mission," Proc. of the SPIE Laser Radar Technology and Applications III Conference, Vol. 3380 (1998).
3. R.T. Menzies and R.M. Hardesty, "Coherent doppler lidar for measurements of wind fields," Proc. IEEE, Vol. 77, pp. 449-462 (1989).
4. M. Huffaker and R.M. Hardesty, "Remote sensing of atmospheric wind velocities using solid state and CO2 coherent laser systems," Proc. IEEE, Vol. 84, No. 2, pp. 181-204 (1996).
5. M.J. Kavaya, S.W. Henderson and C.P. Hale, "Solid-state progress supports coherent laser-radar technology," Laser Focus World, August, pp. 83-93 (1989).
6. W.E. Baker, et.al., "Lidar-measured winds from space: a key component for weather and climate prediction," Bulletin of the American Meteorological Society, Vol. 76, No. 6, pp. 869-888 (1995).
7. R.G. Beranek, et.al., "Laser atmospheric wind sounder (LAWS)," Proc. of the SPIE Laser Applications in Meteorology and Earth and Atmospheric Remote Sensing, Vol. 1062, pp. 234-248 (1989).
8. M.J. Kavaya, et.al., Direct global measurements of tropospheric winds employing a simplified coherent laser radar using fully scaleable technology and technique," Proc. of the SPIE Space Instrumentation and Dual-Use Technologies Conference, Vol. 2214, pp. 237-249 (1994).
9. M.J. Kavaya, et.al., "Remote wind profiling with a solid-state Nd:YAG coherent lidar system," Optics Letters, Vol. 14, No. 15, pp. 776-778 (1989).
10. S.W. Henderson, et.al., "Eye-safe coherent laser radar system at 2.1-micron using Tm,Ho:YAG lasers," Optics Letters, Vol. 16, No. 10, pp. 773-7758 (1991).
11. M.J. Kavaya, "Novel technology for satellite based wind sensing," Proc. of the 1996 AIAA Space Programs and Technologies Conference, AIAA 96-4276 (1996).
12. U.N. Singh, et.al., "Injection seeded, room temperature, diode pumped, Ho,Tm:YLF laser with output energy of 600 mJ at 10 Hz," Proc. of the Advanced Solid State Lasers Conference, OSA AWC1, pp. 322-324 (1998).
13. Gary D. Spiers, The effect of optical aberrations on the performance of a coherent Doppler lidar. Proceedings of the Tenth Biennial Coherent Laser Radar Technology and Applications Conference (1999).
14 P. C. Chen, T. T. Saha, A. M. Smith, and R. Romero, "Progress in very lightweight optics using graphite fiber composite materials," *Opt. Eng.* 37, 666-676 (1998).

15 M. Anapol, L. Gardner, T. Tucker, and R. Koczor, "Lightweight 0.5 m silicon carbide telescope for a geo-stationary earth observatory mission," Proc. SPIE Vol. 2543, 164-172, 1995.

16 Y. W. Hsu and R. A. Johnson, "Design and Analysis of one meter beryllium space telescope," Proc. SPIE Vol. 2543, 244-257, 1995.

17 D. L. Hibbard, "Electrochemically deposited nickel alloys with controlled thermal expansion for optical applications," Proc. SPIE Vol. 2543, 236-243, 1995.